AFRL-RB-WP-TR-2009-3100

AIR VEHICLE TECHNOLOGY INTEGRATION PROGRAM (AVTIP)

Delivery Order 0086: Applied Nonlinear Low Order Response Prediction Methods Evaluation

Salvatore L. Liguore, Dale M. Pitt, and Edward V. White

The Boeing Company

APRIL 2009
Final Report

AIR FORCE RESEARCH LABORATORY
AIR VEHICLES DIRECTORATE
WRIGHT-PATTERSON AIR FORCE BASE, OH 45433-7542
AIR FORCE MATERIEL COMMAND
UNITED STATES AIR FORCE

NOTICE AND SIGNATURE PAGE

Using Government drawings, specifications, or other data included in this document for any purpose other than Government procurement does not in any way obligate the U.S. Government. The fact that the Government formulated or supplied the drawings, specifications, or other data does not license the holder or any other person or corporation; or convey any rights or permission to manufacture, use, or sell any patented invention that may relate to them.

This report was cleared for public release by the USAF 88th Air Base Wing (88 ABW) Public Affairs Office (PAO) and is available to the general public, including foreign nationals. Copies may be obtained from the Defense Technical Information Center (DTIC) (http://www.dtic.mil).

AFRL-RB-WP-TR-2009-3100 HAS BEEN REVIEWED AND IS APPROVED FOR PUBLICATION IN ACCORDANCE WITH ASSIGNED DISTRIBUTION STATEMENT.

*//Signature//

LEONARD SHAW
Project Engineer
Structural Mechanics Branch
Structures Division

//Signature//

ANDREW G. SPARKS, Chief
Structural Mechanics Branch
Structures Division

//Signature//

DAVID PRATT, Technical Advisor
Structures Division
Air Vehicles Directorate

This report is published in the interest of scientific and technical information exchange, and its publication does not constitute the Government's approval or disapproval of its ideas or findings.

*Disseminated copies will show "//Signature//" stamped or typed above the signature blocks.

REPORT DOCUMENTATION PAGE

Form Approved
OMB No. 0704-0188

1. REPORT DATE *(DD-MM-YY)*	2. REPORT TYPE	3. DATES COVERED *(From - To)*
April 2009	Final	26 September 2007 – 26 March 2009

4. TITLE AND SUBTITLE
AIR VEHICLE TECHNOLOGY INTEGRATION PROGRAM (AVTIP)
Delivery Order 0086: Applied Nonlinear Low Order Response Prediction Methods Evaluation

5a. CONTRACT NUMBER
F33615-00-D-3052-0086

5b. GRANT NUMBER

5c. PROGRAM ELEMENT NUMBER
0602201

6. AUTHOR(S)
Salvatore L. Liguore, Dale M. Pitt, and Edward V. White

5d. PROJECT NUMBER
A0F2

5e. TASK NUMBER

5f. WORK UNIT NUMBER
0B

7. PERFORMING ORGANIZATION NAME(S) AND ADDRESS(ES)
The Boeing Company
P.O. Box 516
St. Louis, MO 63166-0516

8. PERFORMING ORGANIZATION REPORT NUMBER

9. SPONSORING/MONITORING AGENCY NAME(S) AND ADDRESS(ES)
Air Force Research Laboratory
Air Vehicles Directorate
Wright-Patterson Air Force Base, OH 45433-7542
Air Force Materiel Command
United States Air Force

10. SPONSORING/MONITORING AGENCY ACRONYM(S)
AFRL/RBSM

11. SPONSORING/MONITORING AGENCY REPORT NUMBER(S)
AFRL-RB-WP-TR-2009-3100

12. DISTRIBUTION/AVAILABILITY STATEMENT
Approved for public release; distribution unlimited.

13. SUPPLEMENTARY NOTES
PAO Case Number: 88ABW 2009-1365, 07 April 2009. Report contains color.

14. ABSTRACT
The objective of this project was to evaluate the nonlinear reduced order modeling prediction method as applied to the acoustic fatigue design of representative fixed-wing aircraft structure and recommend technical improvements. These reduced order methods are applicable to the response of stiffened aircraft structural skins exposed to high aeroacoustic loading. The approach was to develop validation test cases based on actual aircraft structures under flight aeroacoustic loading environments. The Implicit Modal Condensation method was implemented with MSC/NASTRAN. The validation included the prediction of structural responses using full-order degree of freedom methods compared to the reduced order methods. Also, the structural response and predicted fatigue life was compared to available test data. This report documents the validation study of the new nonlinear reduced order structural response prediction method along with the identified benefits, deficiencies, and recommendations for technical improvement.

15. SUBJECT TERMS
structural response prediction, low-order, non-linear

16. SECURITY CLASSIFICATION OF:			17. LIMITATION OF ABSTRACT:	18. NUMBER OF PAGES	19a. NAME OF RESPONSIBLE PERSON (Monitor)
a. REPORT	b. ABSTRACT	c. THIS PAGE			Leonard Shaw
Unclassified	Unclassified	Unclassified	SAR	110	19b. TELEPHONE NUMBER *(Include Area Code)* N/A

Standard Form 298 (Rev. 8-98)
Prescribed by ANSI Std. Z39-18

TABLE OF CONTENTS

Table of Contents iii
List of Figures iv
List of Tables vii
Acknowledgements viii
Glossary of Terminology ix
List of Symbols x
Executive Summary xi
1 Introduction 1
2 Methods, Assumptions, and procedures 8
2.1 Background on Reduced Order Modeling Methods 8
2.2 Implementation of the NLROM Method 10
2.3 Matlab User Interface – NLROM 16
2.4 General Acoustic Fatigue Analysis Process 21
3 Results and Discussion 25
3.1 Verification Test Case – Curved Beam 25
3.2 Validation Test Case – Curved Panel 35
3.3 Validation Test Case – Curved Stiffened Aircraft Panel 51
3.3.1 Comparison to Experimental Data – Curved Stiffened Aircraft Panel 59
3.4 Acoustic Fatigue Design Study 67
3.4.1 Baseline Panel 67
3.4.2 Improved Panel 70
4 Conclusions 75
5 Recommendations 77
5.1 Implementation of Method 77
5.2 Integration of Method 78
5.3 Validation of Method 79
5.4 Practicality of Use 81
5.5 Theoretical Extensions 82
6 References 83
Appendix – Linear static model setup 85
Appendix – Linear modal solution setup 89
Appendix – Nonlinear static solution setup 90

LIST OF FIGURES

Figure 1 - NASTRAN FEM and Results from the ELSTEP Evaluation 2
Figure 2 - Acoustic Fatigue Design Process 3
Figure 3 – Typical High Cycle Fatigue Joint Specimen 4
Figure 4 – Comparison of Linear and Nonlinear RMS stresses 5
Figure 5 - Acoustic Noise Sources 6
Figure 6 - Measured Damping Levels in all Types of Metallic and Composite Structures 7
Figure 7 – NLROM Simulation Procedure, modified from Ref. (2) 11
Figure 8 – Acoustic Pressure Load Cases 11
Figure 9 – Model Setup Steps 12
Figure 10 – Sample 3-mode problem with 26 static load cases, Ref. (8) 13
Figure 11 – Curved Beam Nonlinear Static (Modal) Results for Mode 2, only 14
Figure 12 – Nonlinear Static Analysis of Mode-1 Loads (Snap-thru Analysis) 15
Figure 13 – Matlab Tool – NLROM 17
Figure 14 – Model Solution and Results Input 18
Figure 15 – Selection of Linear Modes 18
Figure 16 – Evaluate Linear Response 18
Figure 17 – Nonlinear Static Solution Setup 19
Figure 18 – Nodal Results Interactive Post-Processing 19
Figure 19 – Nodal Post-Processing 20
Figure 20 – Element Results Post-Processing 21
Figure 21 – Additional NLROM Script Features 21
Figure 22 – Model Check-out Process 22
Figure 23 – Linear Modal Response – Pre-NLROM Process 23
Figure 24 – NLROM Analysis Process 24
Figure 25 – Geometry of Curved Beam 26
Figure 26 – Curved Beam Mode Shapes 27
Figure 27 – Compare NASTRAN Full-Order Linear and Nonlinear Static Deflections 28
Figure 28 – Compare the Linear ROM to the Linear Full-order model 29
Figure 29 - Compare the Nonlinear ROM to the Nonlinear Full-order model 29
Figure 30 – Compare the Nonlinear ROM to the Nonlinear Full-order model 30
Figure 31 – Vertical Displacement, Prms=0.92psi, 3-Modes, Alpha=64., T=2secs 31
Figure 32 – Vertical Displacement, NLROM-IC analysis, 3-Modes, Alpha=64, T=2secs 31
Figure 33 – Mid-Span Vertical Displacement at Prms=0.92psi (NLROM-IC) 32
Figure 34 – Mid-Span Vertical Displacement at Prms=0.92psi (ABAQUS-Explicit) 32
Figure 35 – Linear Mid Span Vertical Displacement Response 33
Figure 36 – Linear Quarter Span Vertical Displacement Response 34
Figure 37 – Nonlinear Quarter Span Vertical Displacement Response 35

Figure 38 – Selected Modes 37
Figure 39 – Out-of-Plane Z-Displacement at the Center of the Panel 38
Figure 40 – Out-of-Plane Z-Acceleration at the Center of the Panel 38
Figure 41 – Stress S22 Top Side, Element at the center of long edge 39
Figure 42 – Increasing Solution Time with Increasing Modes for the NLROM method normalized to a one mode solution. 40
Figure 43 – Comparison of the NLROM method efficiency to the Full-order explicit Solution, a 4-sec time simulation 41
Figure 44 – Gamma (Irregularity Factor) vs. Simulation Time 42
Figure 45 – RMS Response vs. Simulation Time 43
Figure 46 – Comparison of PSDs for Different Time Simulation Durations 43
Figure 47 – Cycles to Failure vs. Simulation Time 44
Figure 48 – Time Signal Amplitude PDF 45
Figure 49 – Time Signal Peak/Valley PDF 45
Figure 50 – Linear Time History Signal 46
Figure 51 – Linear response mean – range plot 47
Figure 52 – Linear Time Signal Range PDF 47
Figure 53 - Linear Time Signal Mean PDF 48
Figure 54 – Nonlinear Time History Signal 48
Figure 55 - Nonlinear Time Signal mean-range Plot 49
Figure 56 – Nonlinear response Range PDF 49
Figure 57 - Nonlinear response Mean PDF 50
Figure 58 – Uncertainty in Cycle Counting Fatigue 50
Figure 59 – Curved Stiffened Panel Test Case 51
Figure 60 – Acoustic Input Spectrum 52
Figure 61 – PSD to Time History 53
Figure 62 – Finite Element Model of Panel 53
Figure 63 – Mode shape for baseline model Mode 1, 281 Hz 54
Figure 64 – Mode shape for baseline model Mode 2, 334 Hz 54
Figure 65 – Mode shape for baseline model Mode 6, 568 Hz 55
Figure 66 – Mode shape for baseline model Mode 14, 873 Hz 55
Figure 67 – NASTRAN Linear RMS Y-Displacement (Inches) 56
Figure 68 – NASTRAN Linear RMS Y-Acceleration (Grms) 56
Figure 69 – NASTRAN Linear RMS Sx-Stress (psi) 57
Figure 70 – NASTRAN Linear RMS Sx-Stress (psi) (Shear Clip Location) 57
Figure 71 – Reference Accelerometer (Node) Locations to be used in Study 58
Figure 72 – Reference Strain Gage (Element) Locations to be used in the Study 58
Figure 73 – Center Bay (on Skin) Y-Acceleration 59
Figure 74 – Clip Radius Corner Stress Sx PSD 59
Figure 75 – NLROM Simulation at Different Load Levels and without Preload 60

Figure 76 – Panel Displacement, NLROM simulation w/ and w/o 3-psi preload 61
Figure 77 – Clip Stress, NLROM simulation w/ and w/o 3-psi preload..... 61
Figure 78 – Stress in the Clip at the Edge of Panel, OASPL = 165 dB, Ps=3psi 62
Figure 79 - Progressive Wave Chamber 63
Figure 80 – Test Panel Failure Mode..... 63
Figure 81 – Test Panel Mounted in Facility Side Wall in Pressure Plate Fixture 64
Figure 82 – Mid Panel Upper RHS Skin Pocket..... 65
Figure 83 – Representative FRF Mid-Stiffener on the Web..... 65
Figure 84 – Reference Strain (Sg3) on the Former. 66
Figure 85 - Reference Acceleration (AC1) at the Center of the Panel Bay. 66
Figure 86 – Unit pressure loading in two separate sets to capture desired panel modes..... 67
Figure 87 – Representative node locations for mode selection 67
Figure 88 – Displacement PSDs for representative nodes and selected modes..... 68
Figure 89 – Plot of fatigue prediction for critical element in baseline panel model..... 70
Figure 90 – Mode shape for improved model Mode 1, 293 Hz..... 71
Figure 91 – Mode shape for improved model Mode 2, 350 Hz..... 71
Figure 92 – Mode shape for improved model Mode 3, 454 Hz..... 72
Figure 93 – Mode shape for improved model Mode 4, 491 Hz..... 72
Figure 94 – Mode shape for improved model Mode 11, 776 Hz..... 73
Figure 95 – Mode shape for improved model Mode 13, 888 Hz..... 73
Figure 96 – Plot of fatigue prediction for critical element from baseline panel model 74
Figure 97 – FEM of Idealized Panel 79

LIST OF TABLES

Table 1 – Mode Frequency Table (*-NLROM Modes)..... 36
Table 2 – Timing Study 39
Table 3 – Life Prediction Results..... 62
Table 4 – Experimental Panel Frequencies..... 64
Table 5 – NLROM Practicality Evaluation 82

ACKNOWLEDGEMENTS

This work is funded by the USAF Air Force Research Lab (AFRL/RBSM). The authors would like to acknowledge the technical support and guidance of Doug Henderson, Leonard Shaw, Robert Gordon, and Joseph Hollkamp of this work. We would also like to acknowledge the technical guidance of our Boeing Consultants: David Groen, Mostafa Rassaian, and Bijan Nejad.

GLOSSARY OF TERMINOLOGY

Term	Definition
RMS	Root Mean Square
CAA	Computational Aero-Acoustics
CPU	Central Processing Unit
FEA	Finite Element Analysis
FEM	Finite Element Model(s)
s-N	Stress – Cycles to Failure Data
TBL	Turbulent Boundary Layer
CSD	Cross Spectral Density
PSD	Power Spectral Density
DOF	Degrees of Freedom
IMC	Implicit Modal Condensation
BC	Boundary Condition
ROM	Reduced Order Model
NLROM	Nonlinear Reduced Order Model
NL	Nonlinear
SOL	MSC/NASTRAN Solution Sequence
EMD	Engineering Manufacturing Development
Grms	RMS acceleration in units of g's
WAFO	Waves Analysis for Fatigue and Oceanography
I/O	Input / Output
ODE	Ordinary Differential Equation
PDF	Probability Density Function
V&V	Verification and Validation
P/V	Peak/Valley

LIST OF SYMBOLS

Symbol	Definition
R	R-ratio
Kt	Stress Concentration Factor
G	Gravity units equal to 386 in/s^2
Psi	Pounds per square inch
t	Skin thickness (panel or beam)
c	Nonlinear static load scalars
M	Mass matrix
K	Linear Stiffness Matrix
C	Damping Matrix
p	Modal displacements
x	Physical displacements
f	Modal Forces
F	Applied force
A	Cubic Stiffness Terms
B	Quadratic Stiffness Terms
f_n	Natural frequency (Hz)
Hz	Units of Hertz (1/second)
dB	Units of Decibels
m_0	Zero spectral moment
m_2	2^{nd} spectral moment
m_4	4^{th} spectral moment
N_{uc}	Number of upward zero crossings
N_p	Number of Peaks
ϕ	Eigenvector or Mode shape
ζ	Modal damping ratio
θ	Nonlinear stiffness terms
γ	Irregularity factor
ω	Circular frequency
σ	Standard Deviation

EXECUTIVE SUMMARY

Acoustic Fatigue is an important design consideration for high speed jet aircraft. High-intensity acoustic loading can cause nonlinear resonant response of aircraft structures. These acoustic loads often crack skins and substructure of aircraft. This fatigue cracking is due to the resonant bending response of lightly damped, stiffened skins exposed to extreme aeroacoustic environments. Cracks typically occur in minimum-gage structures like flaps, fairings, and leading and training edges. Repair of this nuisance cracking is costly. It has been estimated that the total repair cost of sonic fatigue cracking in USAF aircraft exceeds $20M/year, Ref. (1). Hence, there is a need for an accurate, efficient nonlinear prediction method to design acoustic fatigue resistant structures for use early in the design stage of aircraft development programs. These new methods will save life cycle costs due to repairs, and save weight by making airframe structure more efficient.

The objective of this program was the implementation and evaluation of a nonlinear reduced order modeling method applied to acoustic fatigue analysis of aircraft structure. The method was evaluated for its efficiency, practicality, and accuracy as compared to full-order explicit nonlinear transient response analysis. Three validation test cases are presented. The first is a simple curved beam. The curved beam results had previously been published in the open literature. This test case verified our implementation of the method. The second test case was of a curved unstiffened panel, which is representative of an actual aircraft panel. This test case was used to validate the efficiency of the reduced order method compared to full-order methods. The third test case was of an actual stiffened aircraft panel. This test case was used to validate the accuracy of the response and fatigue life predictions from the reduced order method compared to full-order methods and available test data. The general conclusion of the evaluations is that the reduced order method is a suitable and an efficient method for predicting acoustic fatigue of stiffened aircraft panels. Linear response methods have been shown to be lacking in accuracy to predict the correct magnitude or spatial distribution of stresses under high intensity acoustic loading. This provides the need for the nonlinear response methodology for acoustic fatigue design. However, existing full-order nonlinear response methods are complex and expensive to use. The reduced order method has been shown to have equivalent level of accuracy as the full-order methods for the test cases presented. The reduced order method is easily an order of magnitude more efficient in computation time than the full-order methods. The final recommendation from this program is that further spiral developments in methodology of the reduced order methods are warranted, and that further validation is required using a detailed aircraft structure design case.

1 INTRODUCTION

Next generation advanced aircraft will use high strength and lightweight materials that are designed to endure combinations of extreme thermal, static, and acoustic loading. These severe loadings can produce nonlinear structural behavior. To better evaluate potential designs, nonlinear finite element analysis methods need to be used to evaluate structures under these extreme loads. Current acoustic fatigue design methods are based on linear structural analysis with empirical corrections to account for nonlinear behavior. But, these linear analysis methods have been found to be conservative at best, resulting in over designed structures. At worst, these linear methods are inaccurate and not able to capture the correct magnitude or spatial distribution of internal loads and stresses in structures. Acoustic fatigue is an important design consideration for high speed jet aircraft where high-intensity acoustic loading can cause nonlinear resonant response of aircraft structures. Hence, there is a need for an accurate, efficient nonlinear prediction method to design acoustic fatigue resistant structures.

Acoustic fatigue is the dynamic loads problem most often encountered in-service especially on high performance aircraft. This was previously documented in Boeing's AVTIP Delivery Order No 27, "Identification of Dynamic Loads Problems and Solutions", Ref. (2). Although a large amount of effort is directed to sonic fatigue analysis during airframe development, a number of problems have historically appeared after aircraft are in service. In the past, design development analysis methods only considered the skin panels with idealized boundary conditions and plane wave excitation. The adjacent substructure was not included which not only affected the response through inaccurate modeling of boundary conditions, but often experienced failures itself. Based on experience, adequate analysis methods must include:

1. Spatially correlated loading with the proper coherence
2. Static pressure and thermal loads
3. Accurate boundary conditions and the adjacent substructure
4. Determination of the critical vibration modes, that are not necessarily the first or lowest frequency modes

Quick methods for predicting acoustic fatigue are in widespread use, and are relied upon because of schedule and cost constraints common to all programs, and because the methods were thought to be generally conservative. However, these quick methods are generally inaccurate for highly nonlinear acoustic response applications.

Linear response methods have always been used to analyze for acoustic fatigue, even today. In the late 1980's and early 1990's, the development of the hypersonic NASA/USAF National Aerospace Plane (NASP) Program presented new challenges for thermal-acoustic fatigue. The use of new materials, high temperatures, and very high acoustic loads meant that linear methods of analysis were no longer valid. Research was initiated in the area of nonlinear acoustic response analysis and performed as part of cooperative R&D programs with NASA-LaRC, Old Dominion University (ODU) and AFRL. Boeing implemented its first nonlinear response method (called TAPS, for Thermal Acoustic Post-buckled response of Structures) based on the method developed by James Locke (Ref. (3)), and a panel code called NRAP, Nonlinear

Response of Panels based on early work by Professor Chuh Mei, Ref. (4). In the mid 1990's, Boeing evaluated the NASA-LaRC Equivalent Linearization (EL) method which was implemented in NASTRAN using DMAP alters, Ref. (5). This research was primarily driven by the new requirements for High Speed Civil Transport (HSCT) and the High Speed Research (HSR) programs. Boeing worked with NASA on the development of new methods and test techniques for acoustic fatigue. In 2001, Boeing provided NASA-LaRC with an evaluation of the ELSTEP (Equivalent Linearization using a Stiffness Evaluation Procedure) method to assess its ease of use and accuracy. The method was used to predict strains in the Durability Patch test panel for which measured test data were available, Figure 1. This assessment discussed how the method operated, relayed some user experiences, and compared measured response to that predicted by the method. Although, the method was more accurate than the linear methods, it was in fact very difficult to use. There was a steep learning curve to the ELSTEP procedure. There are approximately 40 files to be generated and tracked throughout the process.

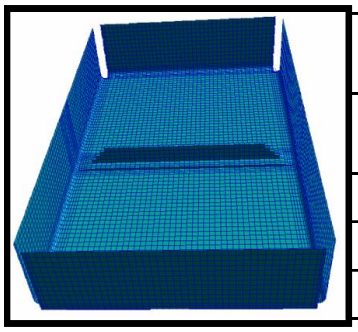

OASPL of Load	**Measured Strain**	**Predicted Strain** *nonlinear*		**Predicted Strain** *linear*	
dB re 0.0002 μbar	μin/in	μin/in	error	μin/in	error
165	956	848	-11%	2415	153%
156	472	476	0.8%	857	82%
144	165	186	13%	215	30%

Figure 1 - NASTRAN FEM and Results from the ELSTEP Evaluation

In the early 2000's Boeing developed new quasi-static nonlinear method (also referred to as the Nonlinear Miles method). This method was based on a quasi-static approach using MSC/NASTRAN. The method used the modal forces from a Solution 103 normal modes analysis as the basis for nonlinear static analysis in Solution 106. This method was essentially a single mode reduced order method similar to the Implicit Modal Condensation (IMC) Method, Ref. (6). The method has been applied with some accuracy on several acoustic response applications.

Analyzing for acoustic fatigue requires a good understanding of the variables used to perform the analysis. For instance, the input loads need to be well defined. The input loads can be a combination of acoustic (noise), structural vibration, shock, thermal, static pressure, or in-plane loads. It's important to understand the static response as well as the dynamic response. Some acoustic fatigue problems consist of high static loads with relatively low acoustic loading, where the acoustic loads alone would not cause fatigue. Static or thermal loads causing buckling instabilities in the presence of moderate to high acoustic loads have created cracking problems. Very high acoustic loads cause a majority of acoustic fatigue problems. Linear dynamic frequency response methods are inadequate for these problems; hence, there is a need for nonlinear reduced order methods that can be efficiently performed in a timely manner in a production environment.

The acoustic fatigue design process is shown in, Figure 2. In the early development phase of new aircraft, the first step in the acoustic fatigue design process is the definition of the internal and

external acoustic environment. If the aircraft is not a derivative aircraft, then the acoustic environment is defined using (a) measured data from similar aircraft, (b) empirical data, (c) wind tunnel testing, or (d) computational aeroacoustics (CAA). The second step in the process is to evaluate all structure in the affected high acoustic zones. This evaluation typically involves using simplified handbook or spreadsheet analysis methods. These methods are essentially quasi-static response methods that use RMS based fatigue approaches. Regardless of the method, the objective is to quickly screen a large portion of the aircraft for potential acoustic fatigue issues. The methods typically rely on conservative design requirements (i.e. adding 3.5dB to maximum expected acoustic loads, conservative s-N curves and structural Kt's, and 2x to 4x factor on Design Life requirements). This is meant to account for the uncertainty in the measured loads, s-N properties, and the modal damping. These methods are all linear in nature. In parallel with the analysis screening, there is a high cycle fatigue allowables test program to generate data for use with detailed finite element analysis.

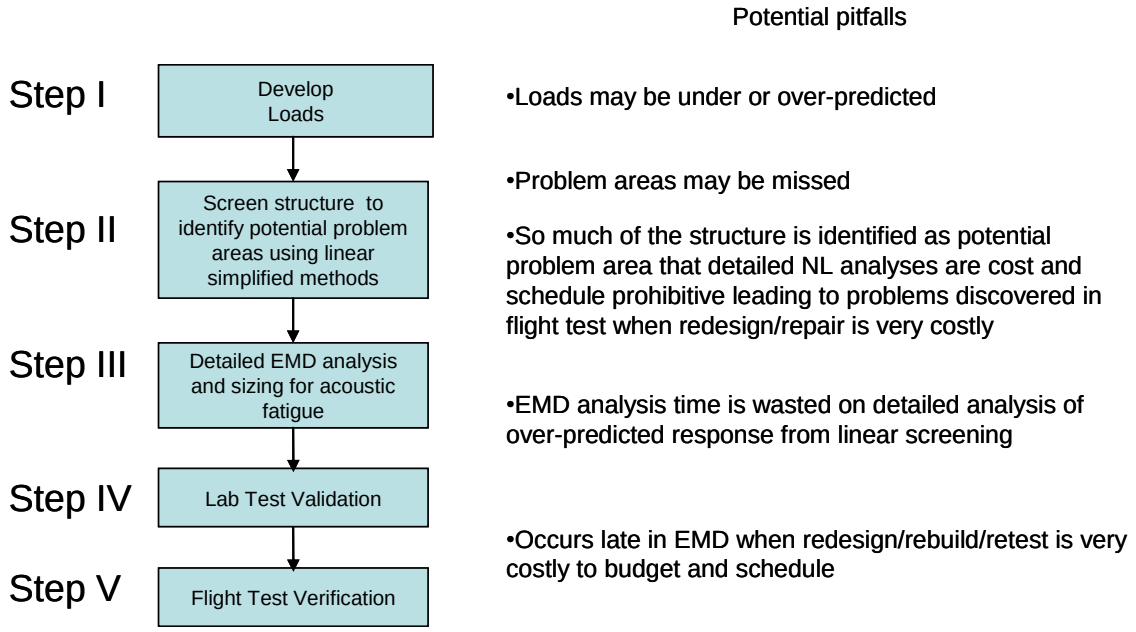

Figure 2 - Acoustic Fatigue Design Process

The third step in the process is to evaluate any structure determined to be critical in Step II. This evaluation most likely is a detailed linear random frequency response Finite Element Analysis (FEA) of the structure. This analysis process is used to finalize the design of the structure. This type of analysis is only performed on a few select critical panels. The effort involved in doing this type of analysis on a new development program is limited by cost, schedule, and availability of expertise.

The fourth step in the process is to validate the analysis in Step III, typically using acoustic chamber testing. This accelerated test will simulate the acoustic levels and durations expected in service. If the test article fails the validation test, then the process starts over with Step III. The fourth step validates the analysis process and design.

The fifth step is flight test validation of the preliminary acoustic design loads. The internal and external noise and vibration environment will be measured for the entire flight envelop and under realistic missions and flight maneuvers. These loads are stored in a database for retrieval and

comparison to the preliminary loads. If the loads from Step V are higher than expected, the acoustic fatigue design process could restart from Step II, if the loads are much higher over most of the aircraft, or at Step III, if only a few critical components are affected.

Acoustic fatigue problems that are caught during the development of an aircraft are not as costly because the changes can be incorporated during the on-going design activity, designs are not committed to production, and numbers of aircraft requiring retrofit are few or none. This process emphasizes the need for better structural dynamic response prediction, better loads prediction, and better fatigue life calculation methods. Problems caught after large numbers of aircraft are in service are very costly, and can cost over $100M over the life of the fleet, Ref. (2).

Even with a well-documented acoustic fatigue design process, there can always be unexpected fatigue problems. The cause of these fatigue problems varies, but a major reason is a screening (Step II) or detailed (Step III) analysis process that incorrectly predicted the response stresses and fatigue life. Linear response analysis methods are not always conservative in the prediction of stresses in the substructure. All analysis methods need models that can accurately predict the correct stress distribution within the structure. Acoustic fatigue typically occurs near the edge of a panel or in the attachment structure at a stress concentration (Kt) detail. These Kt details may be fastener holes, bend radii, machined steps, welds, etc. These allowables are random s-N curves of new materials (Kt=1, R=-1), and allowables of joints (bonded, bolted, welded, etc.) using a specimen as shown in Figure 3. Hence, a detailed FEA needs to model the structure accurately enough to be used with the allowables that are available. For instance, if there are joint allowables then the Finite Element Model (FEM) does not need to model the joint in detail, but it needs to predict accurately the reference stress (note: the reference stress is a stress near the failure point in a low stress gradient location that is easily predicted in an analysis model, and which coincides with the placement of the strain gages on the specimens). The model may also only need to predict the correct loads at a stress detail, and then a "break-out" model with internal (element, grid point or constraint) loads may be used to predict stress in the detailed part.

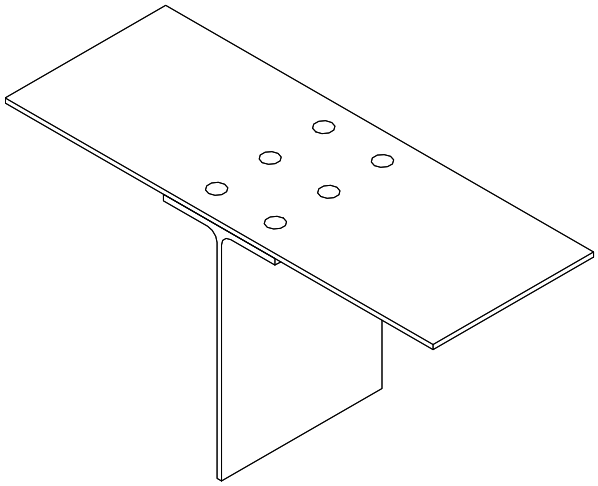

Figure 3 – Typical High Cycle Fatigue Joint Specimen

Another source of error in detailed dynamic response analysis is a model that does not correctly predict the stress and internal loads distribution due to nonlinearity. When a panel undergoes nonlinear membrane response, the linear normal mode response is no longer a good approximation of the internal stress and loads distribution. Membrane response has the effect of

increasing the loads transferred into the attachment structure. Therefore, although linear analysis may over predict response and appear to be conservative, it could in fact predict the incorrect stress distribution which leads to an incorrect fatigue prediction because the stress hot spot is missed. This is demonstrated in Figure 4. This is a simulation of the AFRL Durability Patch panel. The two analyses shown are a linear random frequency analysis, and the other is nonlinear reduced order method using two modes, both at an acoustic loading of OASPL=165dB. The figure clearly shows that linear random response methods can not be expected to accurately predict the correct internal distribution of loads and stresses. The nonlinear reduced order analysis correctly predicted the failure location and the magnitude of the measured RMS strain.

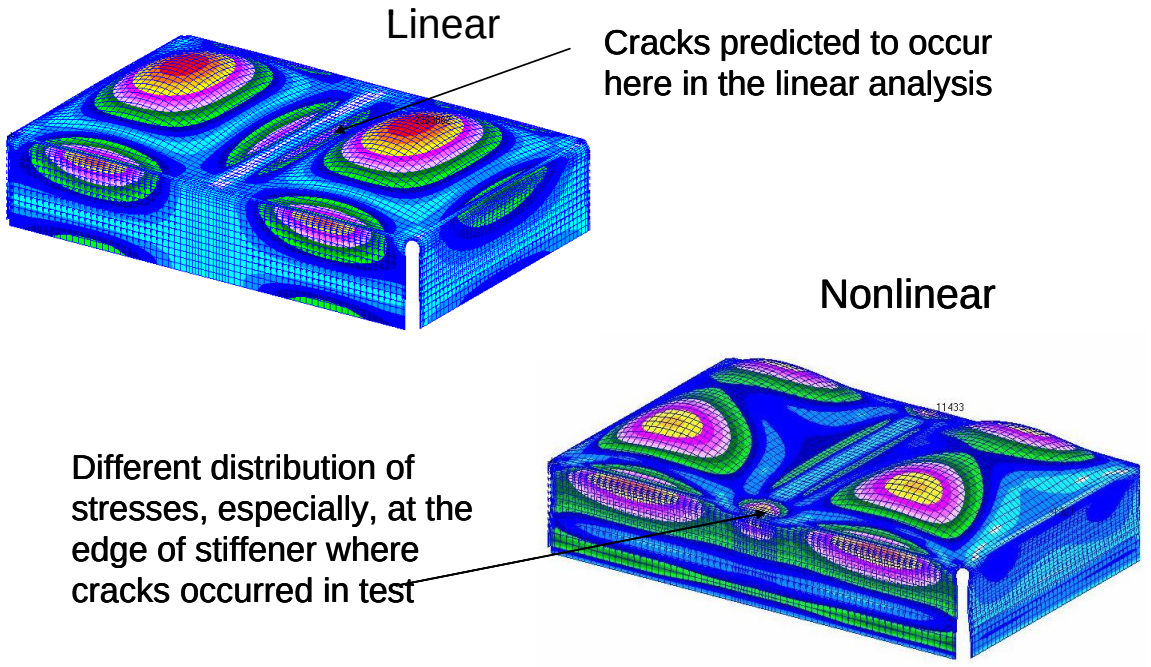

Figure 4 – Comparison of Linear and Nonlinear RMS stresses

This has been the case when large static loads are present which might be causing buckling or nonlinear static response. The presence of large static loads also affects the linear mode shapes and stress distribution.

These types of complex acoustic fatigue problems can only be analyzed using nonlinear geometric transient response analysis. Nonlinear response analysis can be a costly and time consuming analysis; especially, when a detailed FEM is used that may require a 100,000+ DOF to predict stress concentrations near holes, in shear clips, or in integrally machined multi-stepped flanges. The reduced order response approach should allow for larger models with more refined mesh in the fatigue critical details. The mesh density (and element size) limits the use of a full-order physical degree of freedom analysis, since the stable time integration step is dependent on the size of the smallest element in the model. The reduced order modal methods avoid this limitation.

High acoustic loading can come from many sources: engine near field noise, engine exhaust, separated turbulent boundary layer (TBL), shock waves, vortices generated from lift improvement devices, rocket thrust, and high rate gun fire, Figure 5. For acoustic fatigue

analysis, it's important to understand how the acoustic loads are distributed (amplitude) and correlated (phase) over the surfaces being analyzed. Some acoustic load sources are well correlated over a large area (vortex-sheet or explosive blast), while others are not correlated at all (high rate gun fire), and still others are considered partially correlated (or correlated over a small area such as a single panel) with the degree of correlation degrading with distance (separated flow, exhaust impinged flow).

Figure 5 - Acoustic Noise Sources

Another important aspect of the problem is the definition of the structural model. The boundary conditions of the model are very important. Many acoustic fatigue problems are actually in the substructure, so it's important to accurately model the substructure stiffness, since the stiffness is important in the development of nonlinear membrane response of thin skin panels. Hence, correctly modeling the substructure is vital to predicting the correct "Hot Spot" for acoustic fatigue. However, to accurately capture these details requires the use of large models that are not practical for full nonlinear analyses in a production engineering environment. This is another important reason why the reduced order method makes using nonlinear analysis tractable.

The damping of the structure is also an important variable. The damping comes from different sources, such as from the boundary conditions in the form of frictional damping, air pumping from high amplitude response, aerodynamic damping from high speed TBL or vortex flow, and material damping. All of these damping sources need to be accounted for in the acoustic fatigue analysis. For aeroacoustic applications, the aerodynamic damping (and mass and stiffness) can be best predicted using a coupled aeroelastic model (i.e. Solution 146 in MSC/NASTRAN.) Measured lab and flight damping levels in all types of metallic and composite structures, Figure 6, shows that the damping can vary considerably, Ref. (7).

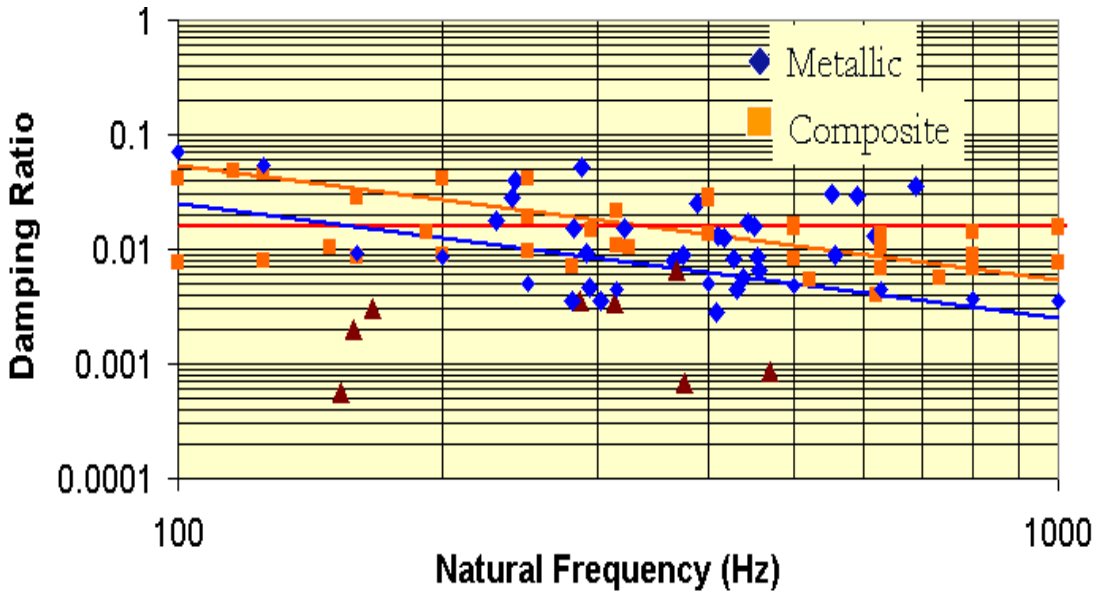

Figure 6 - Measured Damping Levels in all Types of Metallic and Composite Structures

Lastly, while predicting the correct acoustic response is very important the ultimate objective is correctly predicting the fatigue life. Acoustic response is a random amplitude high cycle fatigue problem. Most fatigue data is generated from round bar axial constant amplitude test data at very high loads and low cycles. It's important to understand how to correctly apply the available fatigue data to the nonlinear acoustic fatigue problem. Most linear acoustic fatigue problems use random amplitude RMS beam bending fatigue data, which is directly applicable to most acoustic fatigue problems. However, nonlinear problems use constant amplitude fatigue data and apply cycle counting fatigue methods.

2 METHODS, ASSUMPTIONS, AND PROCEDURES

2.1 Background on Reduced Order Modeling Methods

A linear finite element model produces a system of equations as shown in Eq. (1), where *x* is the time varying vector of nodal displacements; *M*, *C* and *K* are the linear mass, damping, and stiffness matrices. The vector, *f(t)*, represents the nodal force vector as a function of time.

$$[M]\{\ddot{x}(t)\}+[C]\{\dot{x}(t)\}+[K]\{x(t)\}=\{f(t)\} \quad (1)$$

The linear equations of motion can be uncoupled by transforming the physical coordinates, *x*, to modal coordinates, *p*, where *N* is the number of DOF in the finite element model.

$$\{x(t)\}=\sum_{i=1}^{N}\{\phi_i\}p_i(t) \quad (2)$$

Finite element models with a large number of degrees of freedom (DOF) can be reduced to a low order system of modal equations through a modal transformation. The normal mode shapes (eigenvectors), ϕ_i, are the basis vectors, and are computed from the eigenvalue solution of Eq. (1) when f(t)=0. The solution also produces the natural frequencies, ω_i. The mode shapes are scaled so that

$$\begin{aligned}\{\phi^T\}[M]\{\phi\}&=[I], \quad \{\phi^T\}[C]\{\phi\}=[\overline{C}]=diag(2\zeta_1\omega_1,2\zeta_2\omega_2,...2\zeta_n\omega_n)\\ \{\phi^T\}[K]\{\phi\}&=[\overline{K}]=diag(\omega_1,\omega_2,...\omega_N)\end{aligned} \quad (3)$$

Typically only a few modes are retained and the displacement vector is approximated.

$$[\overline{M}]\{\ddot{p}\}+[\overline{C}]\{\dot{p}\}+[\overline{K}]\{p\}=\{\phi^T\}\{f(t)\} \quad (4)$$

For a nonlinear problem, the equation for r^{th} arbitrary mode can be written where θ_r represents the nonlinear stiffness part of the model.

$$[\overline{M}]\{\ddot{p}_r\}+[\overline{C}_r]\{\dot{p}_r\}+[\overline{K}]\{p_r\}+\lfloor\theta_r(p_1,p_2,...p_N)\rfloor=\{\phi_r{}^T\}\{f(t)\} \quad (5)$$

The nonlinear modal equations differ from linear modal equations in that they are coupled through the nonlinear function. Typically for structural applications, the nonlinear function is approximated by quadratic and cubic terms. The general form of the nonlinear function is

$$\theta_r = \sum_{j=l}^{L}\sum_{k=j}^{L} B_r^{jk} p_j p_k + \sum_{j=l}^{L}\sum_{k=j}^{L}\sum_{l=k}^{L} A_r^{jkl} p_j p_k p_l \qquad 6$$

Note that only L modes have been retained in the modal expansion. The general form of the nonlinear function is where the quadratic coefficients, B_r, and the cubic coefficients, A_r, belong to the ‘‘rth’’ modal equation and have indices to denote which group of terms they multiply. The reduced-order system of nonlinear modal equations can be solved by direct time integration, and time histories of the modal displacements result. Time histories of physical displacements are computed from the nonlinear modal displacements.

The nonlinear stiffness terms are evaluated using applied modal load solutions (Ref. 2). First, generate a set of force vectors, $\{F_k\}$, as physically-scaled combinations of the modal basis vectors, and compute nonlinear static solutions for the set of forces,

$$\{w_k\} = \left(\left[K_{Lin}\right] + \left[K_q(w_k)\right] + \left[K_C(w_k)\right]\right)^{-1}\{F_k\} \qquad 7$$

Convert each $\{w_k\}$ and $\{F_k\}$ to the modal domain,

$$\{p_k\} = [\phi]^{-1}\{w_k\} \quad \{f_k\} = [\phi]^T\{F_k\} \qquad 8$$

Each modal equation has the form (only showing the cubic terms for clarity),

$$\ddot{p}_1 + \omega_1^2 p_1 + A_1^{111} p_1^3 + A_1^{112} p_1^2 p_2 + A_1^{122} p_1 p_2^2 + A_1^{222} p_2^3 = f_1 \qquad 9$$

Considering only the static response (ignoring the inertia term) and rearranging,

$$A_1^{111} p_1^3 + A_1^{112} p_1^2 p_2 + A_1^{122} p_1 p_2^2 + A_1^{222} p_2^3 = f_1 - \omega_1^2 p_1 \qquad 10$$

Considering all static modal load cases, a set of equations can be formed for each mode,

$$\begin{matrix}\text{Load Case 1}\\ \text{Load Case 2}\\ \\ \text{Load Case n}\end{matrix}\begin{pmatrix} {p_1}^3 & {p_1}^2 p_2 & p_1 {p_2}^2 & {p_2}^3 \\ {p_1}^3 & {p_1}^2 p_2 & p_1 {p_2}^2 & {p_2}^3 \\ \cdots & & & \\ {p_1}^3 & {p_1}^2 p_2 & p_1 {p_2}^2 & {p_2}^3 \end{pmatrix} \begin{Bmatrix} {A_1}^{111} \\ {A_1}^{112} \\ {A_1}^{122} \\ {A_1}^{222} \end{Bmatrix} = \begin{Bmatrix} f_1 - {\omega_1}^2 p_1 \\ f_1 - {\omega_1}^2 p_1 \\ \cdots \\ f_1 - {\omega_1}^2 p_1 \end{Bmatrix} \qquad 11$$

This set of equations can then be solved using least squares for the nonlinear coefficients. These coefficients are then substituted back into nonlinear modal equation, Eq. (5). This nonlinear

modal equation is then solved using direct time integration. For the time integration, the model has the form below (for a two mode example),

$$\begin{Bmatrix} \ddot{p}_1 \\ \ddot{p}_2 \end{Bmatrix} + \begin{pmatrix} 2\zeta_1\omega_1 & 0 \\ 0 & 2\zeta_2\omega_2 \end{pmatrix} \begin{Bmatrix} \dot{p}_1 \\ \dot{p}_2 \end{Bmatrix} + \begin{pmatrix} \omega_1{}^2 & 0 \\ 0 & \omega_2{}^2 \end{pmatrix} \begin{Bmatrix} p_1 \\ p_2 \end{Bmatrix} + \begin{pmatrix} A_1{}^{111} & A_1{}^{112} A_1{}^{122} A_1{}^{222} \\ A_2{}^{111} & A_2{}^{112} A_2{}^{122} A_2{}^{222} \end{pmatrix} \begin{Bmatrix} p_1{}^3 \\ p_1{}^2 p_2 \\ p_1 p_2{}^2 \\ p_2{}^3 \end{Bmatrix} = \begin{Bmatrix} f_1(t) \\ f_2(t) \end{Bmatrix} \tag{12}$$

The modal transformation is then used to calculate the physical displacements. Nodal response quantities like velocity and acceleration can easily be calculated. But other response quantities like element stress, strain, or internal loads, are calculated in the original FEM. The physical displacements are used as enforced displacements to calculate the element stresses and loads. This operation can be performed on an element by element basis or on the whole model.

Note, only the bending modes are retained in the modal basis set. Nonlinear static load solutions obtained through finite element analysis are used in the estimation process. The effects of membrane stretching on the bending displacements are contained in the static cases and are incorporated into the estimated nonlinear terms for the bending modes. That is, the effects of stretching are implicitly condensed into the nonlinear terms of the bending mode equations. This approach has been referred to as the Implicit Modal Condensation (IMC) method, Ref. (6).

Modal bending amplitudes are computed directly from integrating the model in the method. Physical bending displacements can then be computed from the modal amplitudes, however physical membrane displacements cannot be obtained. As a result, linear membrane stresses and strains which depend on membrane displacements cannot be recovered using the finite element strain-displacement equations. An expansion process is sought to expand the modal bending amplitudes into membrane displacements.

The process requires a transformation matrix or membrane basis set. A procedure was developed to estimate the membrane basis set from the static nonlinear solutions. This process is referred to as the Implicit Modal Condensation Method with Expansion (ICE), Ref. (9). For this program, we only implemented the IMC. But, for some applications, particularly those where the structure is very flat, then the ICE method is required to accurately predict membrane strains.

2.2 Implementation of the NLROM Method

We chose to implement the method based on MSC/NASTRAN commercial finite element analysis software. This implementation required writing a Matlab interface that could read and write results to and from NASTRAN bulk data and output (punch) files. Matlab was then used as the primary tool for computation of the nonlinear stiffness coefficients, the integration of the nonlinear modal equations, and for the computation of the inverse transformation of the results back to physical coordinates. The Matlab interface is also used to setup element stress post-processing operations.

The process just described is called the Implicit Modal Condensation (IMC) method, as described in Ref.s (9) thru (15). The entire simulation procedure is shown in the Figure 7. First,

a finite element model is developed in PATRAN, and linear static (SOL 101) is run to get the applied load nodal forces. Then, the normal mode solution (SOL 103) is calculated in NASTRAN. The mode shapes, frequency table, and grid point force balance is output. The grid point forces are a linear scalar of the eigenvectors. These loads cases are then used in the nonlinear static solutions (SOL 106).

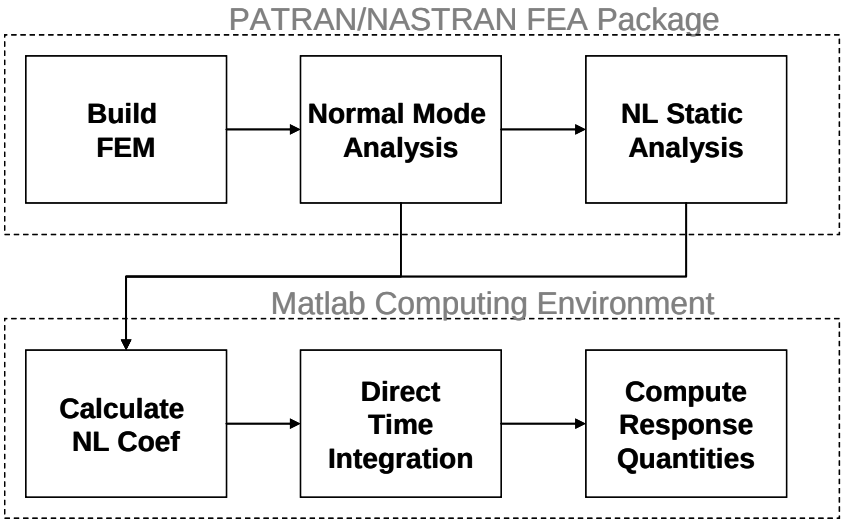

Figure 7 – NLROM Simulation Procedure, modified from Ref. (2)

The first step is to setup the FEM with the acoustic excitation load cases. This is done in PATRAN using the Load/BCs menu. The acoustic loading is defined as a distributed pressure loading over the face of CQUAD4 elements. This is demonstrated for the curved aluminum beam. The beam is 18 inch long by 1 inch wide, 0.09 inch thick, and with an 81 inch radius of curvature. The acoustic loading is defined as two uncorrelated pressure load cases, as shown in Figure 8. These are unit pressure loads, 1 psi. This step is required in order to get the nodal distribution of the applied loads for the modal response calculation. The easiest way to get these nodal forces is by setting up a linear static solution (SOL 101), and requesting the applied loading at the nodes, OLOAD = ALL. A sample SOL 101 input deck is shown in Appendix – Linear Static Model Setup.

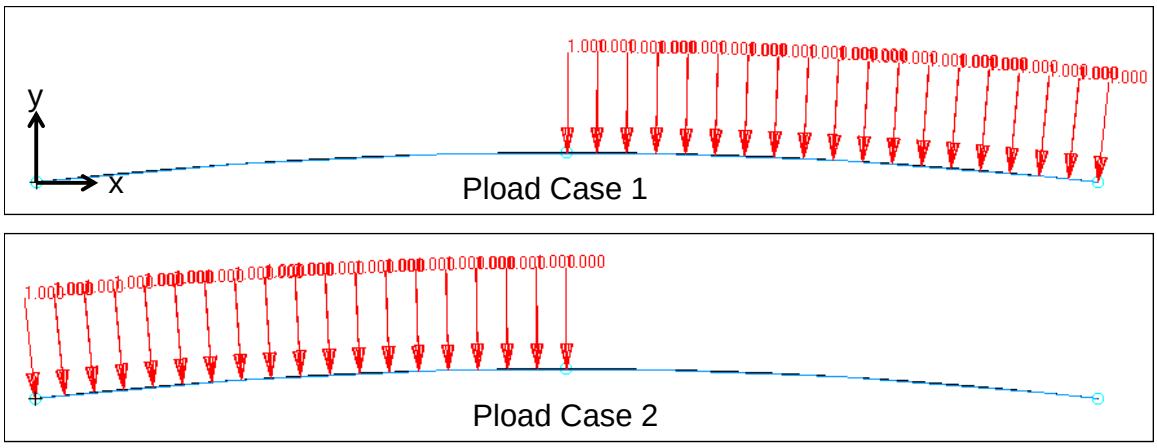

Figure 8 – Acoustic Pressure Load Cases

The next step is the setup and solution of the linear normal mode solution (SOL 103). From this solution, the eigenvectors (VECTOR = ALL), frequencies (eigenvalues), and the grid point forces (GPFORCES=ALL) are requested in the CASE CONTROL. The eigenvectors and frequencies are used in the modal transient response solution and in the evaluation of the nonlinear stiffness coefficients. The grid point forces are used in the nonlinear (modal) static solutions. The grid point forces are a linear combination of the eigenvectors, and represent the internal loads in the model, if the eigenvector was a static deflection shape. The eigenvectors are mass normalized. This is set on the EIGRL card.

```
EIGRL    1       0.      1500.          0                       MASS
```

This is the initial setup process, and it is shown in Figure 9. A sample SOL 103 input deck is shown in Appendix – Linear Modal Solution Setup. The next step is the determination of the nonlinear stiffness coefficients.

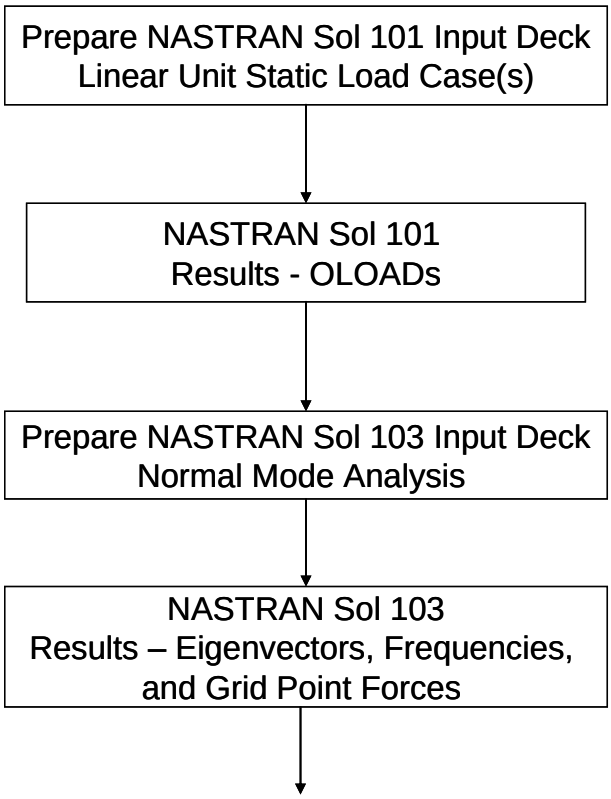

Figure 9 – Model Setup Steps

The number of static solutions is dependent on the number of modes. A one mode solution requires two static solutions, two modes require eight static solutions, three modes require 26 static solutions, and four modes require 64 static solutions, and so on. The number of nonlinear static solutions is given by the combination formula.

$$\binom{n}{K} = \frac{n!}{k!(n-k)!} \qquad 13$$

The total number of nonlinear static analysis is then,

$$\text{Total Number Of NL Static Solution} = \binom{n}{1} \times 2^1 + \binom{n}{2} \times 2^2 + \binom{n}{3} \times 2^3 \qquad 14$$

A sample SOL 106 input deck is shown in Appendix – Nonlinear Static Solution Setup.

The first term in Eq. 14 represents the one mode solution, the second term the two mode combination solutions and the third term all of the three mode combination solutions. The process only requires up to three mode combination solution in order to calculate the coupled cubic nonlinear coefficients. For example, the load cases for the 3-mode model are shown below in Figure 10. These nonlinear static load cases are scaled combinations of the modal vectors, where c_1, c_2, and c_3, are scale factors to modal (grid point force) vectors (1, 2, and 3 respectively). The load scalars are chosen such that the nonlinear static solution results in physically appropriate displacements. In other words, the response has to be nonlinear in order to accurately determine the nonlinear stiffness coefficients.

	load cases												
	1	2	3	4	5	6	7	8	9	10	11	12	13
mode 1	c_1	0	0	c_1	c_1	0	c_1	c_1	0	c_1	$-c_1$	c_1	c_1
mode 2	0	c_2	0	c_2	0	c_2	$-c_2$	0	c_2	c_2	c_2	$-c_2$	c_2
mode 3	0	0	c_3	0	c_3	c_3	0	$-c_3$	$-c_3$	c_3	c_3	c_3	$-c_3$
	14	15	16	17	18	19	20	21	22	23	24	25	26
mode 1	$-c_1$	$-c_1$	c_1	$-c_1$	$-c_1$	0	0	$-c_1$	$-c_1$	0	$-c_1$	$-c_1$	0
mode 2	$-c_2$	c_2	$-c_2$	$-c_2$	0	$-c_2$	0	c_2	0	$-c_2$	$-c_2$	0	$-c_2$
mode 3	c_3	$-c_3$	$-c_3$	$-c_3$	0	0	$-c_3$	0	c_3	c_3	0	$-c_3$	$-c_3$

Figure 10 – Sample 3-mode problem with 26 static load cases, Ref. (8)

Note that for each mode, there is a positive and negative loading condition. This allows for fitting of the nonlinear stiffness coefficients thru the entire range of structural motion. For instance consider the one mode case or load cases 1 and 18 above. Isolating these two load cases, the deflections and loads are output from the nonlinear solutions and the modal forces are calculated using Eq. 8. These modal forces and deflections are then plotted in the Figure 11. In the figure, there are five data points used to fit the nonlinear stiffness coefficients. Note the solution is forced thru an intercept of zero, which is the trivial zero load case. A cubic polynomial is used to fit the load-deflection curve, and the three constants are the A_1^{111}, B_1^{11}, and K_1. These constants are fairly close to those found in Ref. (8). Note, the frequency of this mode is f_n=258.4 Hz, and $f_n = (1/2\pi)*(K_1/M_1)^{0.5}$, where M_1=1.0, mass normalized. This is the general process that is used to calculate the nonlinear modal stiffness coefficient. The process for getting the nonlinear modal terms is fairly straight forward, however, selecting the correct static load scalars and keeping the best modes for the modal solution is critical.

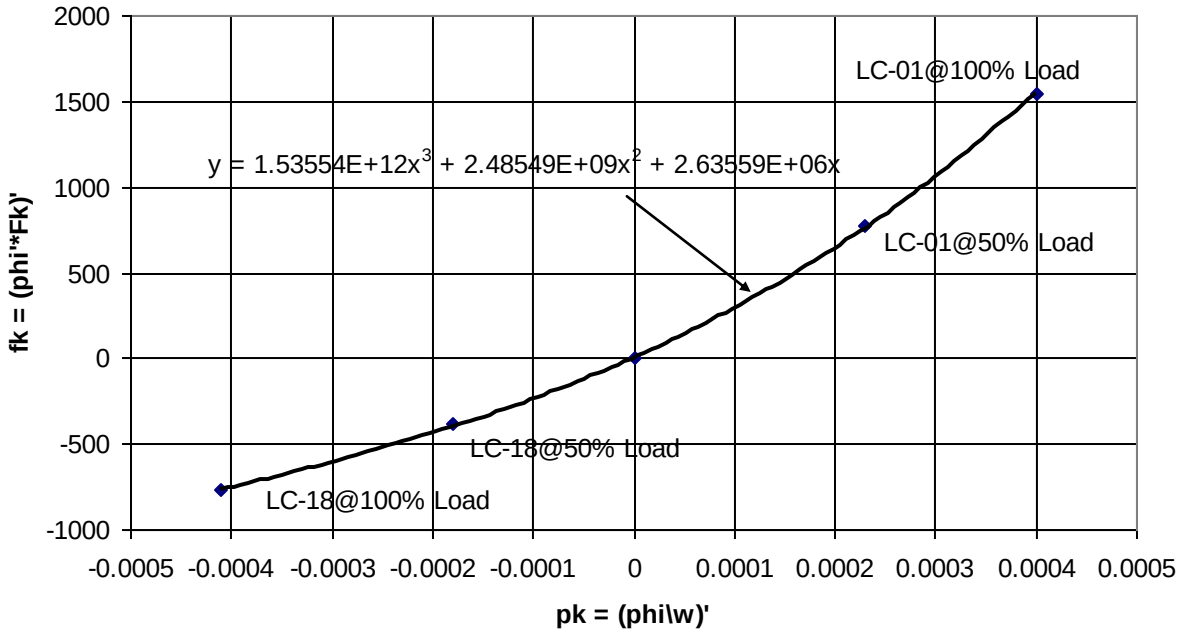

Figure 11 – Curved Beam Nonlinear Static (Modal) Results for Mode 2, only

The nonlinear static load case scalars can be approximated. As a rule of thumb, a thin shell structure will start to under go nonlinear deformation when the deflection is ½ of the thickness. At one times the thickness the structure is nonlinear and at twice it's very nonlinear, and the membrane stiffening effects should be significant. So, we can use this as a guide for making an initial selection of the scalars. Since, the grid point forces are used to generate the load cases, and these are based on mass normalized eigenvectors. The 2*thickness divided by the max value of the mass normalized eigenvector is the approximated scale factor.

$$c_1 = \frac{2t}{|\phi_{\max}|} \qquad 15$$

For the above curved beam test case, the thickness is t=0.09 inch, and the max mass normalized eigenvector was ϕ_{max} = 102. This yields a c_1 = 0.0018. For this analysis, c_1 = 0.002 and $-c_1$ = 0.0004. Note the scalar was not the same for the positive and negative load cases. This is because the beam would snap thru (buckle) under the higher load value in the negative load case. It has not been determined if this is beneficial to the overall accuracy of the NLROM solution, but in general it's assumed that the static solutions are not allowed to buckle, since this would invalidate the cubic polynomial least squares fit of the nonlinear modal stiffness coefficients.

A few things to consider when setting up the nonlinear static solutions:

The load scalars are not arbitrary, and need to produce physically significant deflection results. The loads should not produce a buckled shape. But, they should produce nonlinear deflections,

otherwise, the cubic (hardening) and quadratic (softening) nonlinear stiffness terms will not be correct.

Curved structure, like this beam, is highly sensitive to snap-thru on the negative loading. The snap-thru response is shown in Figure 12. The intermediate results for the nonlinear solution is shown for a modal load scalar of c_1=-0.002. At 40% of this load, the model is snapping thru. The solid curve is the cubic polynomial fit, which is obviously not a good approximation.

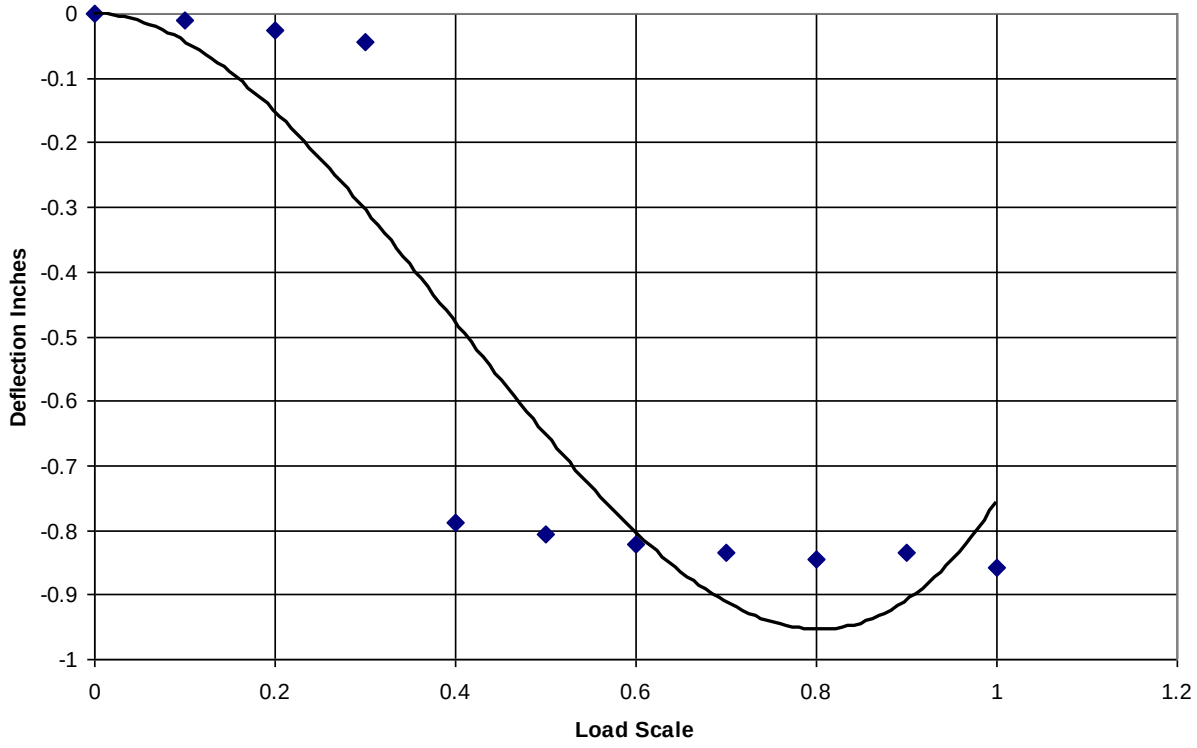

Figure 12 – Nonlinear Static Analysis of Mode-1 Loads (Snap-thru Analysis)

The selection of the nonlinear static load scalars can be an iterative process. The user needs to be prepared for this and not initially select a lot of modes for the solution. It's best to select only the primary modal contributors first, and tweak the scalars for the modes. For the higher order modes, the load scalars can usually be set at much lower values. The nonlinear hardening and softening effects seems to diminish with increasing modal order, or at least this effect is less important. Typically, the level of acoustic energy decreases with frequency for most aero-acoustic fatigue applications. Hence, for the higher order modes, there doesn't seem to be much shifting in natural frequencies or peak broadening. This is based on observed test data, which will be presented in this report.

Also, the higher order modal combination load cases typically produce solution convergence problems if the load scalars are too high. It's possible to go into the input deck and change the troubling load cases on an individual basis, but if you're running a 20 mode solution which requires 9920 combination loads cases, then this can be a daunting task. Hence, it seems best to just set the higher mode scalars at a single lower value that won't produce any solution problems.

This seems best as long as those modes don't significantly contribute to the overall critical stress response.

The general rule of thumb found in this study is that the primary modal contributors should produce deflections up to one to two times the thickness, and the higher order modes can be much less but at least half the thickness.

2.3 Matlab User Interface – NLROM

The NLROM method is not a standard analysis procedure in any commercial FE code. Hence, the calculation of the nonlinear stiffness terms and the integration needs to take place outside of any standard analysis package. We chose to use Matlab for our primary computation tool because it's easy to develop a graphical user interface, matrix calculations are easily programmed, and the nonlinear equations are conveniently solved using Matlab ODE solver. The following describes the NLROM Matlab Tool that was used to perform all of the studies described in this report.

As previously mentioned MSC/NASTRAN was selected as the structural analysis code that would be the basis for the model. NASTRAN was chosen because it is our most widely used structural analysis tool, and it's our standard method for performing acoustic response calculations. ABAQUS was also considered. ABAQUS is our standard nonlinear structural analysis tool, and is primarily used for nonlinear transient response calculations. But, since we didn't require these aspects of ABAQUS, we went with a tool that has the widest base of use in NASTRAN.

The setup for the Linear Static and Normal Mode Solutions of the NASTRAN model are done in PATRAN. The models (bulk data files, or *.bdf) can be run using PATRAN's Analysis Manager or by running the NASTRAN windows executable program. The second option can be performed in the Matlab tool.

Below is a screen shot of the NLROM Tool, Figure 13. The tool was written for Matlab R2007b. There are MEX files compiled with the script. These MEX files are C++ programs that perform certain I/O functions. The script is generic and runs on most versions of Matlab, but the C++ functions need to be recompiled using the user MEX utility.

There are four different functions to the Matlab tool: (1) Model I/O and Solution, (2) ODE Solution, (3) Nodal Response Post-Processing, and (4) Element Post-Processing Setup. These operations will be explained as they pertain to the evaluation process.

First, there is the linear model solutions and results I/O, Figure 14. As previously mentioned, these models are setup in PATRAN, but they can be submitted to NASTRAN from this tool. This is just for convenience. But more importantly, the PUNCH results from NASTRAN are scanned and the results are read into Matlab.

At this point, the linear modal transient response can be calculated and nodal or element post-processing can be performed. On the interface, we can select a range of modes or just a list of modes, and also a prescribed modal damping ratio, Figure 15. It's important to understand what the linear response is before running the nonlinear response, Figure 16. From the linear response, we can quickly estimate the critical modes to the structural response. This aids in the selection of modes to use in the nonlinear solution. This doesn't guarantee the best selection of modes but it does yield a good first estimate. Also, we get an initial estimate of the response, which we can compare to the nonlinear solution.

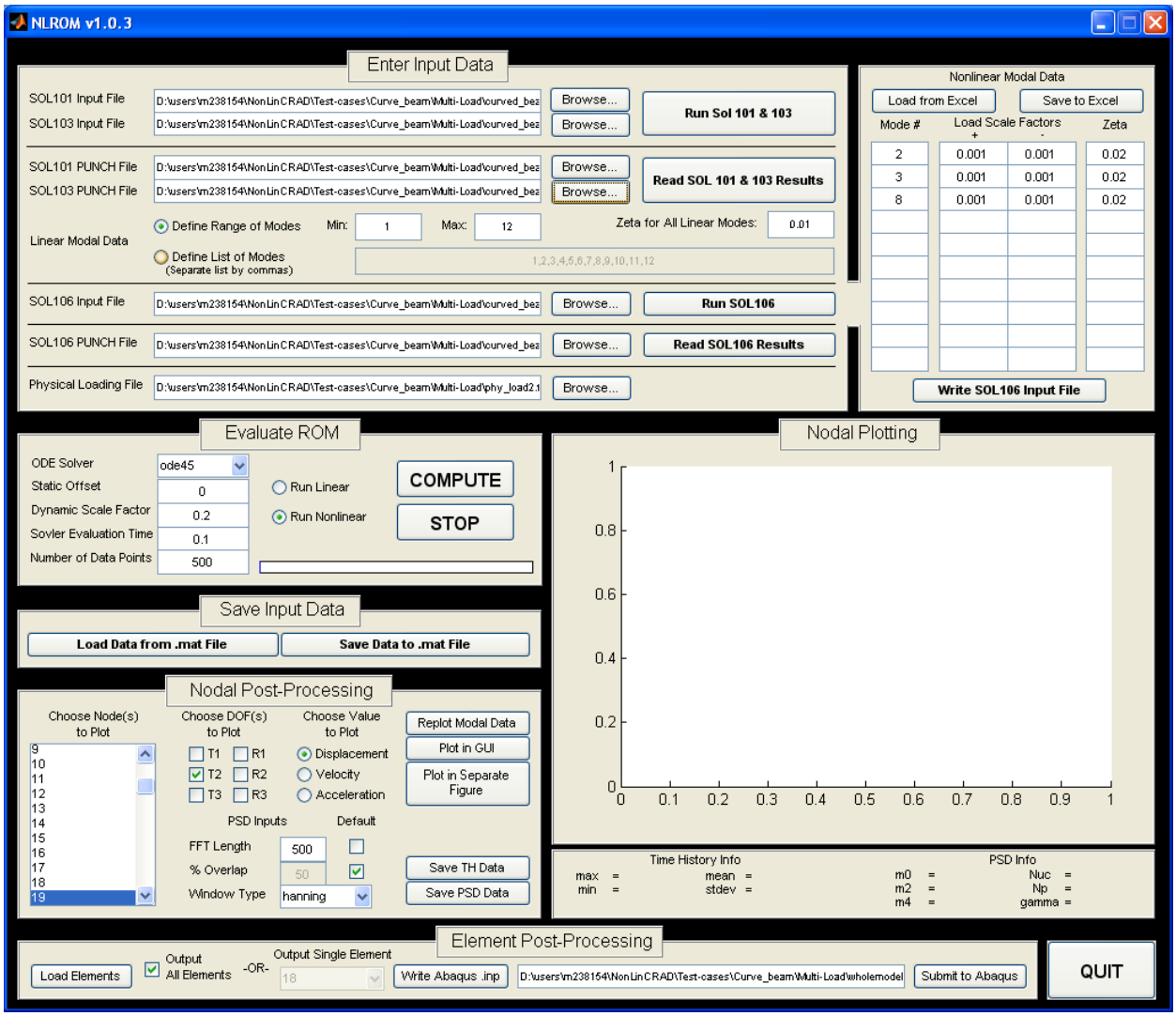

Figure 13 – Matlab Tool – NLROM

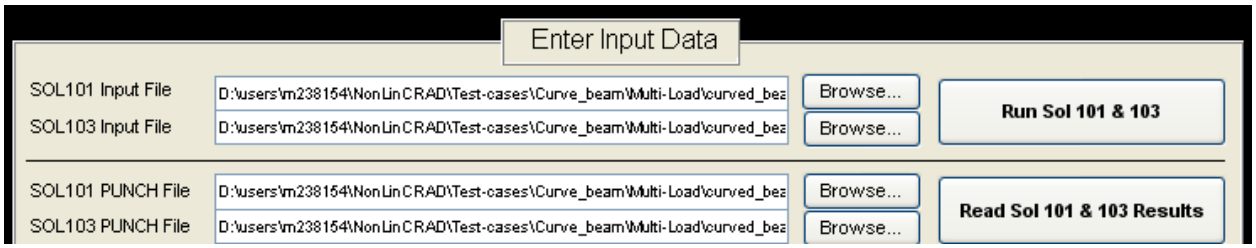

Figure 14 – Model Solution and Results Input

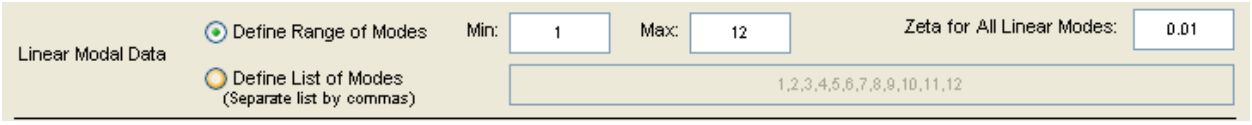

Figure 15 – Selection of Linear Modes

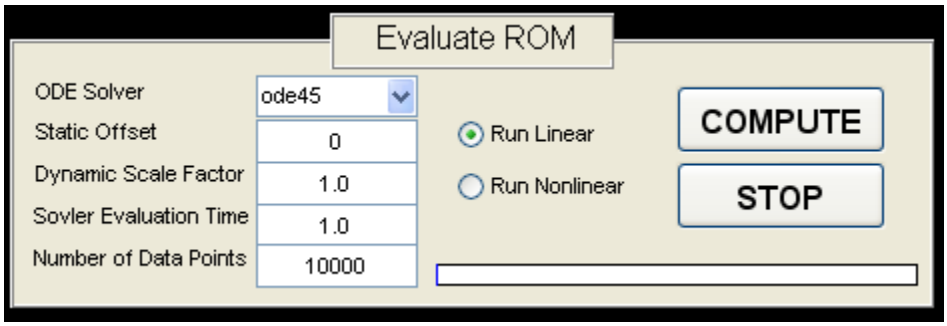

Figure 16 – Evaluate Linear Response

The next step is selecting the modes and setting up the nonlinear static solutions, Figure 17. This is easily performed in the interface. The mode numbers, their scale factors (+ and -), and the modal damping ratio is listed in the table. Matlab sets up the NASTRAN SOL 106 model. This is a huge time saver. This could be done in PATRAN, but it would be a very tedious and error prone process. The Matlab script writes out all of the modal load cases combinations. The tool is currently limited to 10 mode solutions, and this is just because it doesn't seem practical to run thousands of nonlinear static solutions. The user can submit the job from the interface. This submits the job locally on the same machine. Or, the user can submit the job to a network computer cluster outside of the Matlab tool. But once the solution has completed, the user reads the displacement results back into Matlab. The script also calculated the nonlinear modal stiffness terms (A's and B's), and it's ready to perform the ODE solution. A key result that comes out of the nonlinear static solution is the max displacements for each load case. These results are output to an ASCII file. The user can quickly scan this file and determine if the nonlinear solutions produced structural significant displacements.

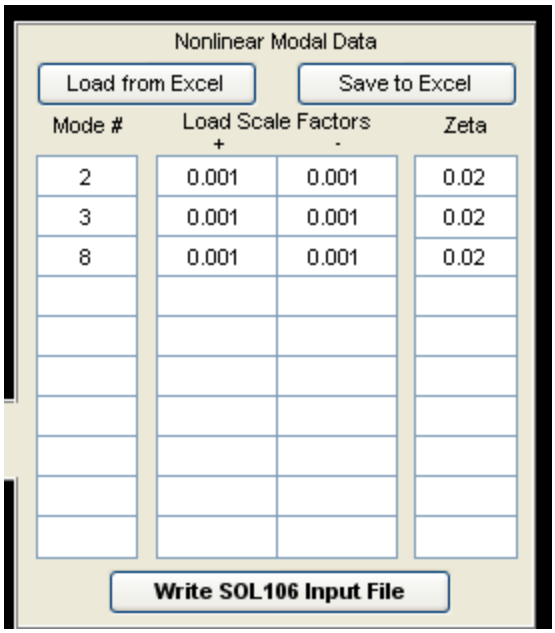

Figure 17 – Nonlinear Static Solution Setup

Once the ODE solution has been performed, the user can perform post-processing of node results (Displacement, Velocity, and Acceleration) for any Node and DOF in the model, Figure 18. The physical results are displayed as a time history and a PSD. The time history statistics (Min, Max, Mean, and Standard Deviation of the time history) and PSD statistics (m_0, m_2, m_4, N_{uc}, N_p, and γ) are also given, Figure 19. The statistics m_0, m_2, and m_4 are zero, second, and fourth spectral moments, respectively. These are calculated using the WAFO routine, spec2mom. N_{uc} and N_p are the number of upward zero-crossings, and number of peaks, respectively. Gamma, γ, is the irregularity factor. A $\gamma = 1$ means that for every valley there is a corresponding peak. A sine wave or narrow band signal would produce a γ=1.0. If $\gamma < 0.5$, then the signal is a wide band process. If it's close to zero, then its broad band white noise process. Being able to post-process the nodal results interactively is a great asset. This allows the user to quickly scan thru displacement response to make sure the solution seems reasonable. It's entirely possible at this point that the user might want to rerun the nonlinear modal static solutions, and formulate a different nonlinear modal model with different modes or based on different scalars.

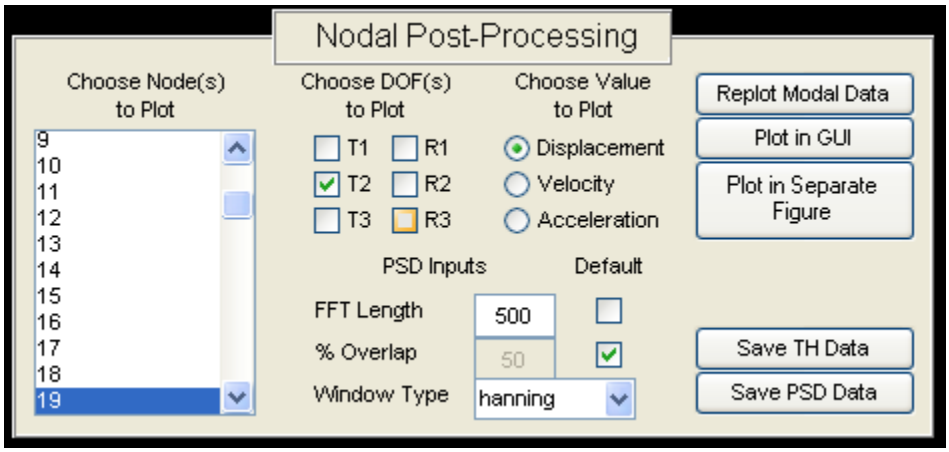

Figure 18 – Nodal Results Interactive Post-Processing

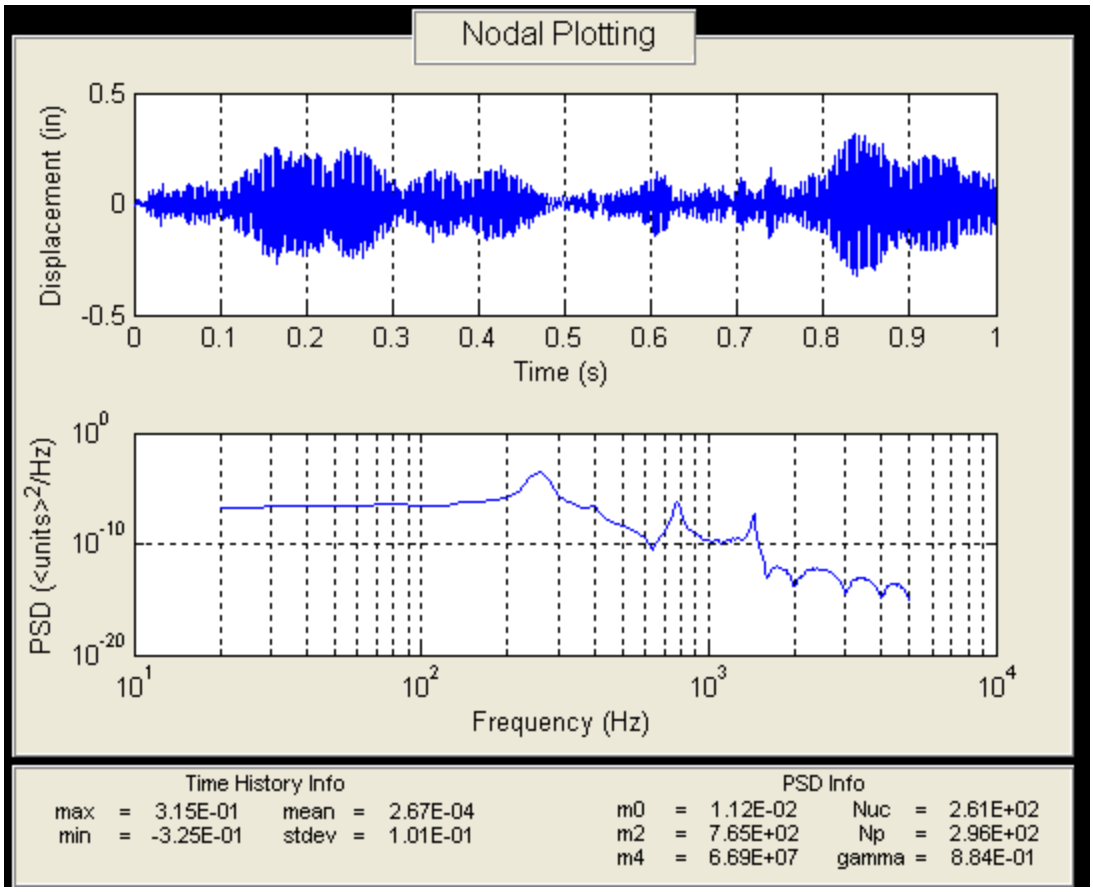

Figure 19 – Nodal Post-Processing

The final step is to post-process the element results, Figure 20. From the NLROM tool, the user has two options. The first option is to output displacement time histories for every DOF attached to a single element. This sets up an explicit time integration solution in ABAQUS. The nodal displacement time histories are applied as enforced displacement boundary conditions. ABAQUS was chosen for its convenience of setting up this type of problem. NLROM reads the SOL 101 model, and extracts out the selected element grid point and grid point coordinates. Also, the material properties, and shell properties are also read into Matlab, and output to the ABAQUS model. The second option is to output whole model results. The method uses the original modal grid point forces, and the nonlinear static load cases. Based on the modal response, RMS response is calculated for each mode to the applied acoustic loading. When the SOL 106 model was run, the script found the translation DOF that gave the highest response. The script then calculates the time history response for these same translational DOF. These become a reference to scale the modal load cases. The script then sets up a new SOL 106 model, with new RMS based scale factors. The user would run this model and review the results in PATRAN. The model would yield useful information related to distribution and magnitude of the stress, strains, and loads in the model. These results are not used for the fatigue calculation, but more for pin-pointing the critical stress hot spots. After post-processing the whole model results, the analyst should then post-process this critical element(s) time history solution. The final step is to take the element stress time history and calculate the fatigue life.

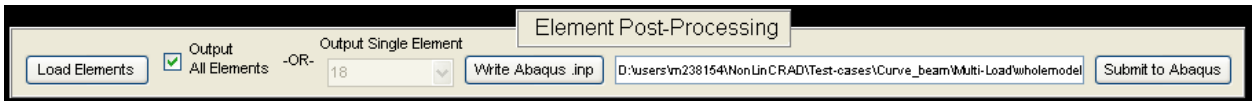

Figure 20 – Element Results Post-Processing

There are other features to the NLROM tool that are very useful, Figure 21. The first is being able to save the current Matlab matrices in a database. This allows the user to reload this database later to auto-fill in all of the enter information and model results. The second feature is being able to scale the acoustic loading without having to generate a new loading file. A static offset can also be added to the loads. Shown in the figure, the integration parameters Solver Time, and number of output points can be controlled. Also, any of Matlab's ODE solvers can be chosen. This is useful if one solver is having numerical difficulties.

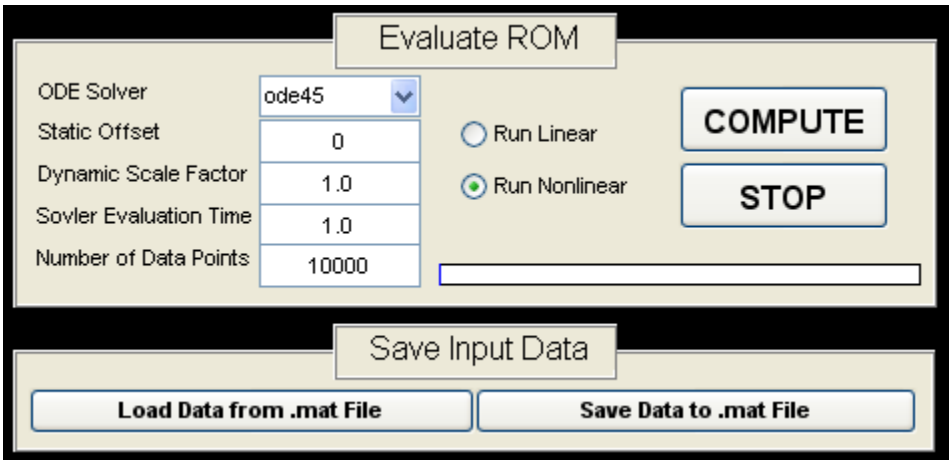

Figure 21 – Additional NLROM Script Features

2.4 General Acoustic Fatigue Analysis Process

In this section, the process for using the NLROM method is described. There are several steps that are common between the linear random frequency response solution, the nonlinear full-order solution, and the reduced order solution. This includes building the FEM, defining the acoustic loading, and performing the fatigue calculations. The primary goal is to predict fatigue life. This requires calculating element stress time histories. The problem with nonlinear analysis is that the critical stress location is not necessarily known a priori. Random transient response solutions require extensive memory if all element stress components time histories is to be output. So usually, only a small set of critical elements and nodes are included in the output request sets.

The process starts with the Model Checkout phase, as shown in Figure 22. These are the common steps between the linear methods and nonlinear reduced order methods. The analyst starts by developing the FEM. Then, the acoustic load case is defined (i.e. apply the pressure). Then, the normal mode and unit linear static pressure runs are performed. This is part of the standard analysis process. Here the analyst is checking for the rigid body modes, checking the model mass, checking the loads, etc. The analyst may also check static and modal element stresses and nodal displacements. The element stresses are scaled to the mode shapes, but it is

useful to determine which elements will have the highest stresses for selected modes. Similarly, the unit static pressure (which is the acoustic load condition(s)), also yield information about which elements might have the highest response when the nonlinear transient response is run. Therefore, this process is performed first, and it determines which modes might be important and which reference results from elements and nodes need to be reviewed during the nonlinear analysis.

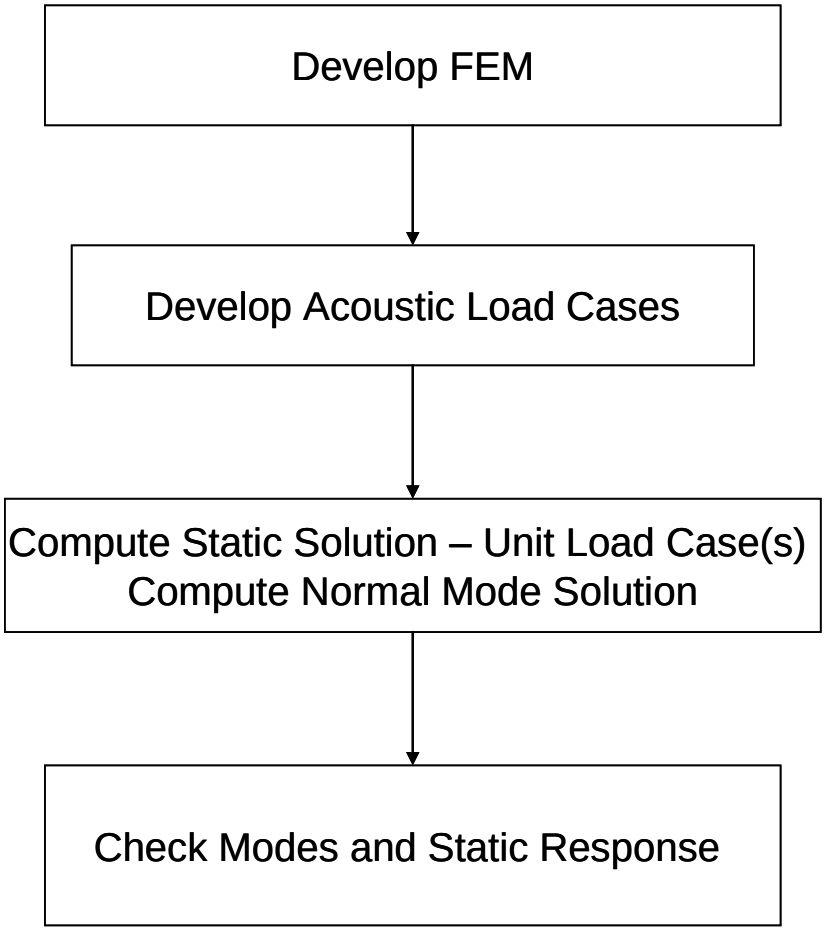

Figure 22 – Model Check-out Process

Once the unit static and normal modes solutions have run, then the analyst selections modes that will be with in the frequency range of the acoustic excitation. Then, before setting up the NLROM, the analyst performs a linear modal transient response solution, Figure 23. This step runs the linear modal transient response with the actual acoustic load condition(s). From these results, the analyst can better determine the modes to use for the nonlinear analysis. The user has selected reference nodes and elements based on the linear normal mode solution. They will review the linear nodal displacements and element stresses at these previously identified reference locations.

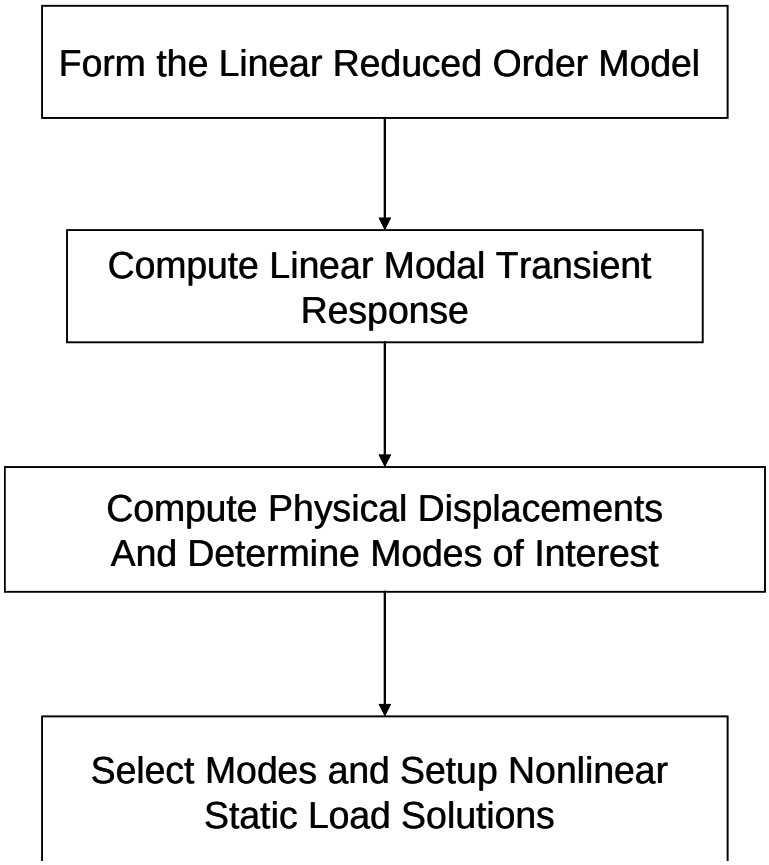

Figure 23 – Linear Modal Response – Pre-NLROM Process

The next steps in the process are to setup and run the nonlinear response, Figure 24. First, the analyst runs the nonlinear static solutions and calculates the nonlinear stiffness terms. Then, the analyst computes the nonlinear modal transient response. The analyst will then review the displacement (or accelerations) at the reference nodes. Based on the modal response, the analyst then selects elements to post-process for the stress time history. The analyst may also elect to review the nonlinear static solutions that were run to get the nonlinear stiffness terms. The analyst needs to scale these results to the max or RMS modal displacement based on the nonlinear response. From these results, the analyst can also determine or verify the elements initially selected for the element output reference set. The analyst performs the post-processing analysis, output the element stress time histories, and then performs the fatigue analysis. The process repeats for each element that's part of the reference set.

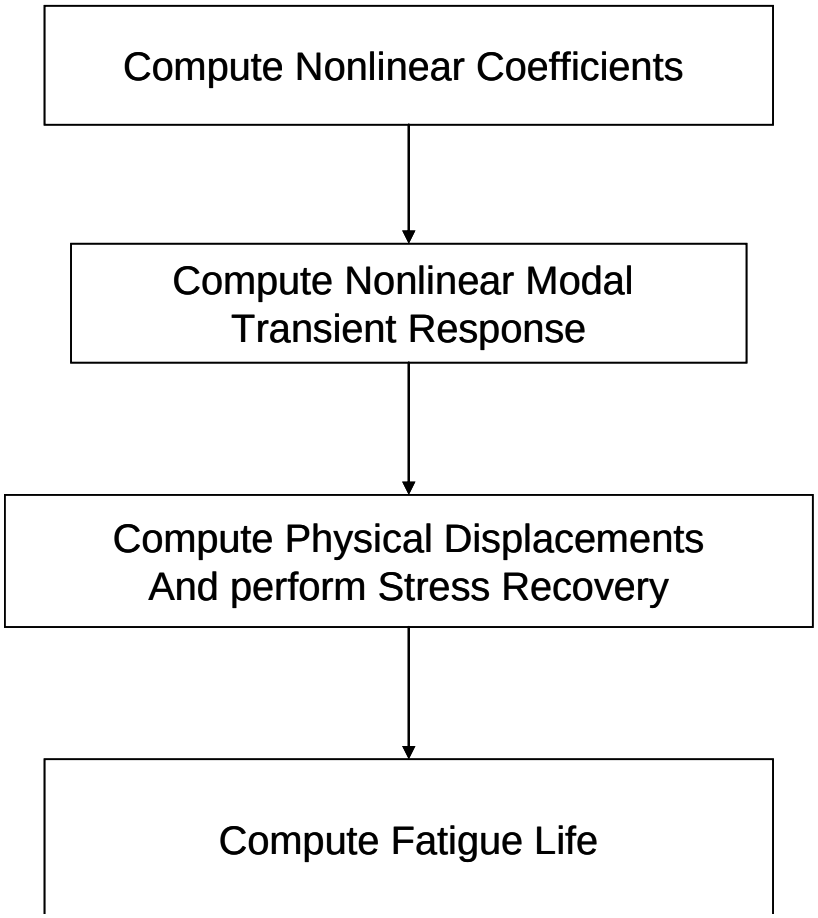

Figure 24 – NLROM Analysis Process

3 RESULTS AND DISCUSSION

In this section there are three test cases described. The first is a clamped-clamped curved beam. This beam are previously been studied in the open literature. This test case was used to verify our implementation of the NLROM method. The second test case was a simply-supported curved panel. This test case was used to validate the efficiency of method. The third test case was a stiffened aircraft panel. This test case was used to validate the accuracy of the method as compared to linear reduced order response methods and to nonlinear full-order response methods. Finally, this last test case was used to demonstrate the practically of using the method in a design study.

The list of accuracy and practicality criteria includes:

- Accuracy of predicted response, such as strain, deflection, and acceleration in terms of max levels, average levels, RMS levels, range and amplitude distributions, zero crossing frequency, peak frequency, and higher moment statistics of distributions
- Accuracy of predicted fatigue life based on time history spectra, RMS levels and zero crossing frequency
- Efficiency and practicality of use, which includes benchmarking CPU usage, model development requirements, user interaction, and user expertise level

3.1 Verification Test Case – Curved Beam

The first verification test case is the clamped-clamped curved beam, Figure 25. The beam is 0.09 inches thick with aluminum material properties. The curved beam test case has been previously studied in Ref.s (10) and (14). The properties of the beam are aluminum and the boundary conditions are clamped-clamped. The acoustic pressure loading is a flat excitation spectrum from 0 to 1500Hz. The applied pressure is assumed to be fully correlated. The spectrum is adjusted for different rms levels (0.23 psi, 0.46 psi, 0.65 psi, and 0.92 psi), as consistent with the above references. The finite element model has 74 nodes, and 36 quad elements. The load is applied as two uniform load cases over each half of the beam. The input files for the beam test case can be found in the Appendices of this report. The first 12 modes are shown in Figure 26.

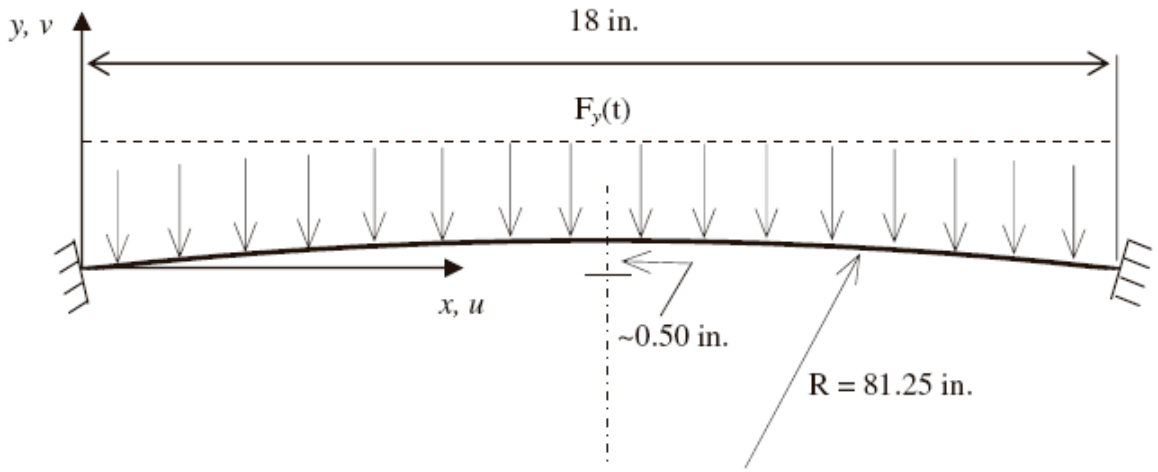

Figure 25 – Geometry of Curved Beam

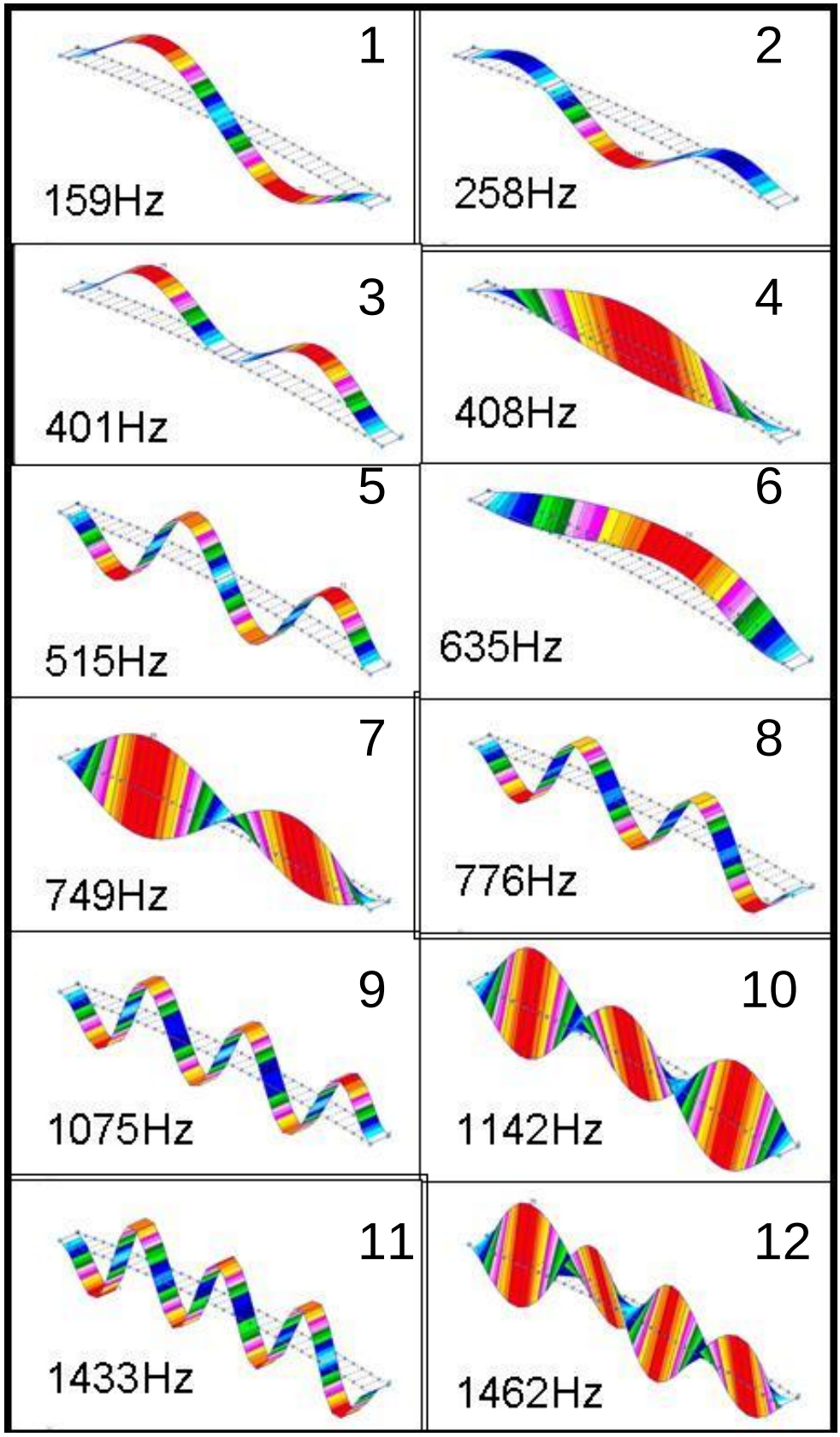

Figure 26 – Curved Beam Mode Shapes

First, we want to verify the model. This is easily accomplished by applying a unit static load (a constant 1-psi from 0 sec to 2 sec) to the model and comparing the reduced order response to the full-order linear and nonlinear static analysis. In Figure 27, the static deflection shape is shown. The static deflection is the steady-state deflection at the end of the 2 second time simulation. This is shown for both linear and the nonlinear full-order static analysis. Next, we compare the reduced order linear model compared to the full-order, Figure 28. The comparison of the nonlinear deflection shapes are shown in Figure 29 and Figure 30, for out-of-plane and in-plane translational degree of freedom, respectively. Both reduced order models used the first 7 bending modes. These plots show that the reduced order models capture the correct linear and nonlinear static stiffness characteristics. Next, the dynamic characteristics will be verified.

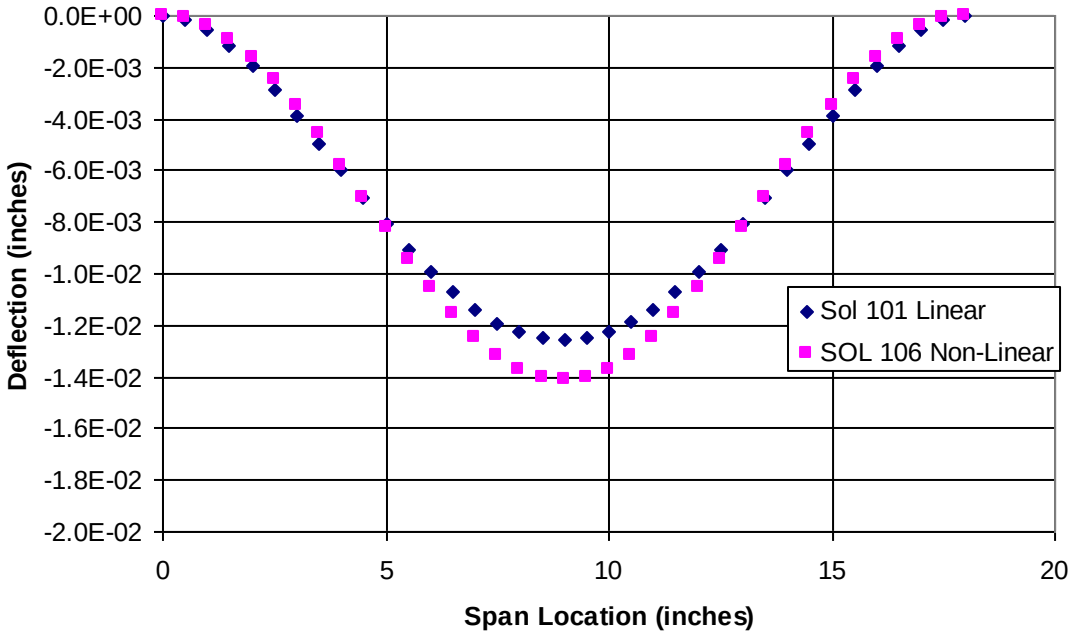

Figure 27 – Compare NASTRAN Full-Order Linear and Nonlinear Static Deflections

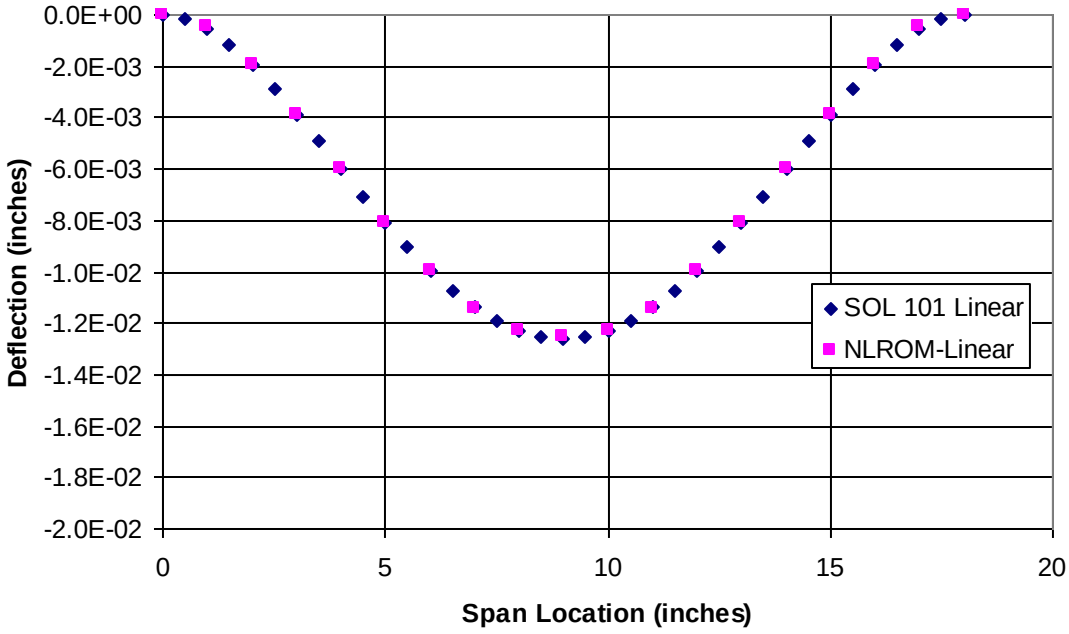

Figure 28 – Compare the Linear ROM to the Linear Full-order model

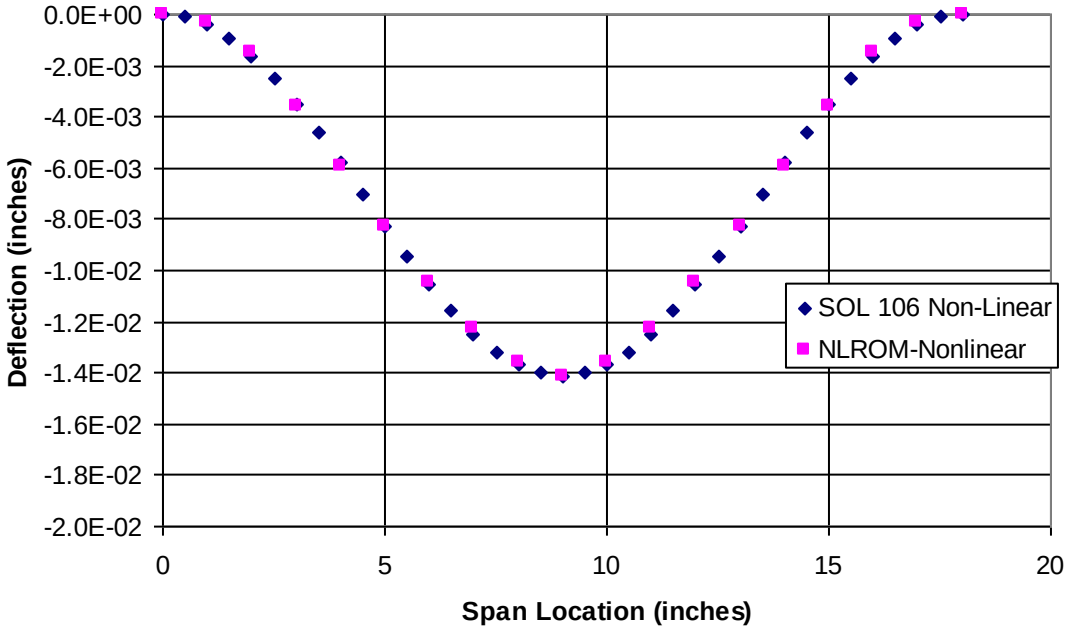

Figure 29 - Compare the Nonlinear ROM to the Nonlinear Full-order model

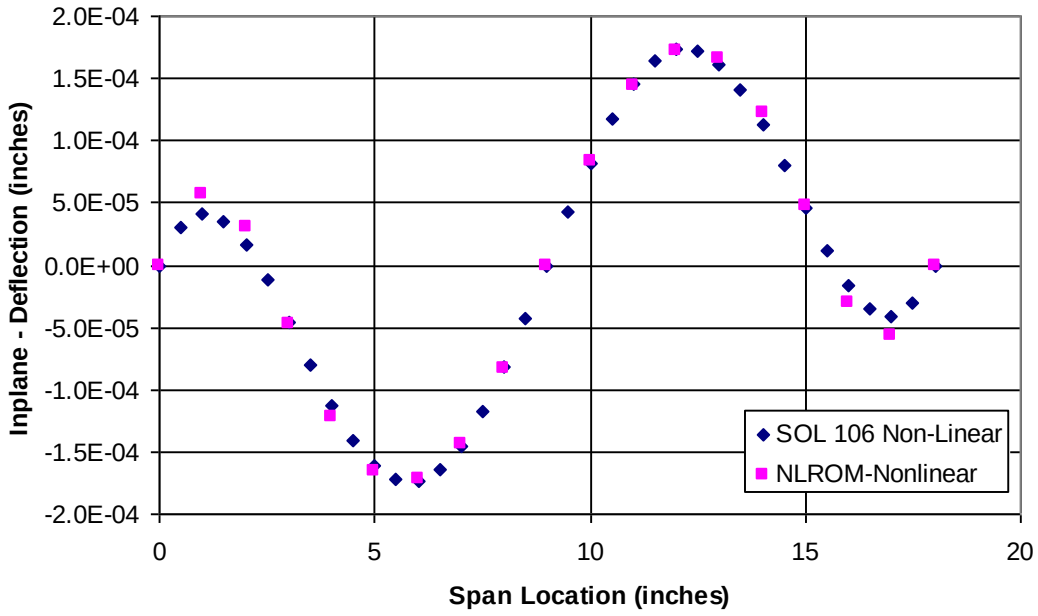

Figure 30 –Compare the Nonlinear ROM to the Nonlinear Full-order model

For the response comparison, the mid and quarter span vertical displacements are calculated for comparison to full-order integration method. The full-order integration method uses Abaqus/Explicit analysis. The reduced-order and full-order analysis use a similar model of 36 linear quads. For the full-order analysis, the model was run for 2 seconds and 64000 output history time intervals. Both mass and stiffness proportional damping (e.g. mass proportional, *Damping, ALPHA=64, where Alpha=$2*\zeta*\omega_n$) is used. The explicit integration took 3 minutes to solve with mass proportional damping, and 55 minutes with the stiffness proportional damping. The implicit analysis took 1 hr and 55 minutes for the same 2 second simulation. All times are for a single processor Dell Workstation.

For this test case, the RanStep analysis was also run, Ref. (17), using the same NASTRAN model, and assuming only three symmetric modes in that analysis for comparison. The results for the IMC, RanStep, and Abaqus/Explicit analysis are shown in Figure 31. The IMC NLROM method compares well to the Abaqus/Explicit analysis. The RanStep analysis was run with only bending modes for comparison. Also, the NLROM analysis was run at different magnitudes of loading from Prms = 0.23 to 0.92 psi. The results are in Figure 32. At the highest loading 0.92psi, the model is starting to snap-thru, as seen in the time history plot, Figure 33. The Abaqus analysis also shows slight snap-thru, Figure 34.

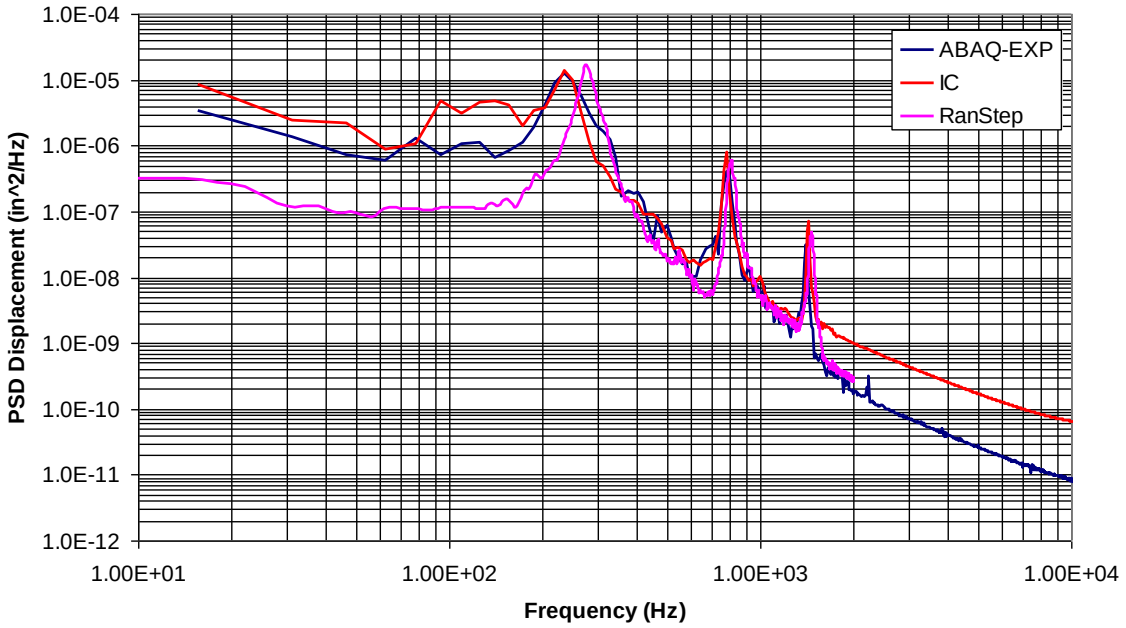

Figure 31 – Vertical Displacement, Prms=0.92psi, 3-Modes, Alpha=64., T=2secs

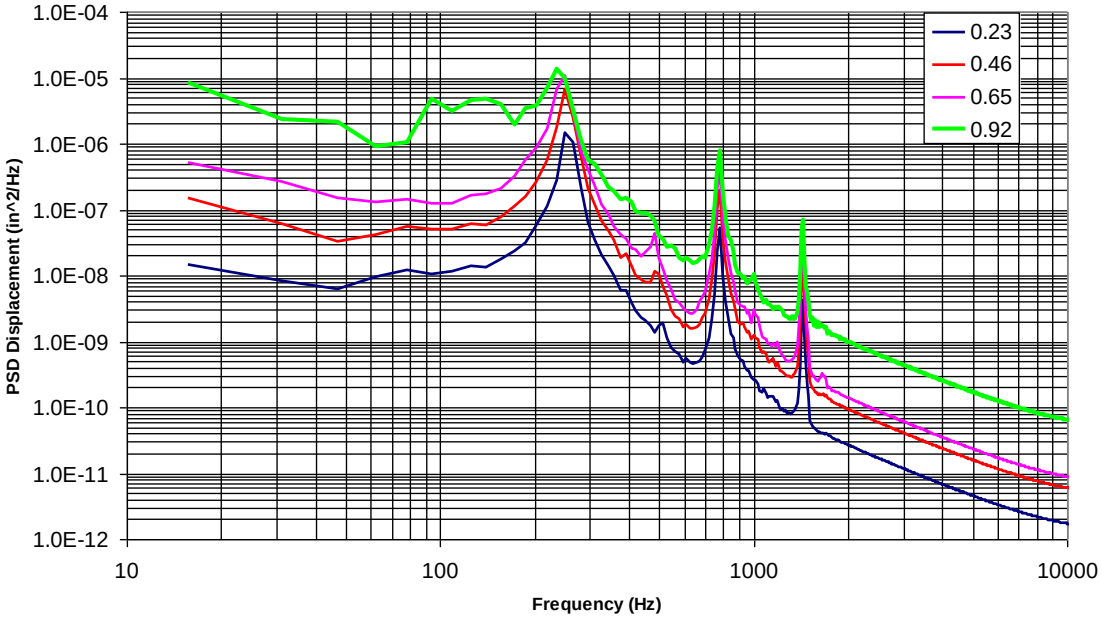

Figure 32 – Vertical Displacement, NLROM-IC analysis, 3-Modes, Alpha=64, T=2secs

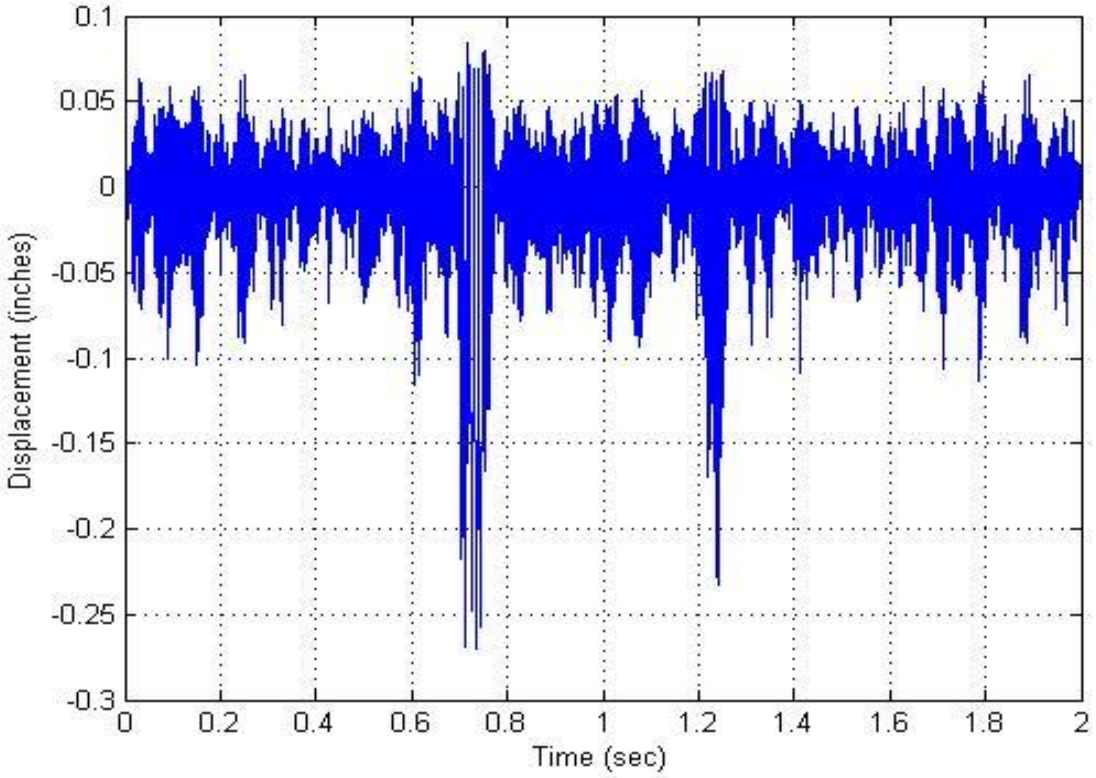

Figure 33 – Mid-Span Vertical Displacement at Prms=0.92psi (NLROM-IC)

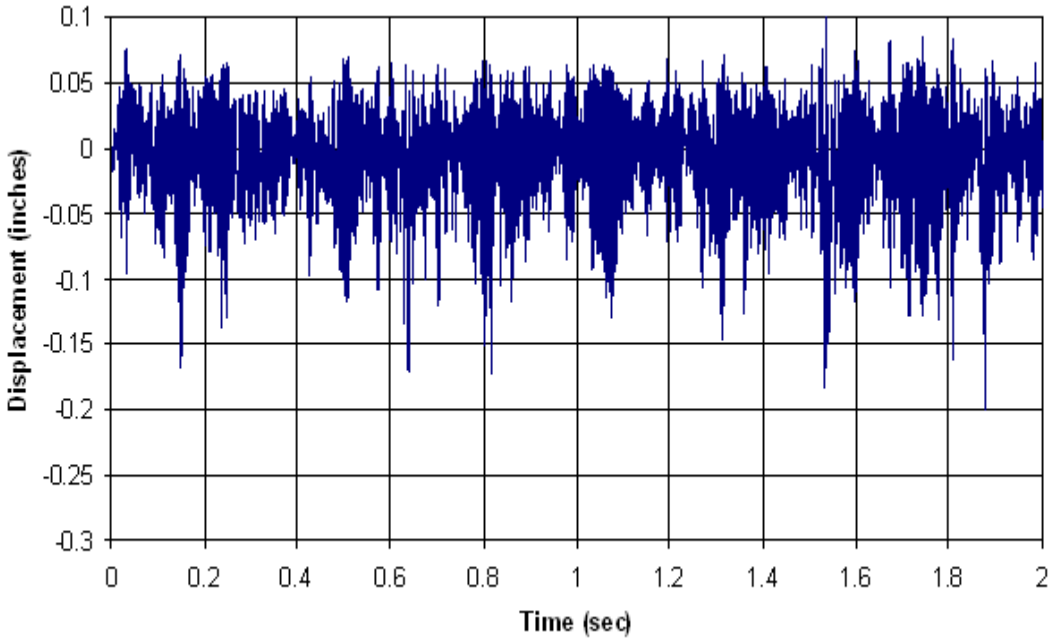

Figure 34 – Mid-Span Vertical Displacement at Prms=0.92psi (ABAQUS-Explicit)

The following is a demonstration that verifies the use of higher-order and asymmetric modes in the model. For the above study, the acoustic loading was fully-correlated, meaning the acoustic

loading time history was the same for both load cases, as shown in Figure 8. For this study, the Modes 1, 2, 3, 5, 8, 9, and 11 were selected. The loading is defined as two load cases that each covers half of the beam. In the first case, the loads are correlated, and in the second case the loads are uncorrelated. First, the linear modal response results are presented below. In Figure 35, the two different load conditions are shown for the mid-span response. There is little difference in the response (same peak frequencies); although, the correlated response is slightly higher. In Figure 36, the quarter span response shows how the asymmetric modes get excited in the uncorrelated loading condition but not the correlated loading condition.

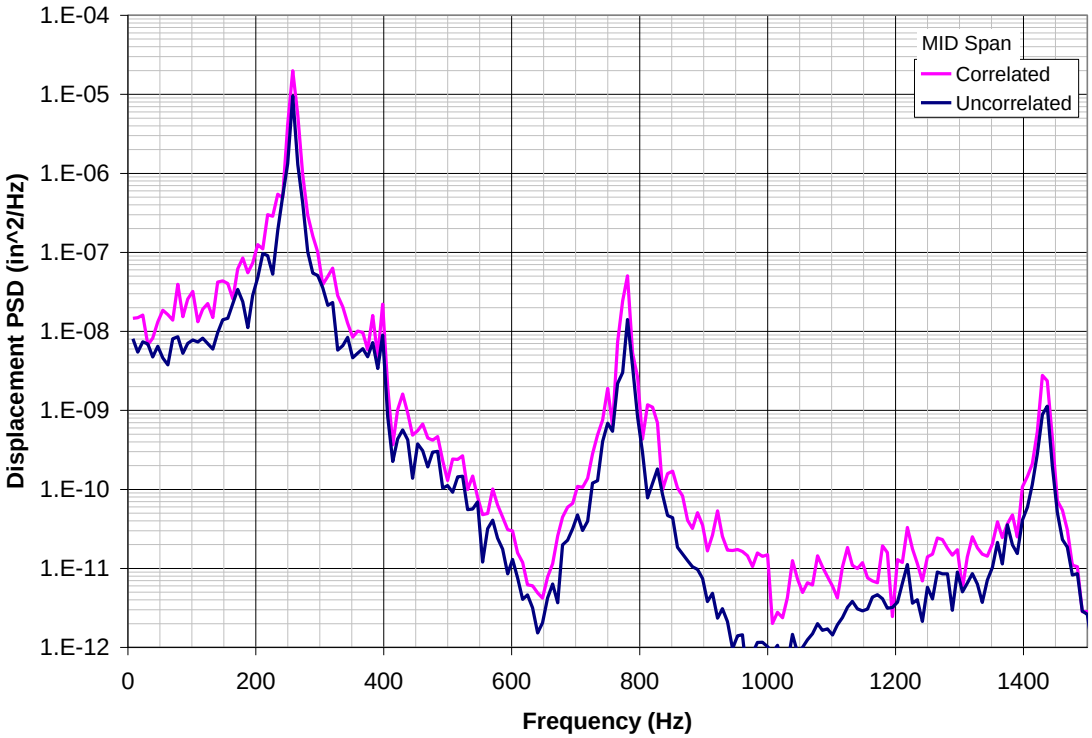

Figure 35 – Linear Mid Span Vertical Displacement Response

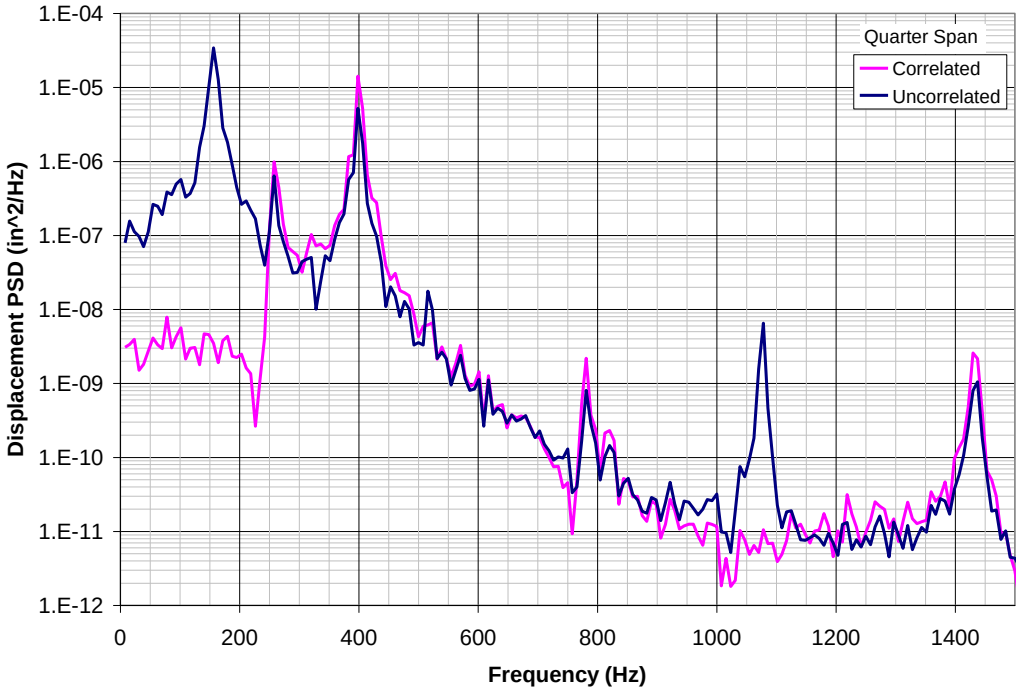

Figure 36 – Linear Quarter Span Vertical Displacement Response

Next, the nonlinear reduced order response is shown for the quarter span location, Figure 37. In this case the correlated loading also excites the asymmetric modes included in the model. This highlights the importance of including symmetric as well as asymmetric modes in the response. In this case, the asymmetric mode is the lowest mode, and there is significant response in this mode. In most separated flow applications, the acoustic loading is fairly uncorrelated over the surface of the skin. The phasing of the loading is significantly influenced by the convection velocity of the propagating noise source.

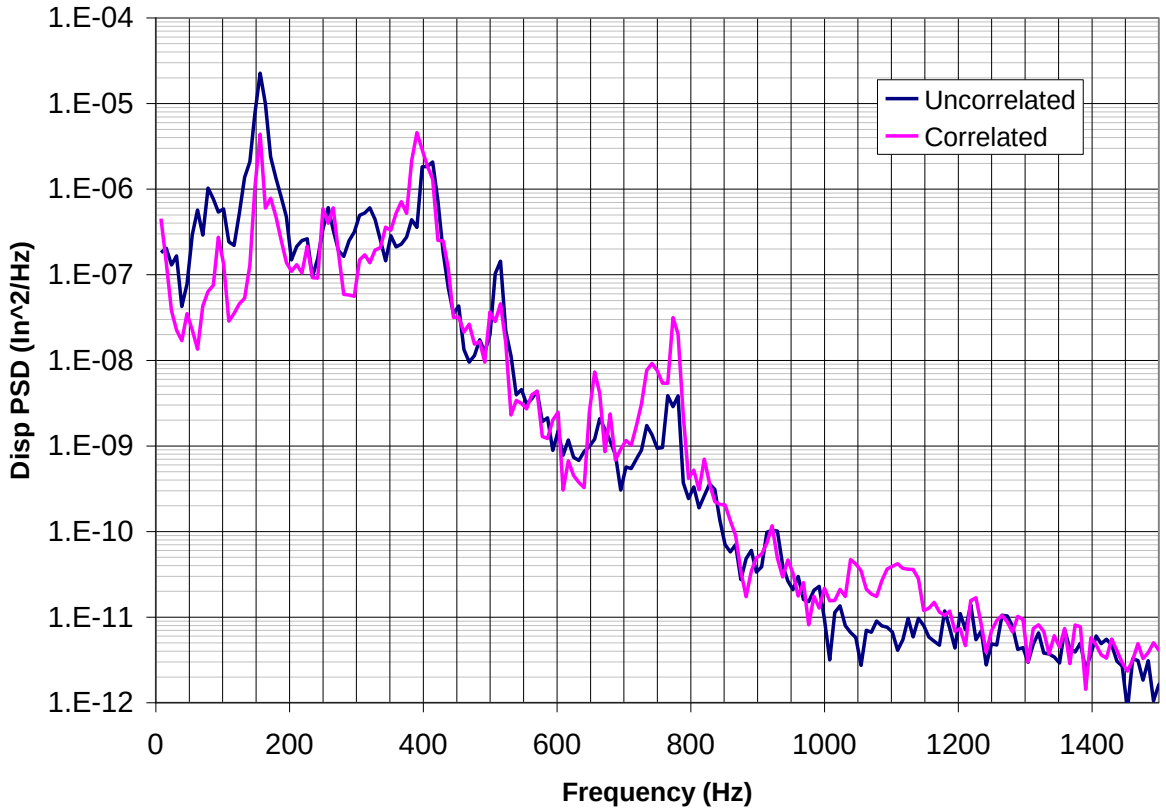

Figure 37 – Nonlinear Quarter Span Vertical Displacement Response

In general, for acoustic fatigue applications, the loading will most likely be separated turbulent boundary type flow, and the loading over a typical aircraft skin panel, will be fairly uncorrelated. The exact degree of correlation needs to measured or modeled. Hence, it's important to include asymmetric modes in the response since these can get excited thru the nonlinear coupling terms in the reduced order equations.

The section showed that we correctly implemented the NLROM method. Both the static and dynamic behavior of the model was demonstrated as compared to existing full-order methods. We also implemented the capability to model complex acoustic load definitions, with multiple load cases. The linear reduced order model demonstrated the expected behavior, and the NLROM demonstrated the expected modal coupling effect that occurs. In the next section, we validate the efficiency of the method compared to the full-order method.

3.2 Validation Test Case – Curved Panel

The second test case examines the accuracy and efficiency of the NLROM method. The test case is an aluminum panel 24.5 inches x 11 inches x 0.071 inches thick with curvature of R_c =135 inches, and with simply-supported boundary conditions. The acoustic loading is a separated turbulent boundary layer spectrum at an OASPL=163dB, and is applied as a single uniform load. The explicit solution uses Abaqus while the NLROM method uses NASTRAN. The FEM uses 1078 quadrilateral type elements (S4R and CQUAD4, respectively). But otherwise the models have the same mesh size, element types, and materials. The NLROM model uses five modes and both simulations are run for T=4 sec. In this case, the NASTRAN

and Abaqus normal vibration modes and frequencies match fairly closely (Table 1). The nodal displacement and acceleration PSDs at the center of the panel and the element stress at the center of the long edge are shown below, in Figure 39 thru Figure 41. The response magnitude and spectrum also match very well up to 500Hz.

Table 1 – Mode Frequency Table (*-NLROM Modes)

Mode # - Order	NASTRAN Sol 103 (Hz)	Abaqus STEP, Frequency (Hz)
1-(1,1)	228*	228
2-(1,2)	235*	236
3-(2,1)	239*	239
4-(3,1)	267*	269
5-(2,2)	279	282
6-(4,1)	318	320
7-(3,2)	342	346
8-(5,1)	396*	401
9-(4,2)	421	428
10-(2,3)	494	501

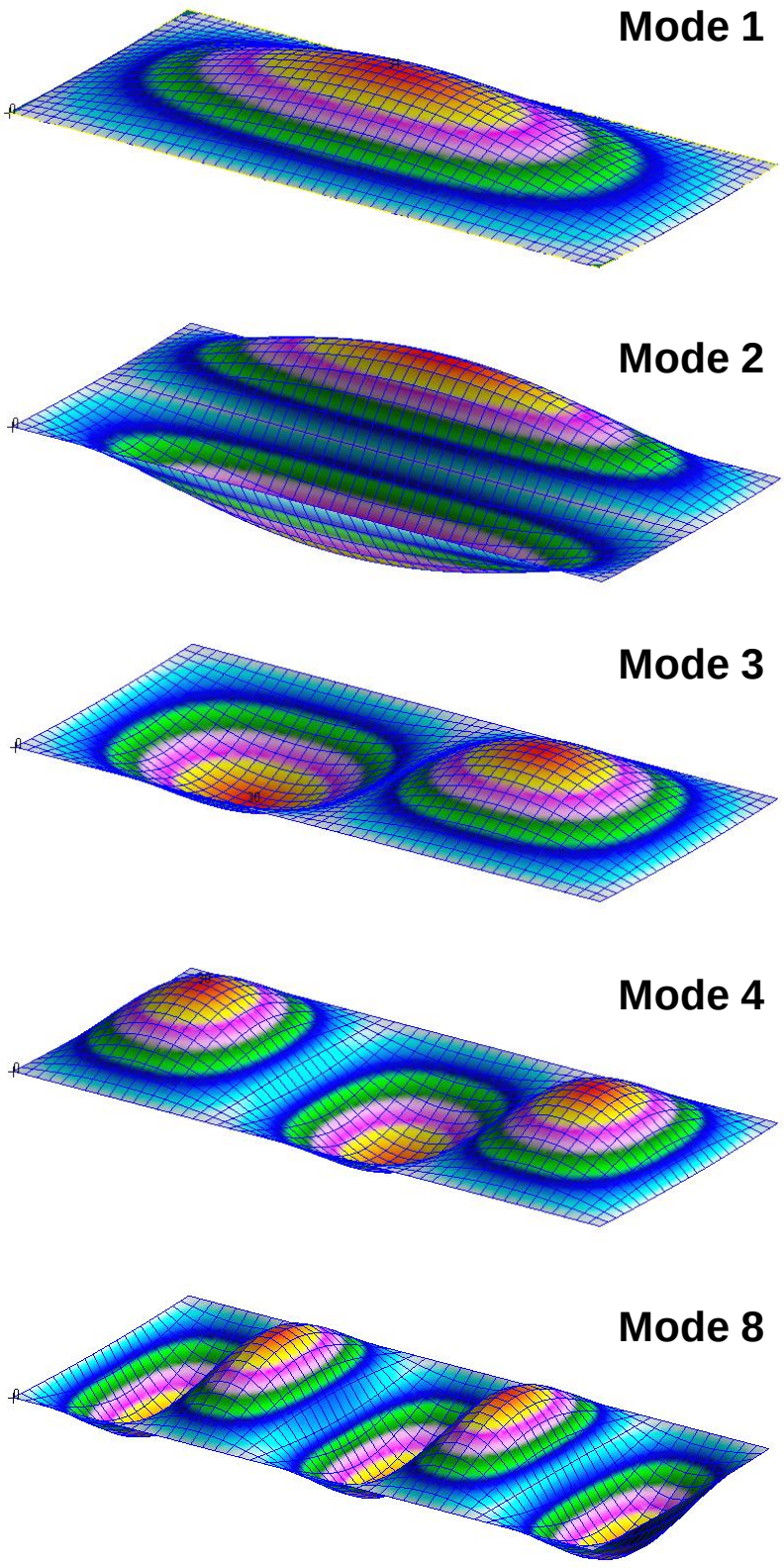

Figure 38 – Selected Modes

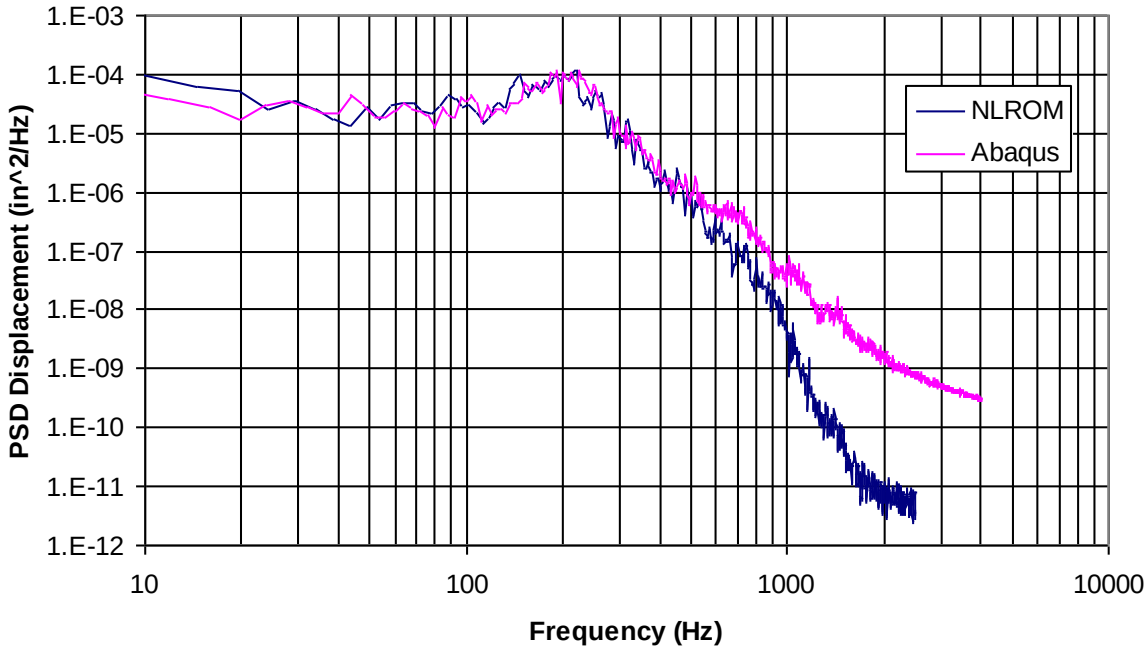

Figure 39 – Out-of-Plane Z-Displacement at the Center of the Panel

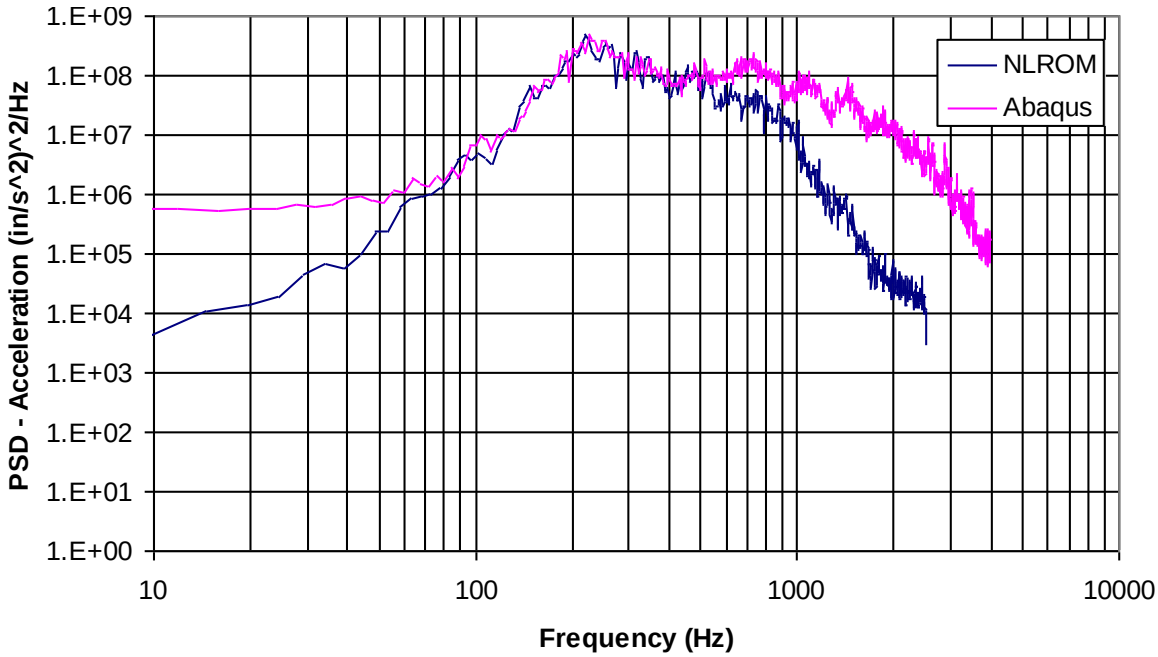

Figure 40 – Out-of-Plane Z-Acceleration at the Center of the Panel

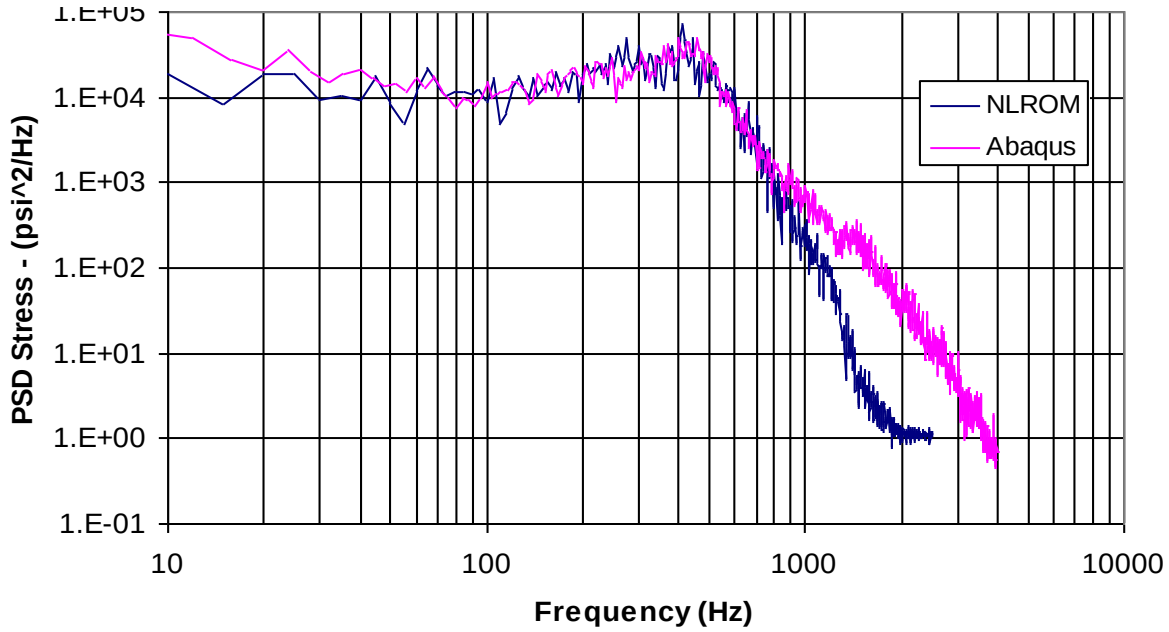

Figure 41 – Stress S22 Top Side, Element at the center of long edge

The accuracy of NLROM has been validated, so now we'll evaluate the efficiency for this we'll perform a timing study as compared to the full order explicit FEA. For this study, three different meshes were used: 0.25", 0.50", and 1.0" element size. Each model was run thru an Abaqus/Explicit solution, and the NLROM process. Solution times were recorded and the timing results are presented. The timing results are listed in Table 2. The table shows for models of different mesh refinement that run time for a nonlinear static (NASTRAN, SOL 106) and nonlinear (Abaqus, *Dynamic, Explicit) analysis increases.

Table 2 – Timing Study

Curved Panel Refinement Study				
		Stable	1-NL static Run	1-sec Explict Run
#Nodes	~DOF	DT (sec)	(sec)	(sec)
312	1560	4.06E-06	3	200
1050	5250	2.07E-06	9.98	1560
4456	22280	1.04E-06	40.2	13370

The solution time of NLROM method is generally not dependent on the integration time (or at least this is a small part of the total solution time.) The big cost for the NLROM method is the solution of the nonlinear static runs which increases with increasing modes and model DOF, Figure 42. The full order explicit FEA is linearly dependent on solution time. The prime factors are the stable time integration step, and the number of DOF in the model. The stable time step is dependent on the size and stiffness of the smallest element. In this study, all elements have the same size and properties for each model.

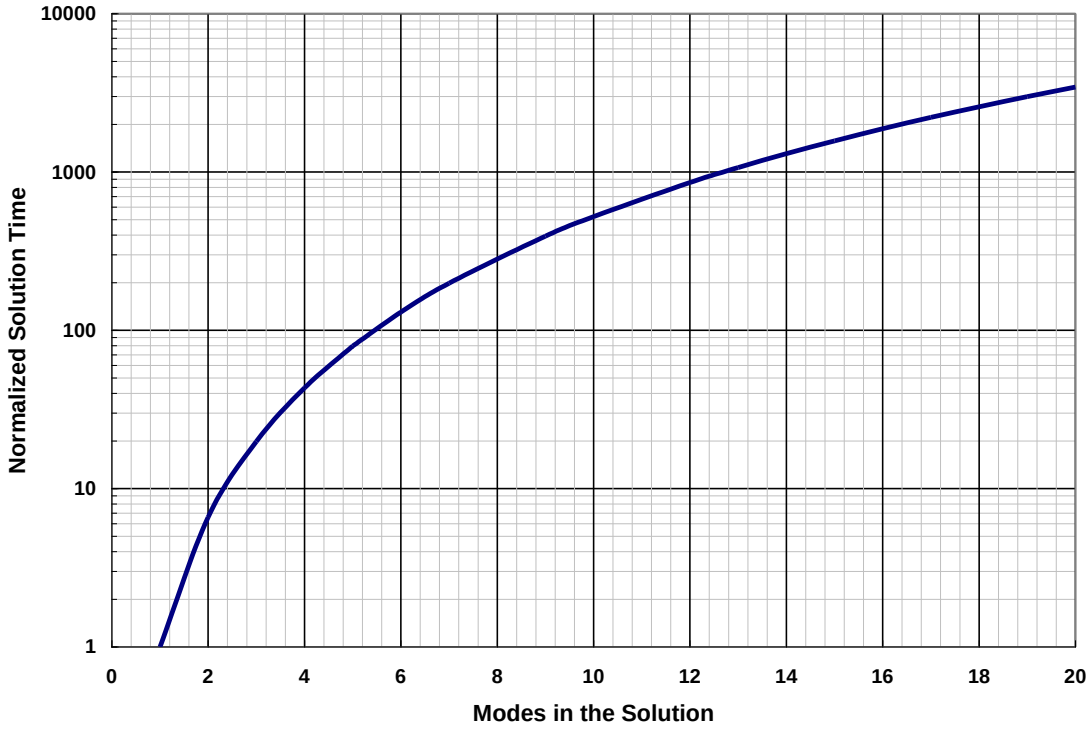

Figure 42 – Increasing Solution Time with Increasing Modes for the NLROM method normalized to a one mode solution.

Figure 43 is a comparison plot for a 4 sec simulation. The dashed lines are the CPU time for the explicit solutions of the three different mesh densities. The points are NLROM solution times for the different meshes with increasing number of modes. The plot shows that there is a point where the full-order analysis is more efficient than the NLROM. In general, small models will run very quickly in a full-order analysis, and the break even point with a NLROM analysis would be with a few modes. The real benefit of the NLROM method is when large refined models are used. A large refined model with only a few modes can be two orders of magnitude more efficient to run than a full-order explicit solution. The second major benefit of the NLROM method is the re-computation time. If the user chooses to change the magnitude of the acoustic loading, or change the damping level, then this requires a completely new computation of the model. While for a NLROM, the model can be quickly re-analyzed for a new acoustic load case or if the user chooses to determine the sensitivity of the response to changes in the damping.

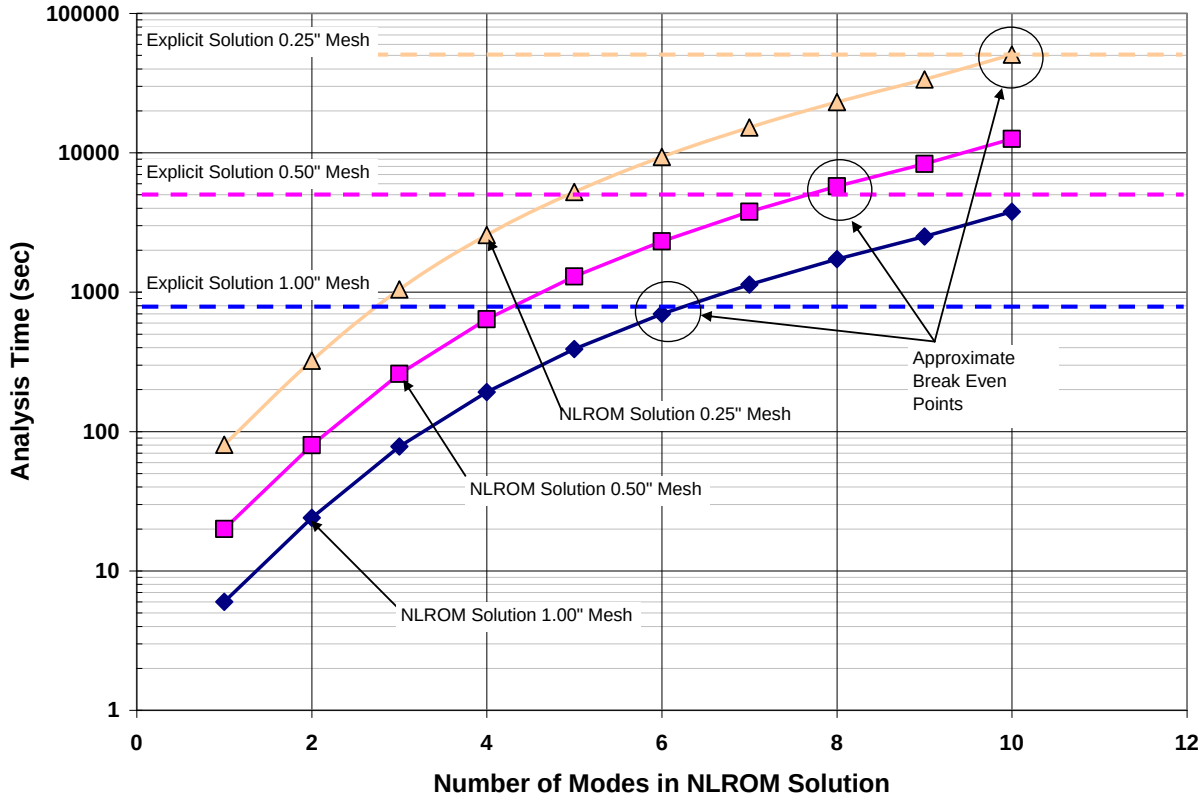

Figure 43 – Comparison of the NLROM method efficiency to the Full-order explicit Solution, a 4-sec time simulation

When performing transient response simulations for fatigue analysis, it's also important to consider the appropriate sample rate and time duration of the simulation. The sample rate mainly affects the higher order modal response. Although, these modes aren't usually the main contributors to the structural response that causes fatigue, they do affect the linearity of the response, because when higher order modes are included in the response the crest factor (Peak Response / RMS Response) is higher. A high crest factor means that there are higher peaks in the response (i.e. >3 * RMS or 3σ). It's the higher peaks in the response that is generally most affected by nonlinearities. For instance, the 1σ peaks probably are not affected, the 2σ are somewhat affected, 3σ peaks are a lot affected, and those peaks >4σ are greatly affected. By increasing the sample rate, the linearity of the response is affected, which affects the distribution of peaks and valleys in the response and this affects the fatigue life.

The higher-order modes are also coupled to the lower order modes thru the nonlinear stiffness coupling terms. This allows for some flow of energy between these modes. Certainly, the energy can flow both ways from the low modes to the higher modes and visa versa. Hence, it's important to include in the model all modes that make a significant contribution to the response and/or that are with in the frequency range of the excitation. Therefore, the sample rate should be four times the highest frequency included in the model with allowance for any stiffening effects. A sample rate less than this requirement will result in some amount of aliasing of the higher-order modes. If the higher-order modes are aliased then the coupling effects to the lower order modes will be less and there is less energy flow. Finally, this can affect the overall nonlinear response.

The length or duration of the time simulation has a similar effect. Generally, the longer the simulation time the higher the probability that large crest factors will be observed in the response. This is best observed by calculating the gamma factor, γ. In Figure 44, the gamma factor is converging with time simulation. There is a similar trend with the RMS and PSD, Figure 45 and Figure 46. The PSDs show very little change above 4 seconds. Similarly, the fatigue life is also converging, Figure 47. Somewhere about 5 or 6 seconds is sufficient for this application.

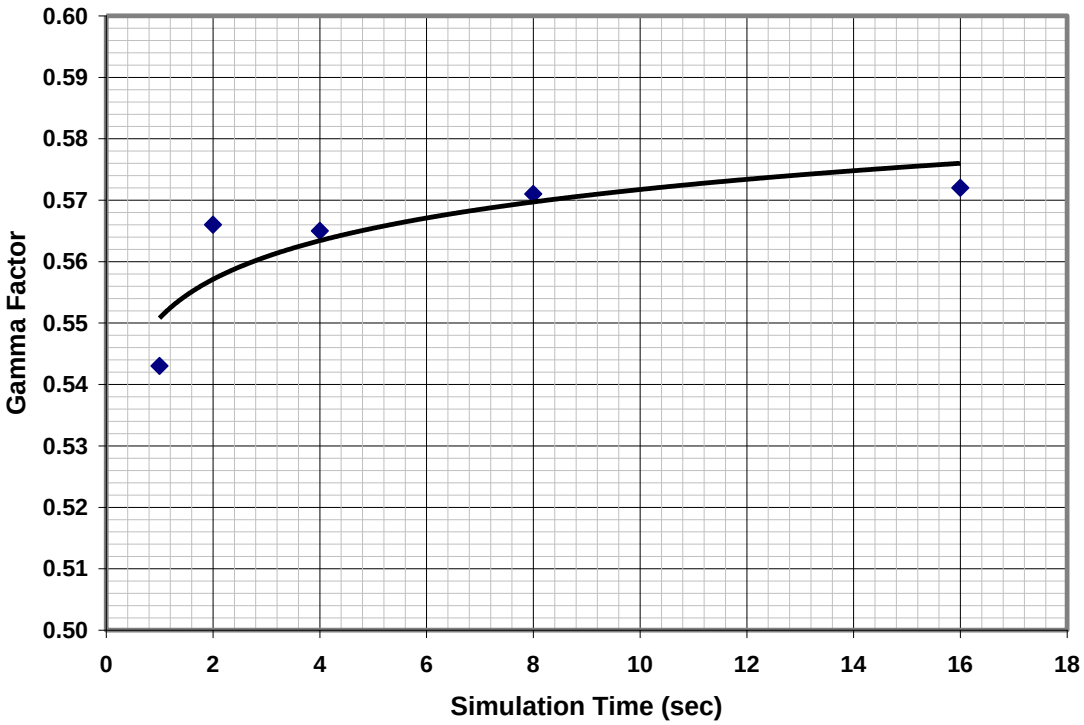

Figure 44 – Gamma (Irregularity Factor) vs. Simulation Time

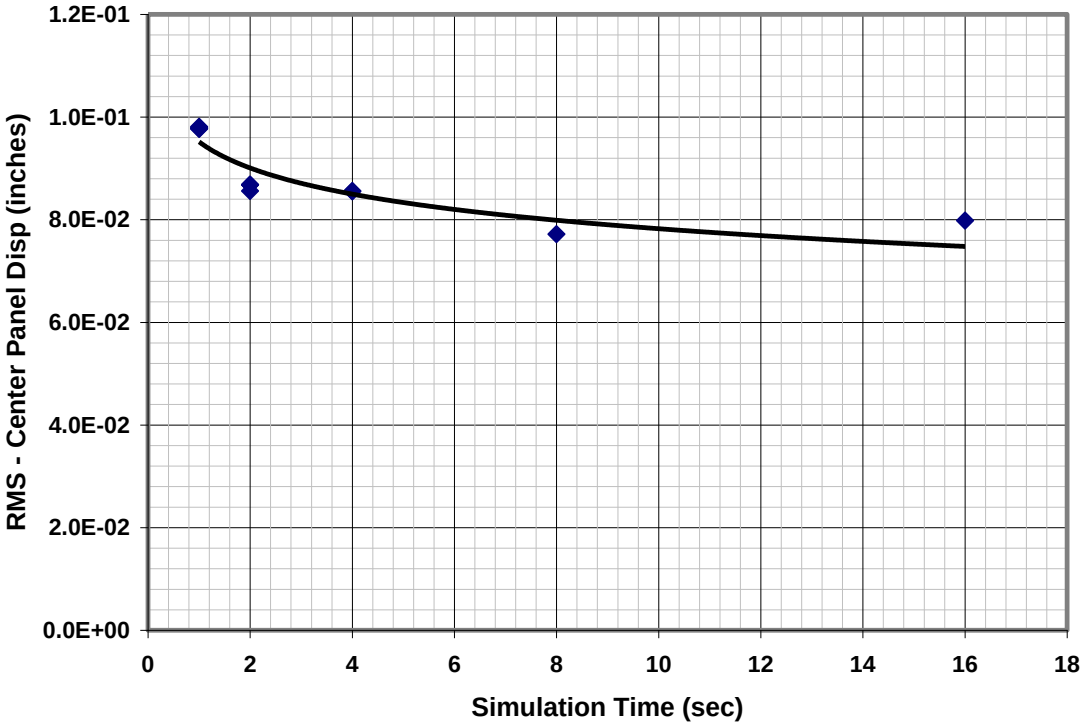

Figure 45 – RMS Response vs. Simulation Time

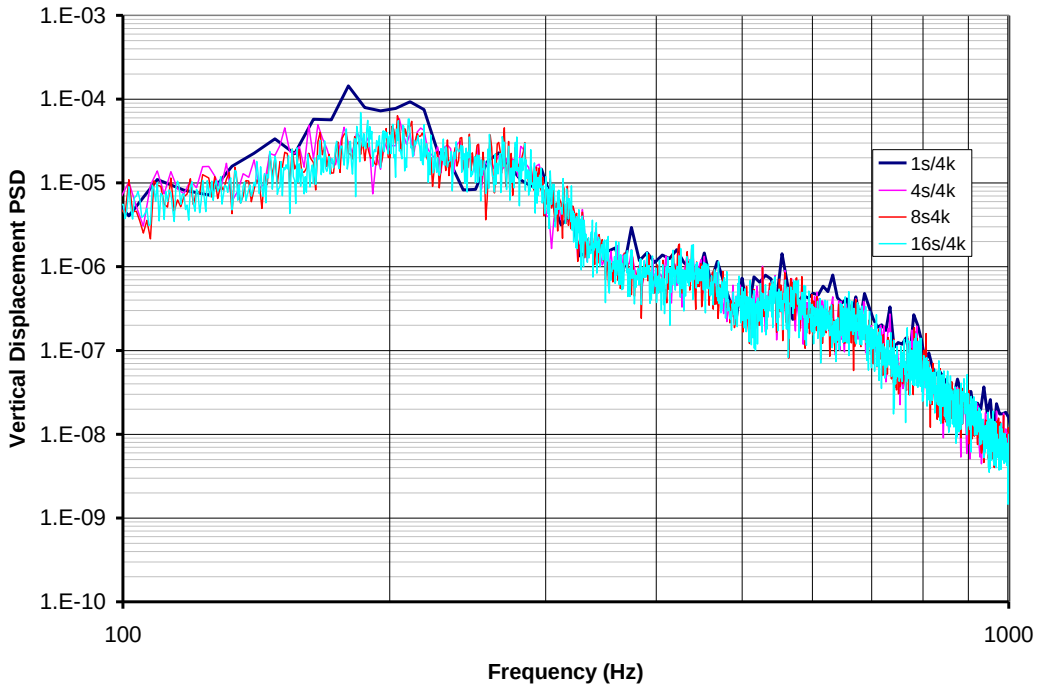

Figure 46 – Comparison of PSDs for Different Time Simulation Durations

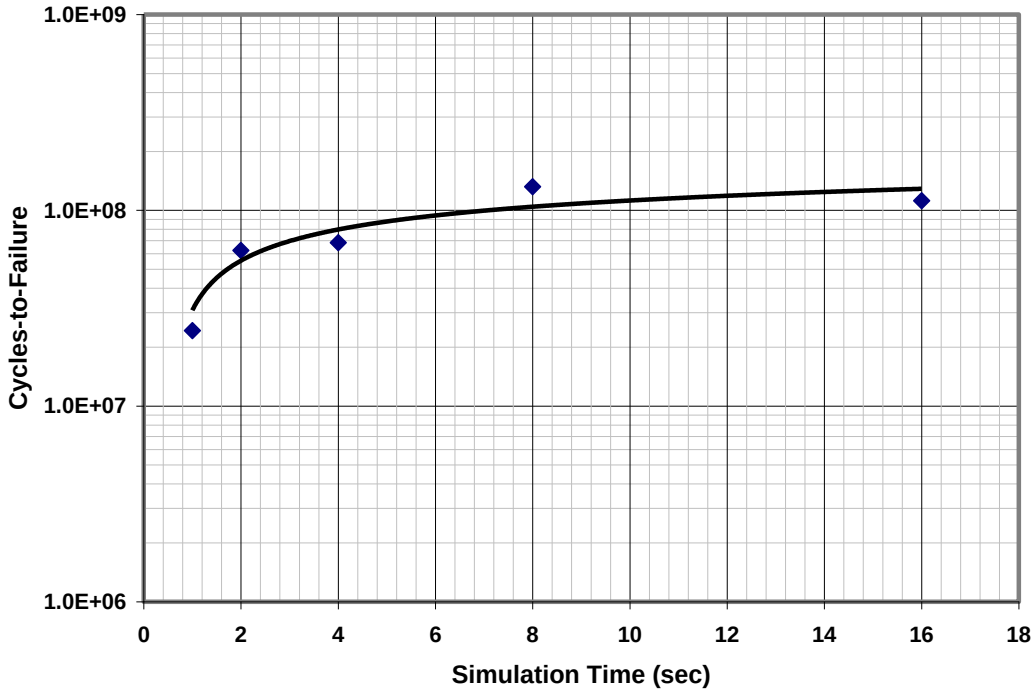

Figure 47 – Cycles to Failure vs. Simulation Time

Hence, the length or duration of the time simulation has a significant effect on the simulation results. In general, the longer the simulation time the higher the probability that large crest factors (Peak / RMS) will be observed in the response. It is known that most of the damage in high cycle fatigue is done by the 2 σ to 3 σ peaks. This can be easily shown by performing a RMS spectrum block type fatigue calculation. However, in real situations the peak/valley distributions do not follow classical Rayleigh distributions, and the fatigue life can be greatly influenced by the presence of high peaks greater than 4σ.

The following is a simple example that demonstrates which stress range produces the most fatigue damage based on linear response and stress-life (no material nonlinearity) damage principles. Assuming a normal distribution to the response, then the percent of stress ranges per spectrum block would look like Figure 48, with most of the Peaks and Valley cycles occurring below one standard deviation (σ). However, most of the damage occurs due to peak/valley cycles in the higher 2.5σ to 3.0σ range, Figure 49. Also, even though they occur very infrequently, the stress ranges in the 4+ σ range can produce significant damage. This helps to demonstrate the point that fatigue life is dependent on the distribution of stress (P/V) range. In summary, the longer the simulation time is run out, then the higher the likelihood that a high stress range will occur. Secondly, the higher stress range cycles tend to occur when higher order modes are contributing to the response to produce a more wide-band response.

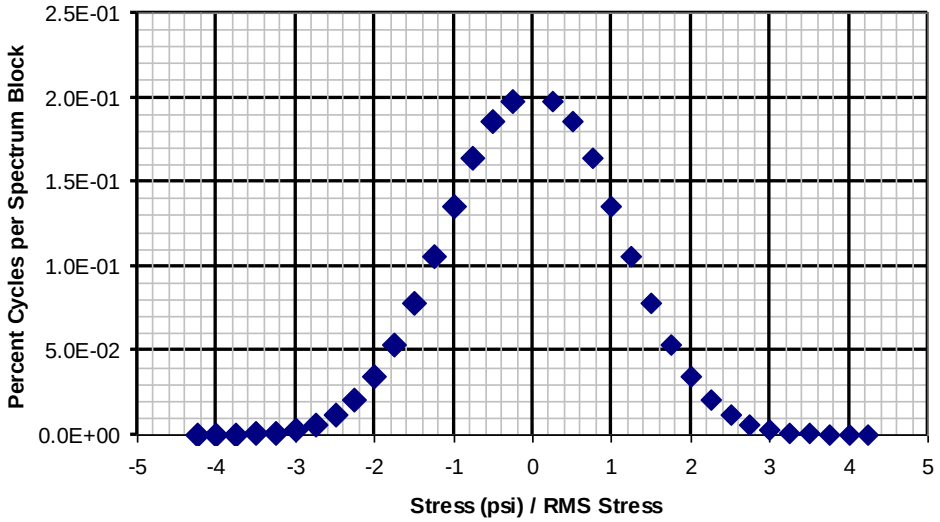

Figure 48 – Time Signal Amplitude PDF

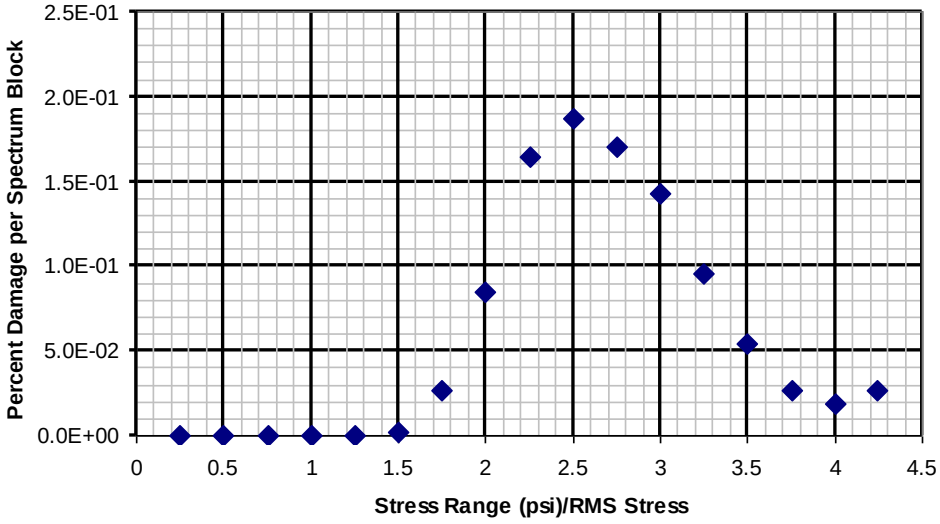

Figure 49 – Time Signal Peak/Valley PDF

It was stated, that the nonlinear response does not produce a Normal or Rayleigh stress range response, and this will be demonstrated. More than likely the nonlinear stress range will be skewed to the lower stress range side of the distribution and the peak (kurtosis) will be sharper. This is due to the nonlinearity effects increasing with increasing stress range. Consider the center panel vertical displacement response distributions from the simulation of the curved panel, where ΔT=8sec at a sample rate of F_s= 4000 Hz. The simulation was run both linear and nonlinear. The linear results are shown below in Figure 51 thru Figure 53. As expected for the linear analysis, the range is Rayleigh distributed and the mean is Normal distributed. The interaction between the mean and range also takes a standard shape. The nonlinear response time signal in Figure 54 shows the one-sided response that is typical of a curved panel (i.e. the panel is stiffer in one direction than the other in bending.) The relationship between the mean and range also shows the snap-thru behavior which is typical of curved panels. Finally, the distributions of the mean and range of the nonlinear response has a much more positive kurtosis

than the linear distributions, Figure 55 thru Figure 57. The main conclusion that needs to be drawn from this study is that the simulations need to be performed with a sample rate high enough to capture the higher order modal response contribution. The higher order modes have an effect on the distribution of the response and the nonlinearity of the response. The primary modes of interest are typically going to be the lowest order modes, but if the higher order modes couple (or phased) with the lower order modes, then this affects the nonlinearity of the lower order response. Also, the duration of the simulation needs to be long enough to adequately capture the statistics of the response. In general, the longer the time simulation are run out, then the more peaks and valleys that are accumulated in the response. With more peaks and valleys added to the response (also called a spectrum block), then the less uncertainty in the fatigue life predictions. For a recent acoustic fatigue study, it was shown that the uncertainty in fatigue life is directly related to the N_p (number of positive peaks statistic), Figure 58. This was determined using Monte Carlo analysis with the spectrum block being randomly generated, and the fatigue being calculated for each spectrum block. Note, the duration was also allowed to vary. This produced the plot shown in Figure 58. The scatter in life is the uncertainty about the mean life prediction. For instance, if the *Log(Life Scatter)* = 1.0, then the standard deviation on the fatigue life prediction is a factor of 10. Note: If the response is narrow band random, then the irregularity factor = 1.0, and $N_p = F_s * \Delta T$.

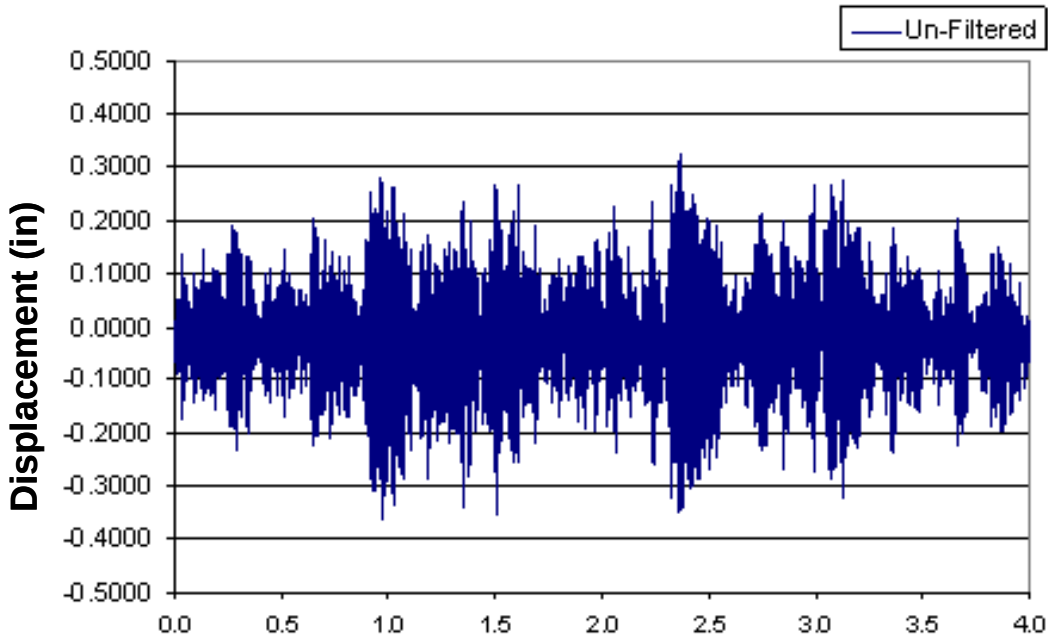

Figure 50 – Linear Time History Signal

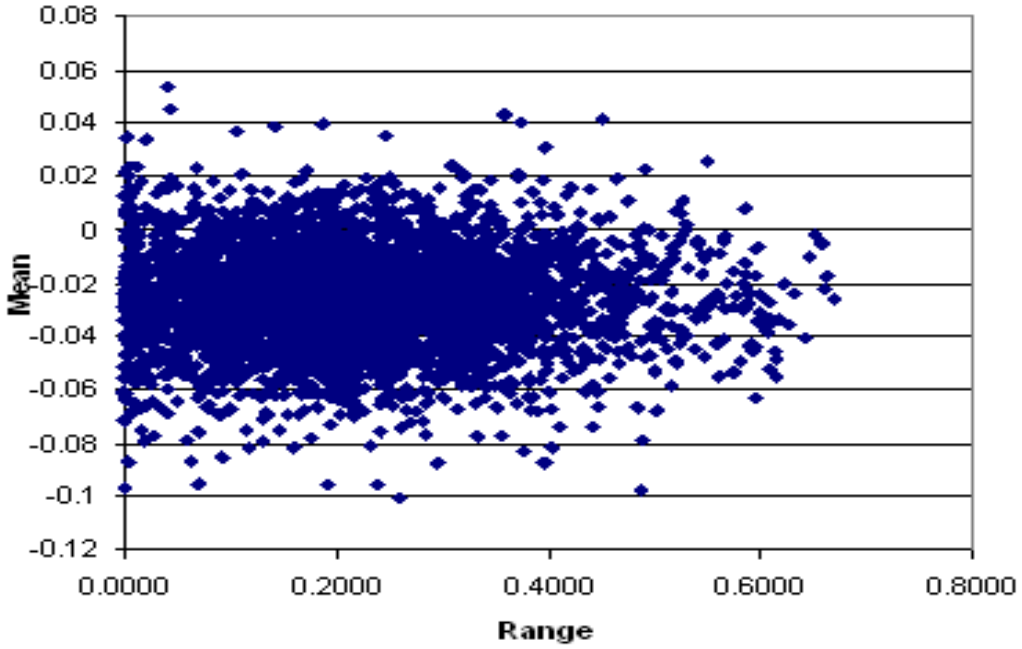

Figure 51 – Linear response mean – range plot

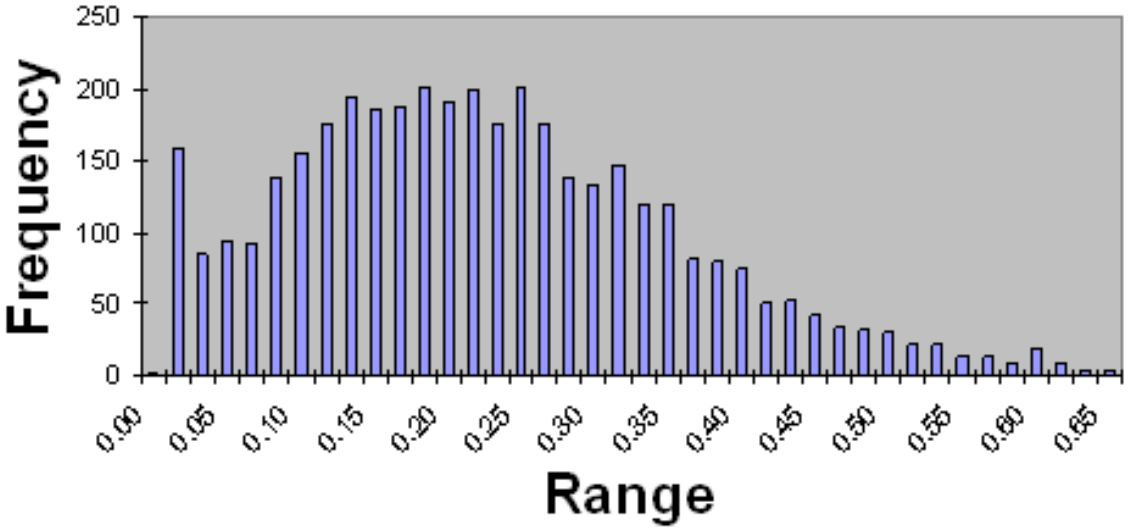

Figure 52 – Linear Time Signal Range PDF

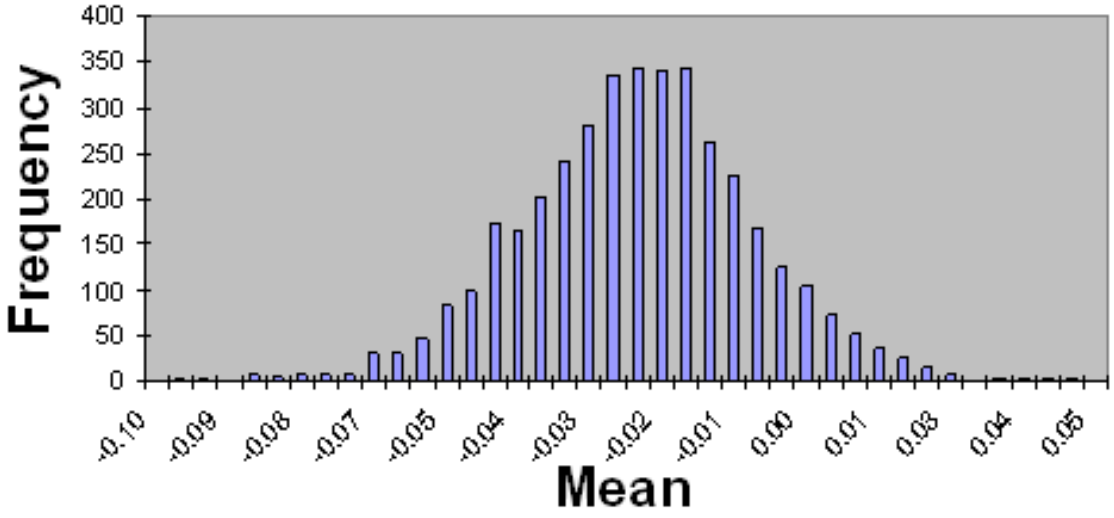

Figure 53 - Linear Time Signal Mean PDF

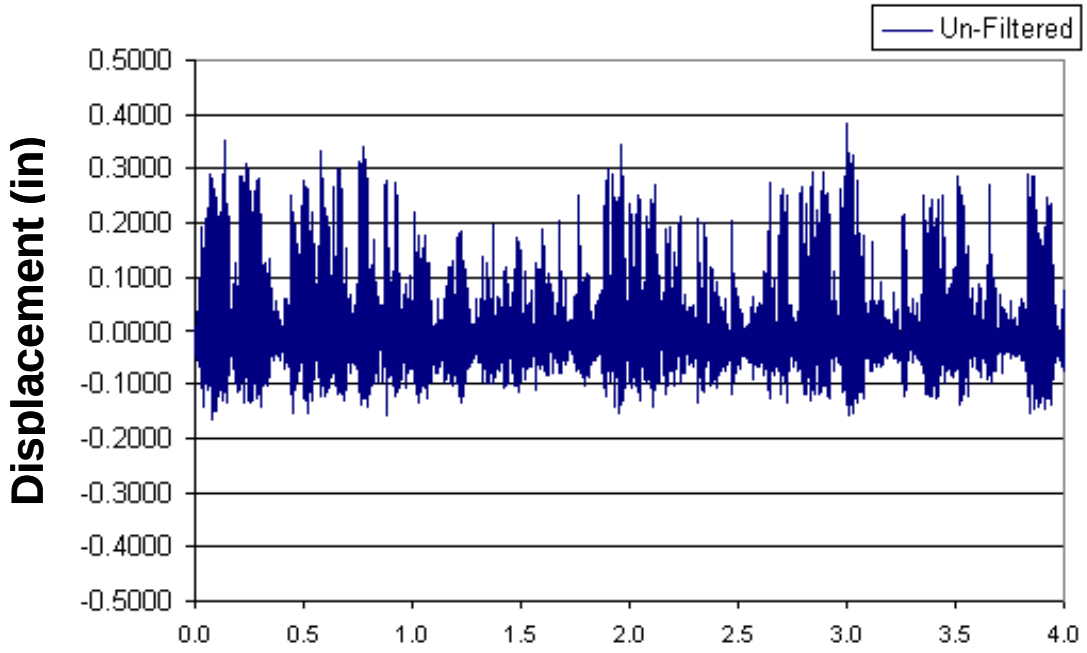

Figure 54 – Nonlinear Time History Signal

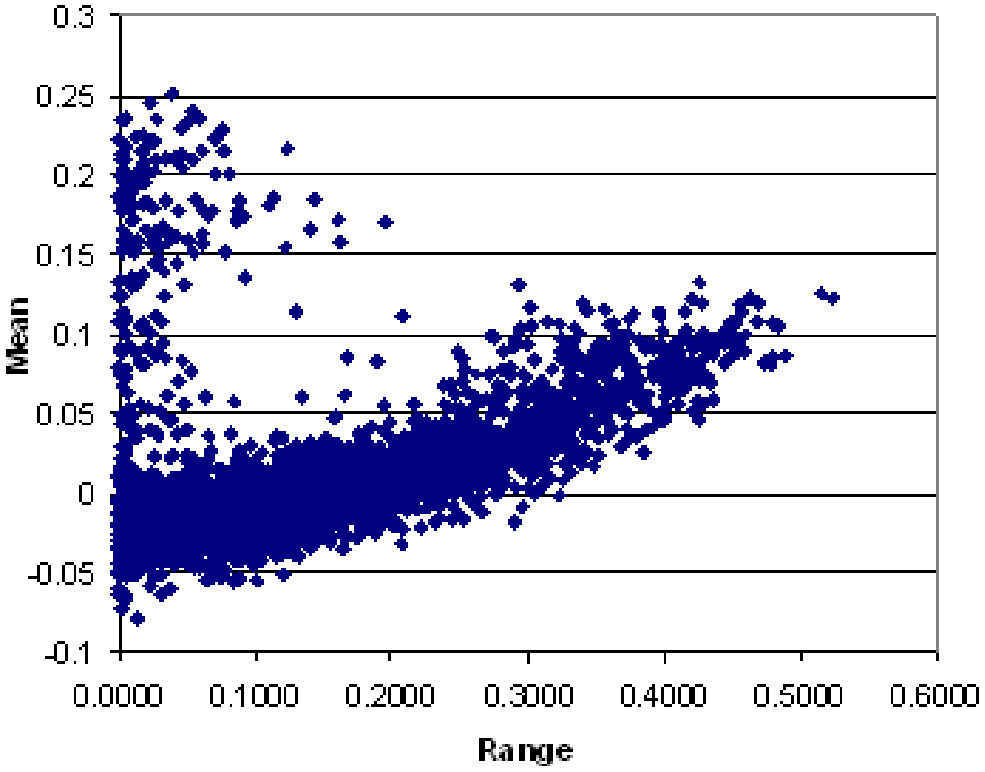

Figure 55 - Nonlinear Time Signal mean-range Plot

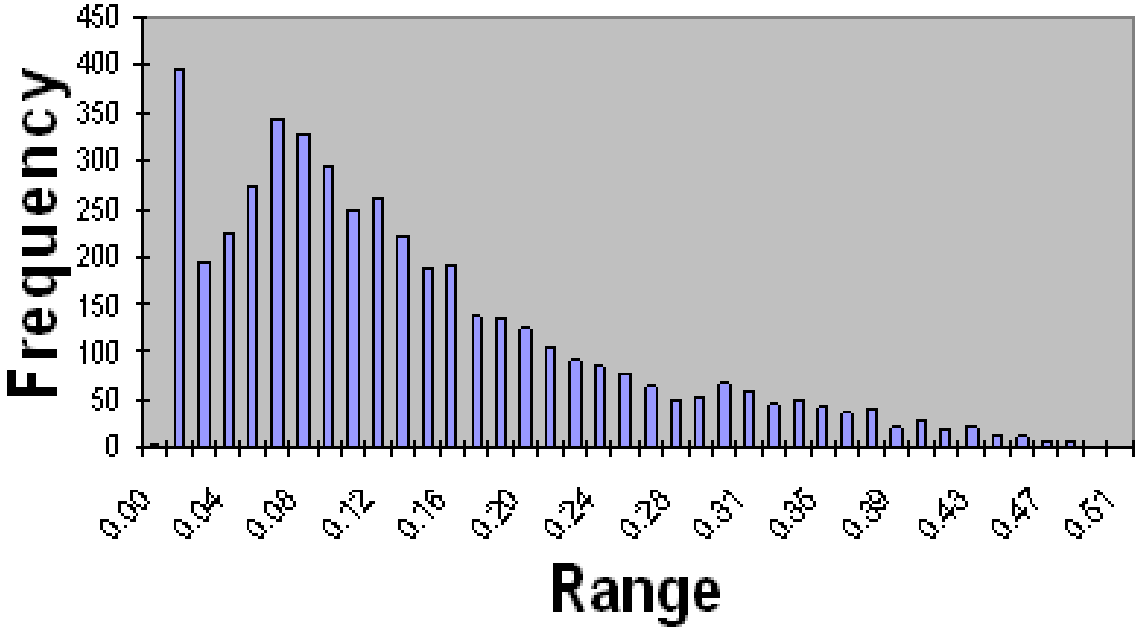

Figure 56 – Nonlinear response Range PDF

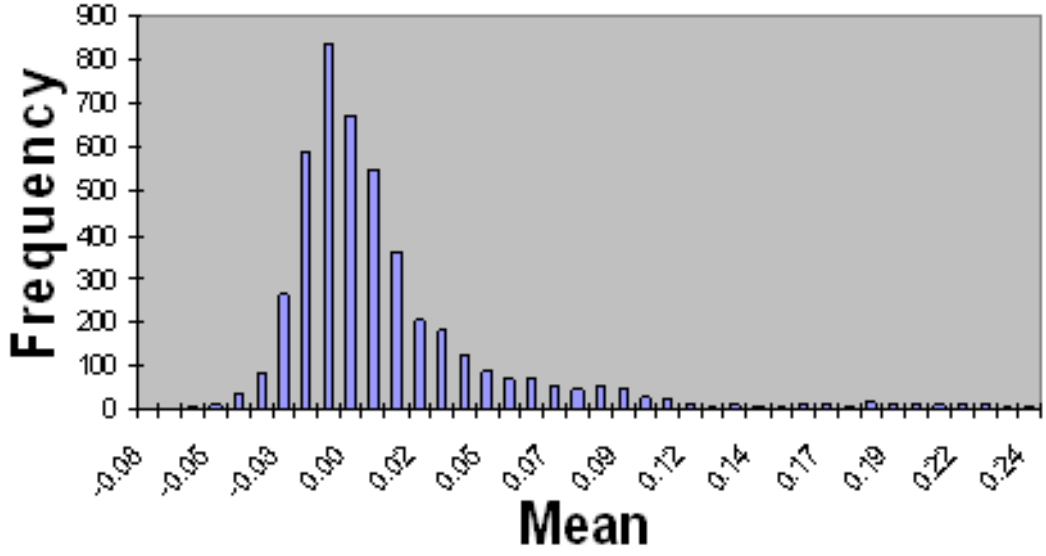

Figure 57 - Nonlinear response Mean PDF

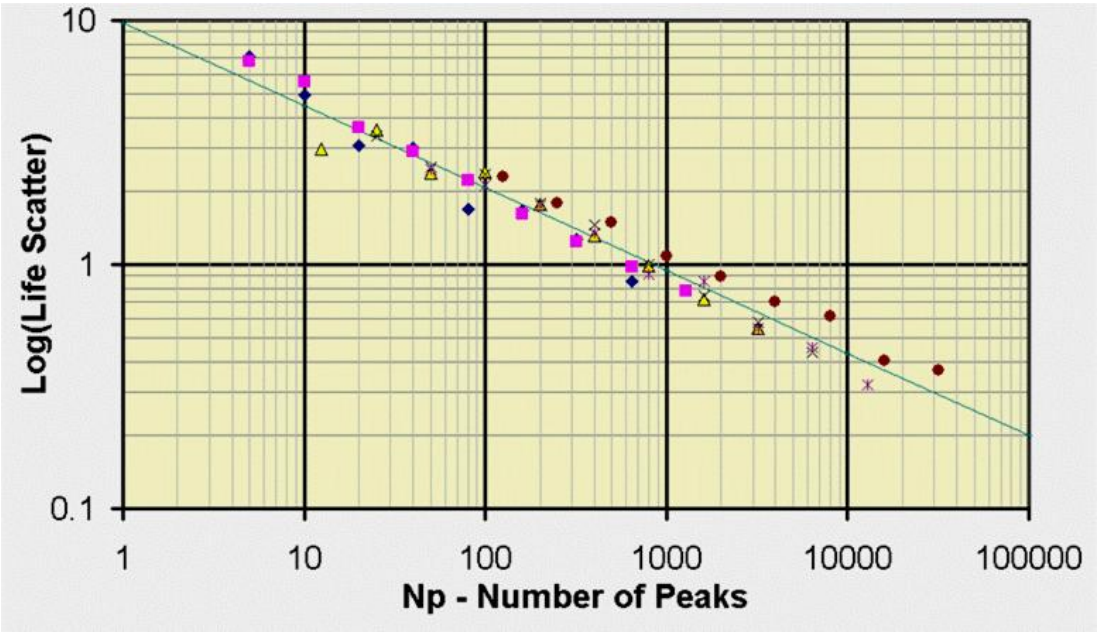

Figure 58 – Uncertainty in Cycle Counting Fatigue

This test case demonstrated the efficiency of the NLROM method. A timing study was performed that clearly shows that the efficiency of NLROM method compared to the full-order method improves significantly as the size of the model increases, and as the length of the time simulation increases. These are significant factors in the computation of acoustic fatigue life, as demonstrated. The next section describes a test case of an actual aircraft panel.

3.3 Validation Test Case – Curved Stiffened Aircraft Panel

The final test case was a curved stiffened panel shown in Figure 59. The panel was 16 in by 14 in, 0.071 in thick, with 0.06- and 0.04-in chem-milled pockets. The skin panel was clamped along all edges and the stiffener pinned at both ends. The first step is to perform an evaluation study. The evaluation study will compare the results (response and fatigue life) based on the nonlinear reduced order and full-order transient response, and the linear frequency response analysis. The objective is to compare the accuracy and efficiency of the NLROM method, as compared to the other analysis methods. The test data was the basis for setting up the analysis, and to correlate the models.

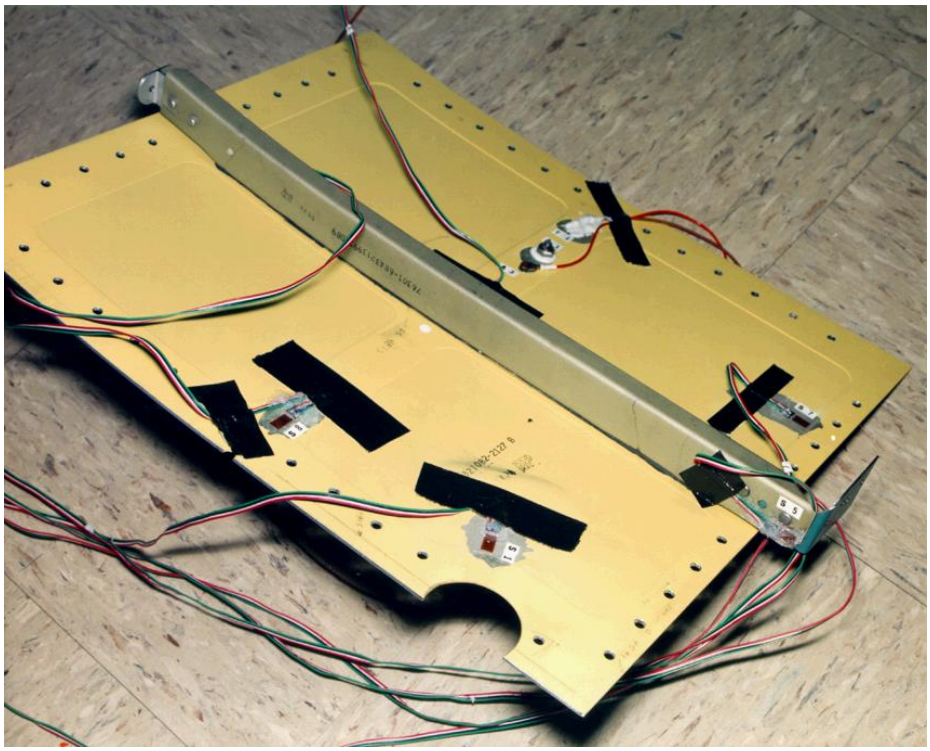

Figure 59 – Curved Stiffened Panel Test Case

The second step is to use the NLROM method and perform a design study based on this test case. Using linear methods, the original design fix was a heavy I-beam stringer in-place of the lighter-weight C-channel. Note: This design has not experienced any failures in service. The design fix was very conservative based on the linear analysis methods available at the time. We will use the NLROM method and look at redesign alternatives. The objective is to the use the NLROM tool as part of a design study and to determine how effective the method is as a design tool.

The overall objectives are:

1. Develop a model that best represents this typical aircraft test panel
2. Predict the response under realistic loads
3. Compare the responses predicted from the reduced order model to a full-order physical degree of freedom model
4. Compare trends to available test data
5. Predict and compare fatigue life

6. Evaluate the Accuracy and Practicality of the method as a design tool

The analysis plan for the curved stiffened panel is to compare the NLROM analysis with (1) NASTRAN Linear Frequency Response Analysis, and (2) Abaqus Nonlinear Transient Explicit. The acoustic input loads are based on an acoustic chamber test. The goal isn't to correlate to the test data, only to use the test data as a basis for setting up the model.

The loading scenario is a shock-induced/turbulent boundary layer (SI/TBL) aero-acoustic noise source (OASPL = 165 dB). The input spectrum is shown below, Figure 60. This spectrum is directly input into the NASTRAN linear random frequency response. For the Abaqus analysis, the spectrum is converted into a time history using MatLab WAFO routine (Ref. (16)) "spec2dat", Figure 61. For all analyses, the two load cases setup is used. A progressive wave with both a phase shift and spatial correlation degradation was assumed.

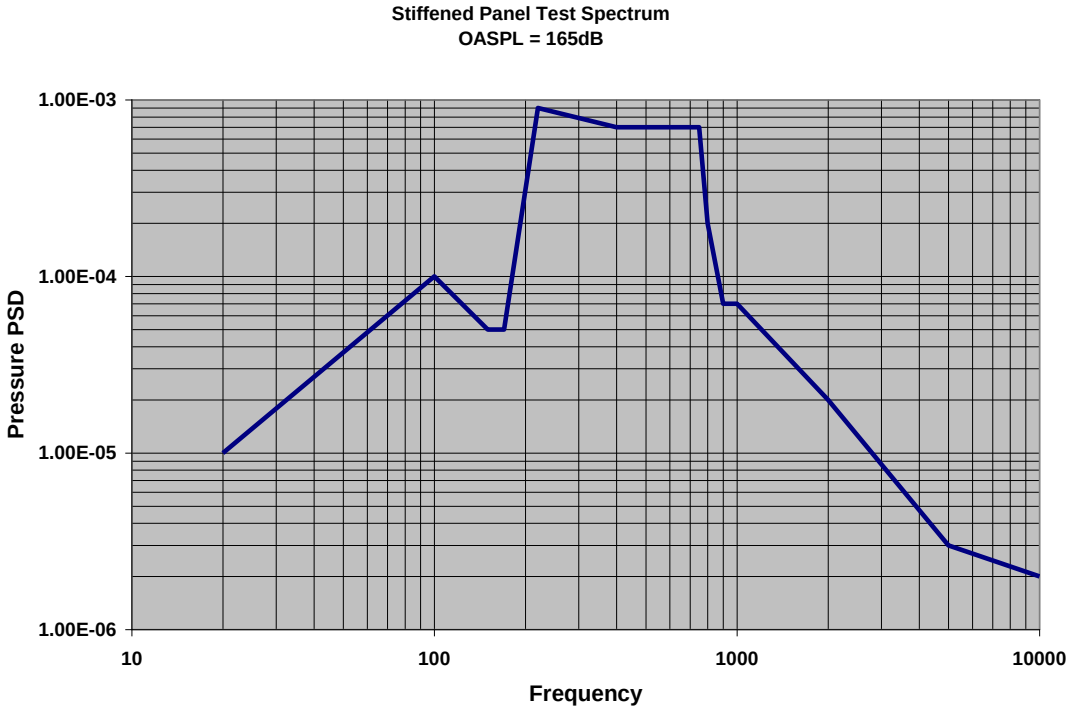

Figure 60 – Acoustic Input Spectrum

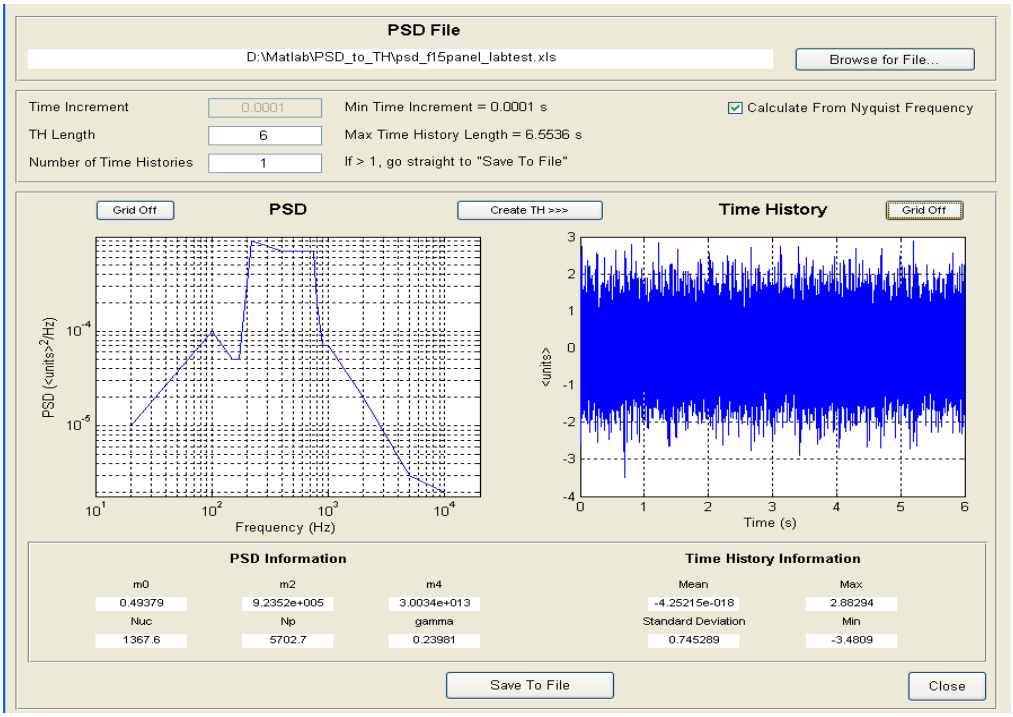

Figure 61 – PSD to Time History

The finite element model that is being used is shown in below, Figure 62. The model has 12202 quad elements and 12542 grids. The modes from the baseline model included in the building of the NLROM are shown in Figure 63 through Figure 66. For this initial study, linear Nastran Random Frequency Response, and the Abaqus Nonlinear Explicit Transient analysis were run. The explicit analysis takes approximately 24hrs of CPU time/second of simulation time. The results below are for only a 2.5 sec simulation.

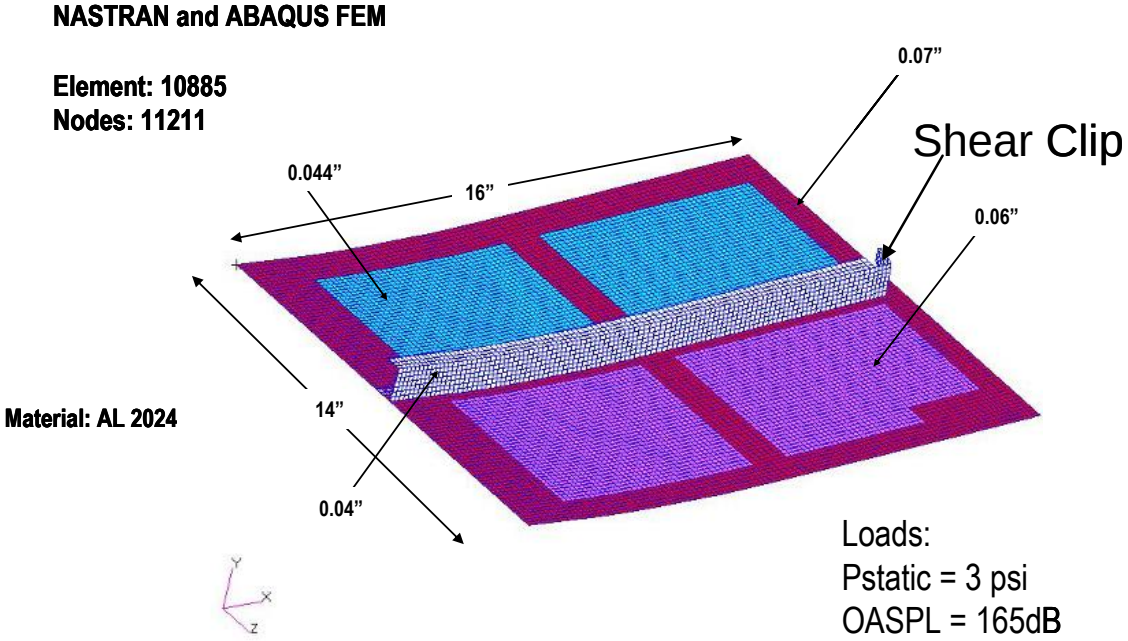

Figure 62 – Finite Element Model of Panel

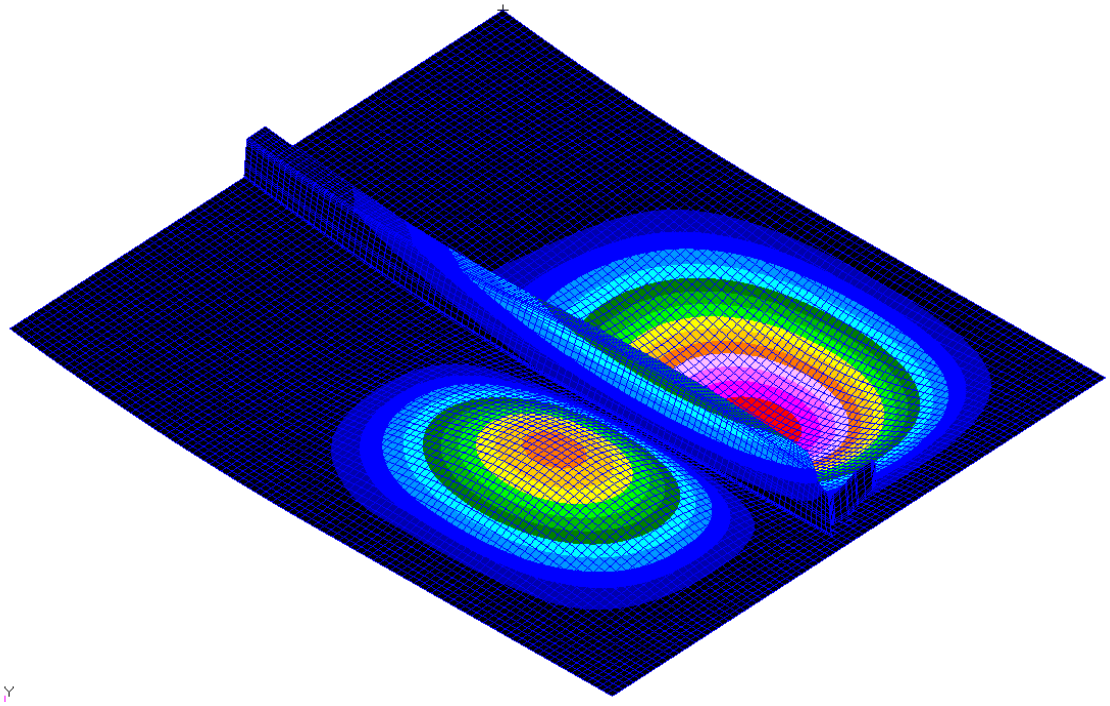

Figure 63 – Mode shape for baseline model Mode 1, 281 Hz

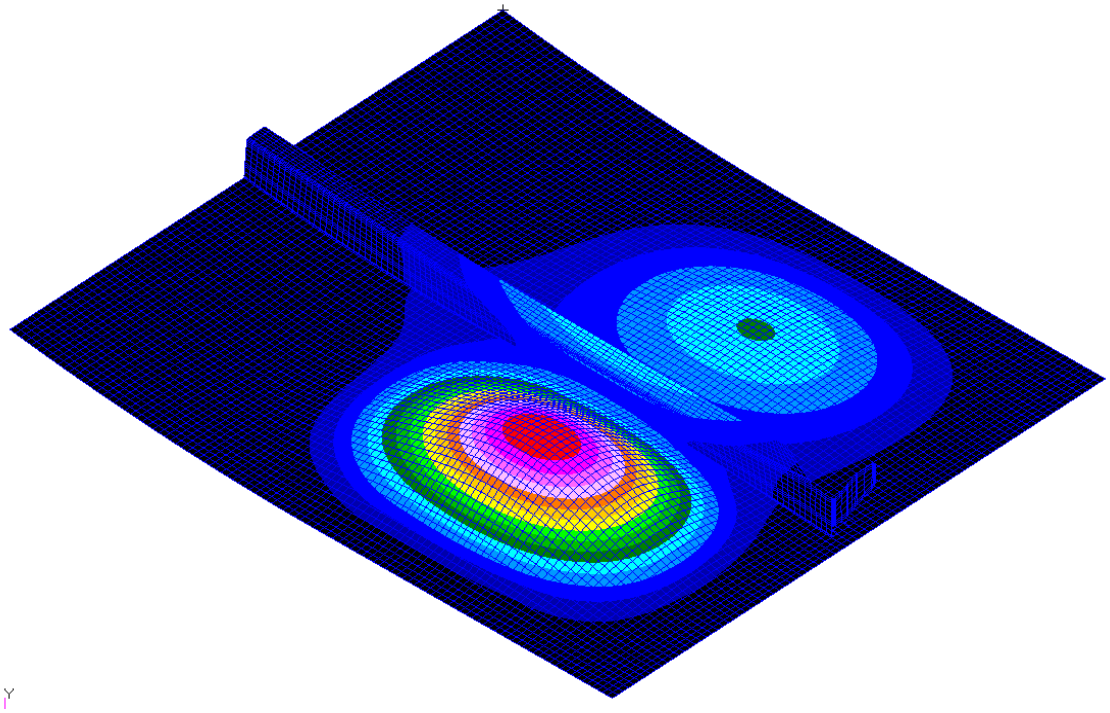

Figure 64 – Mode shape for baseline model Mode 2, 334 Hz

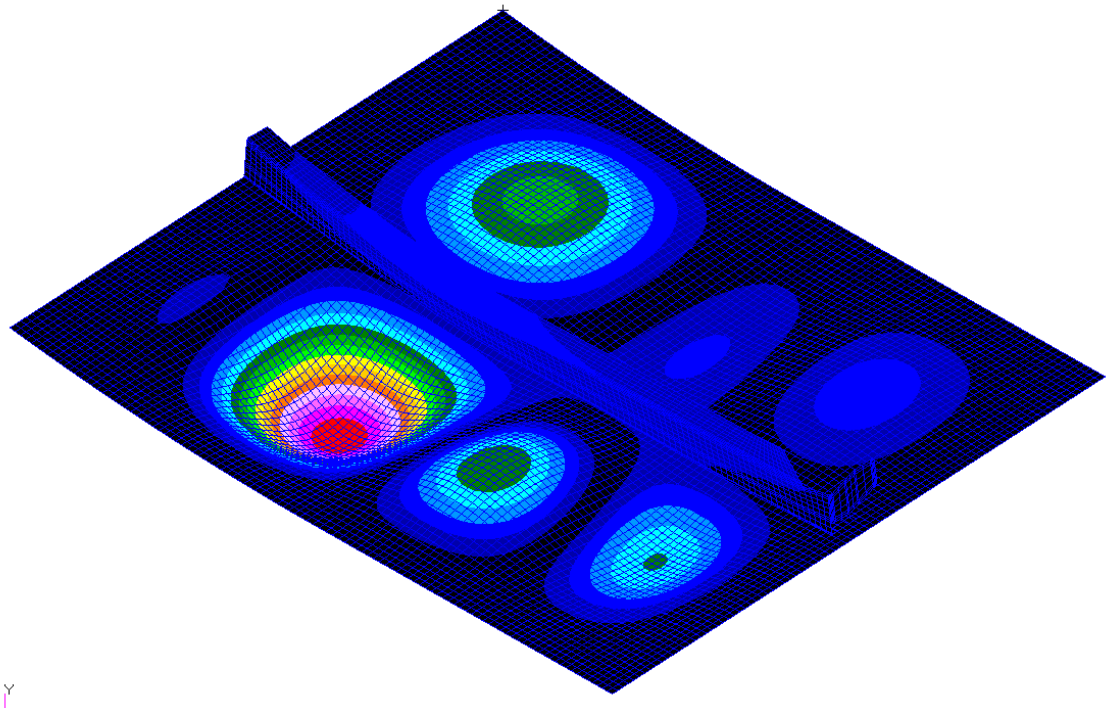

Figure 65 – Mode shape for baseline model Mode 6, 568 Hz

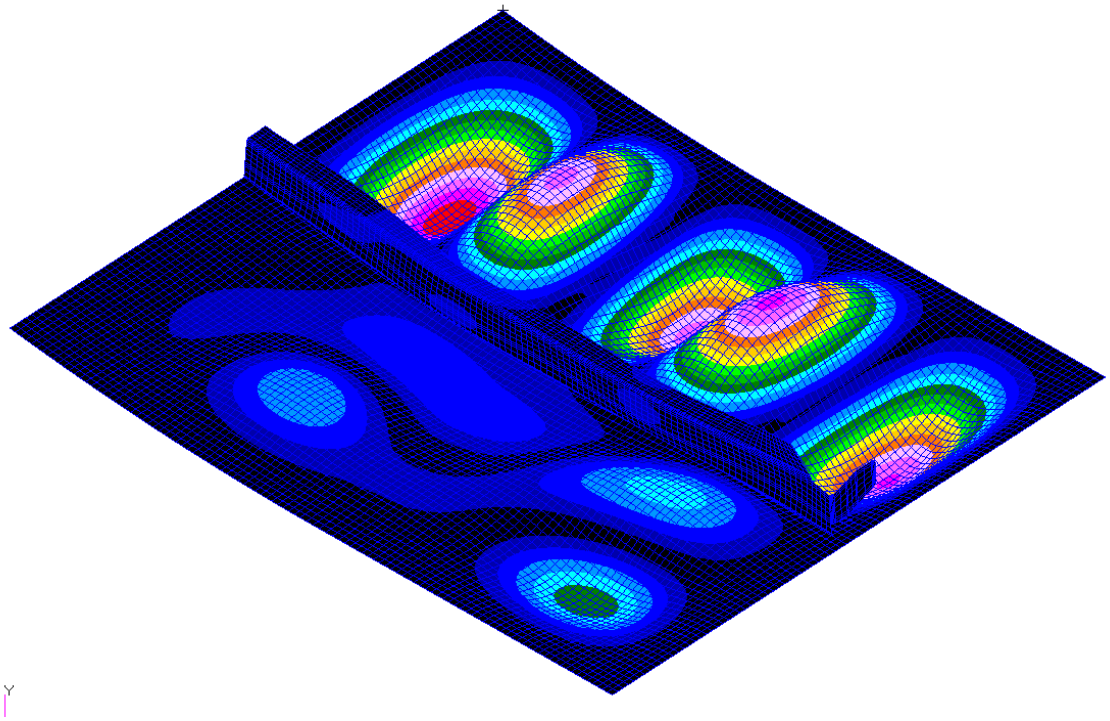

Figure 66 – Mode shape for baseline model Mode 14, 873 Hz

The linear NASTRAN results are shown in Figure 67 thru Figure 70. The normal RMS displacement is shown in Figure 67. The center bay displacements are most certainly nonlinear

since they are two to three times the skin thickness. The acceleration is shown is Figure 68. The RMS stress is shown in Figure 69 and Figure 70. The max RMS stress is at the edge of the panel, but there is a hot spot in the integral shear clip. We know from testing that the shear clip is the critical fatigue location.

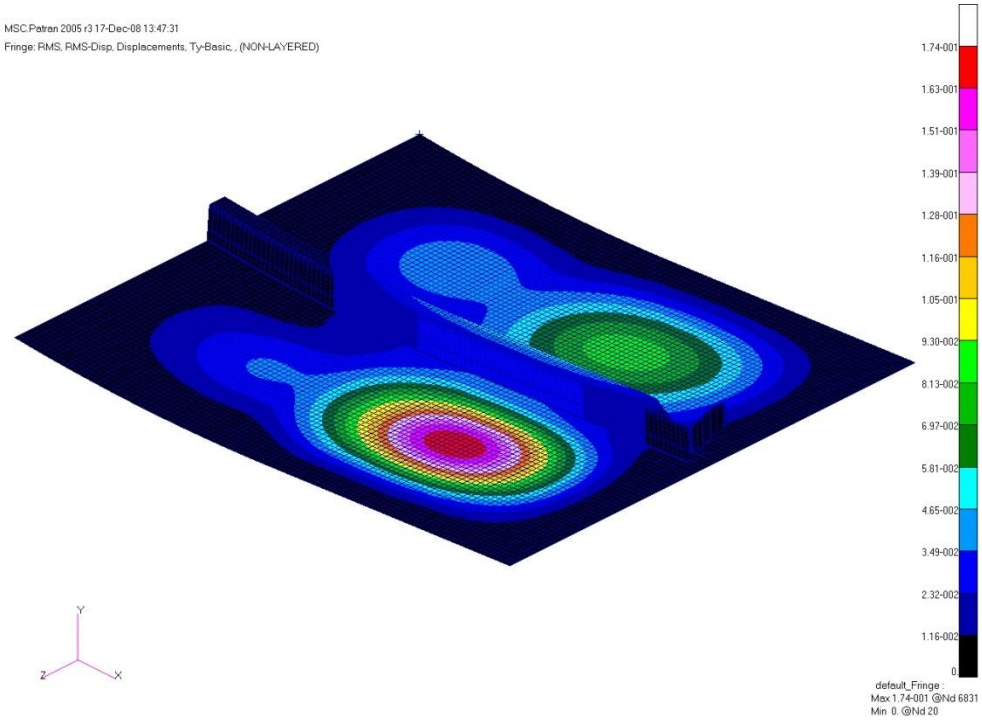

Figure 67 – NASTRAN Linear RMS Y-Displacement (Inches)

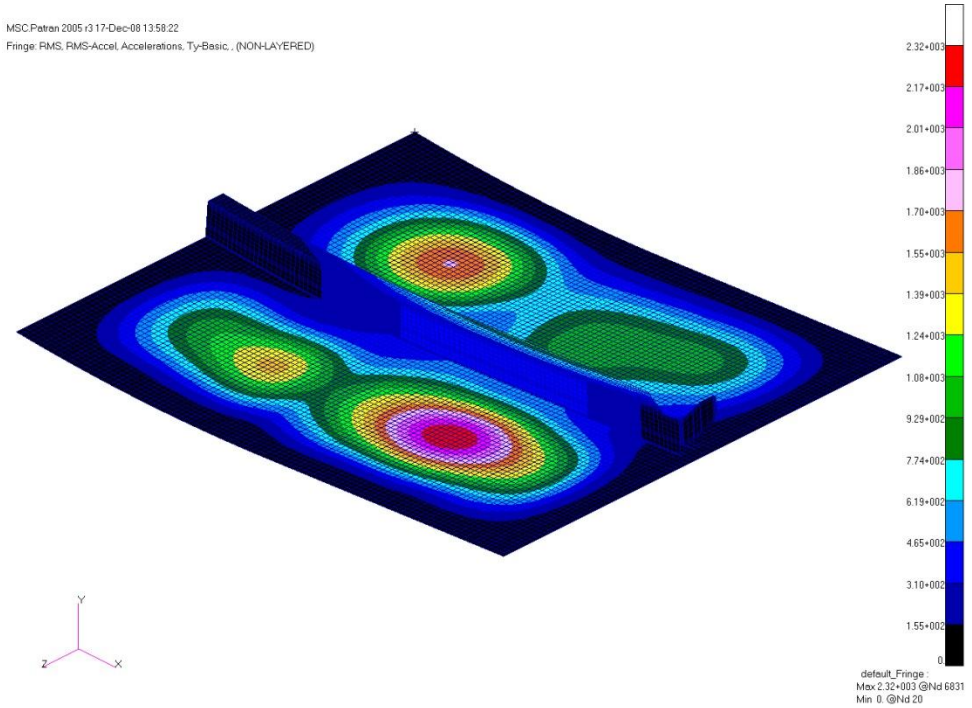

Figure 68 – NASTRAN Linear RMS Y-Acceleration (Grms)

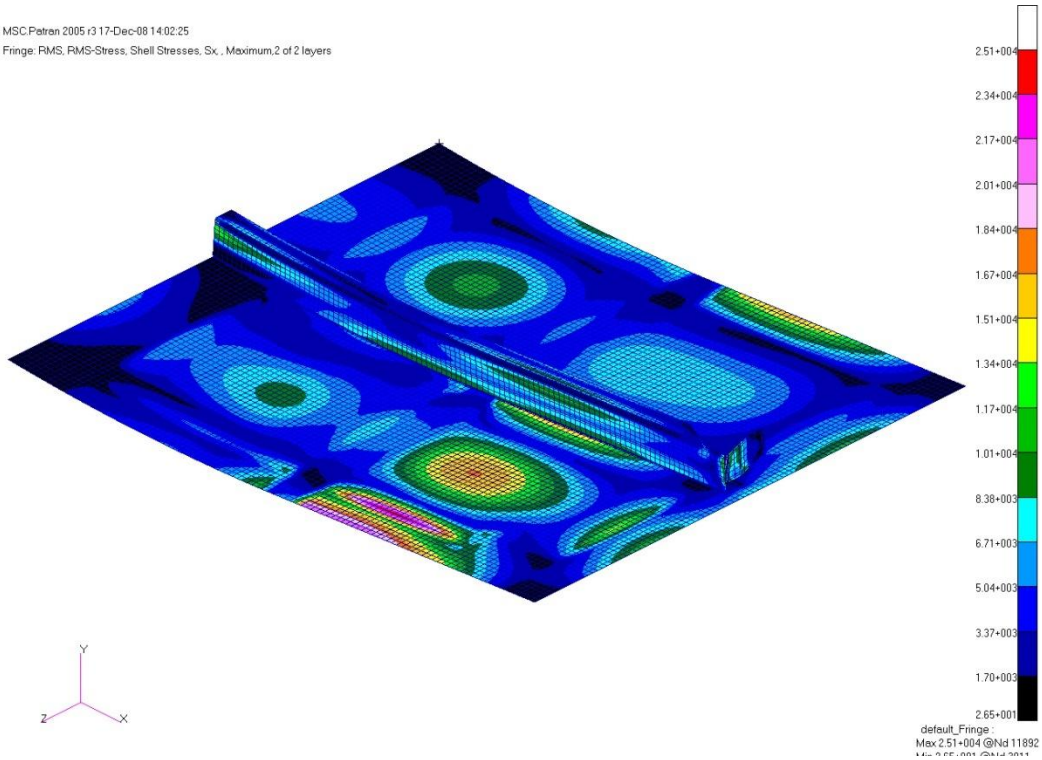

Figure 69 – NASTRAN Linear RMS Sx-Stress (psi)

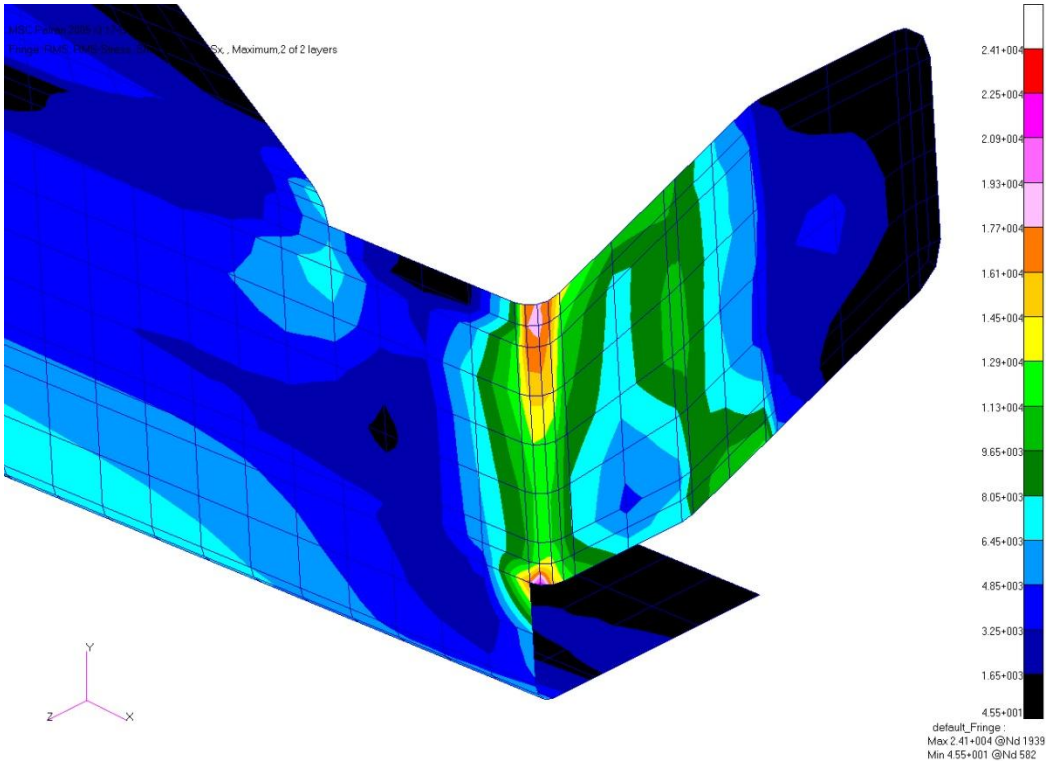

Figure 70 – NASTRAN Linear RMS Sx-Stress (psi) (Shear Clip Location)

The reference strain gages (element) and accelerometer (node) locations are shown in Figure 71 and Figure 72. A few comparison PSDs between linear random frequency response and

nonlinear explicit response are shown in Figure 73 (acceleration in the skin bay) and Figure 74 (stress in the clip). The peaks in the nonlinear response are generally lower with noticeable shifts in frequency. It can be concluded that the linear response is much more conservative.

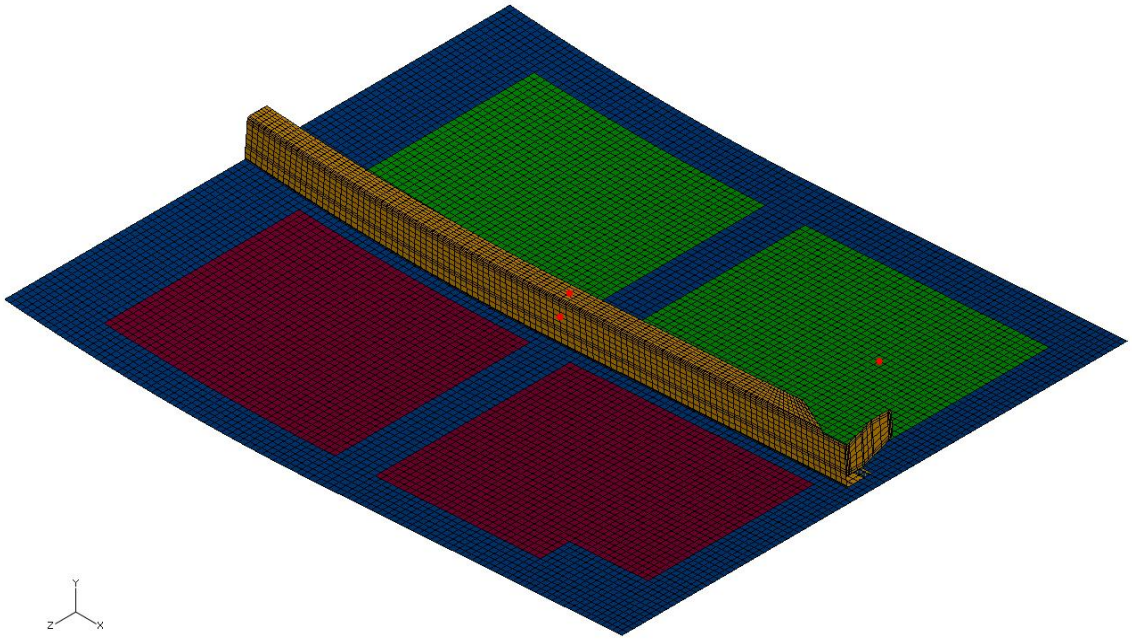

Figure 71 – Reference Accelerometer (Node) Locations to be used in Study

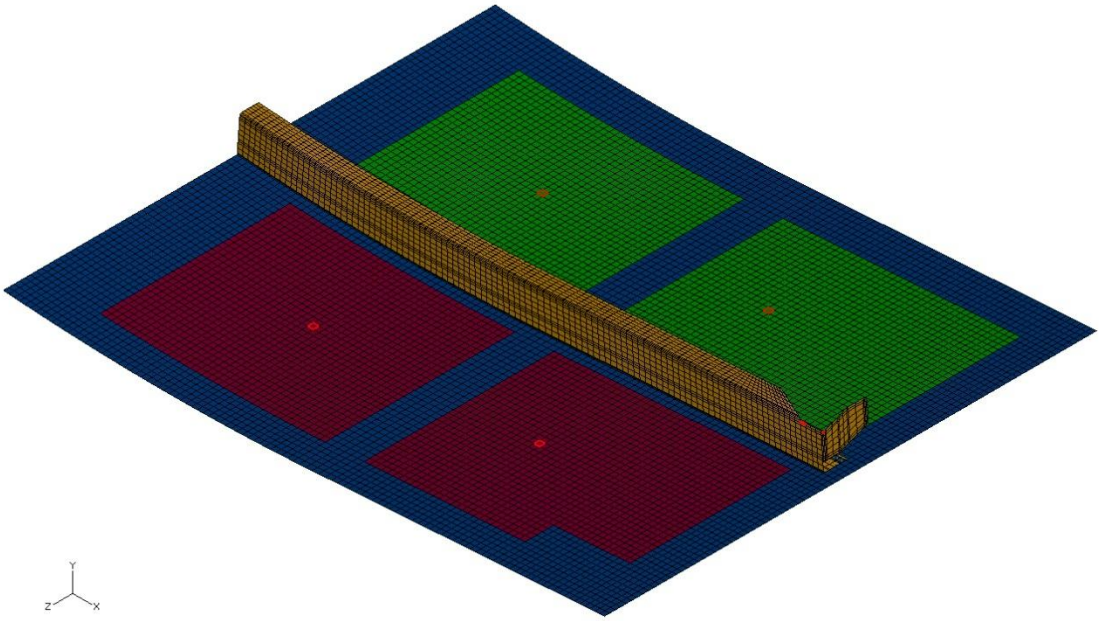

Figure 72 – Reference Strain Gage (Element) Locations to be used in the Study

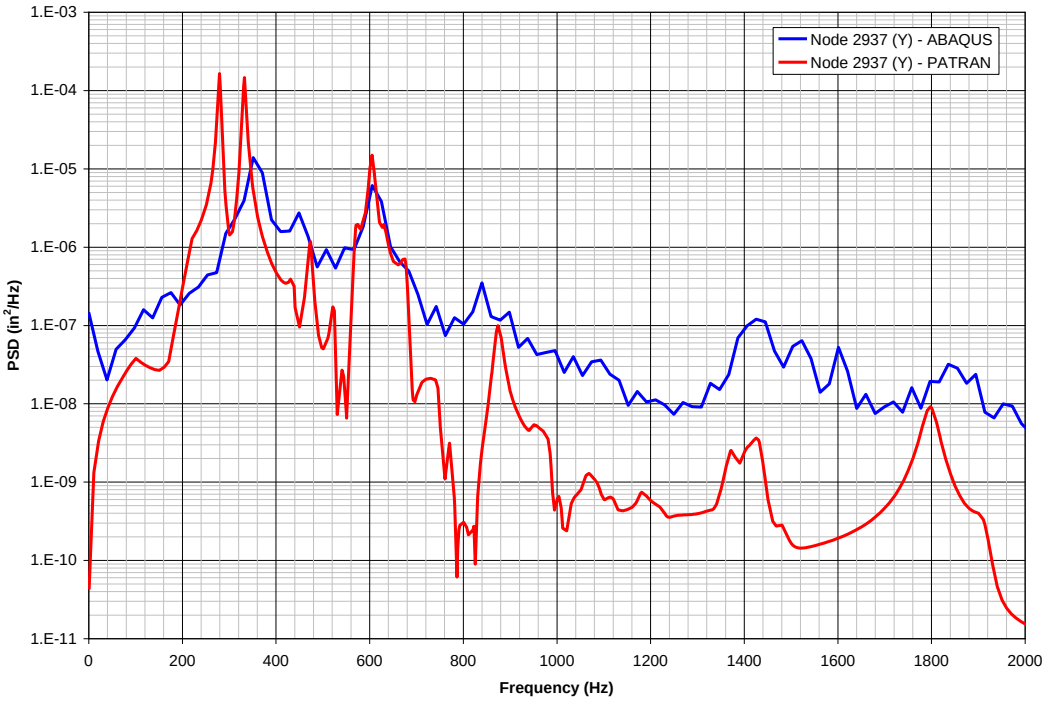

Figure 73 – Center Bay (on Skin) Y-Acceleration

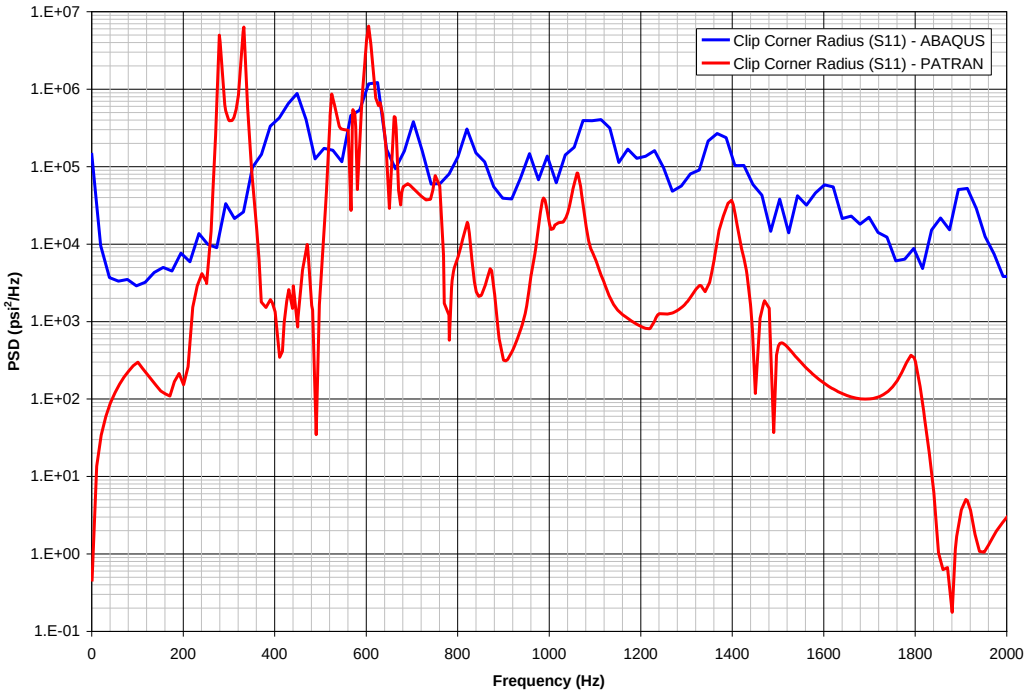

Figure 74 – Clip Radius Corner Stress Sx PSD

3.3.1 Comparison to Experimental Data – Curved Stiffened Aircraft Panel

The NLROM results are compared to the ABAQUS/Explicit solution, as well as to available laboratory test data. Essentially, this is an analysis-to-analysis comparison. The NLROM model used five modes. The acoustic loading was applied as two independent load cases with each

applied over half of the panel. This allowed for asymmetric mode response. The load cases are essentially independent (having no correlation). The damping was set zeta = 0.02. The time integration was $\Delta T=1/4000$ Hz. The NLROM analysis was run at several OASPL levels, as shown in Figure 75. The general nonlinear stiffening behavior is clearly seen as panel frequencies increase and the peaks broaden. The model was also run with a static preload of 3 psi. The static preload effect on the panel response is shown in Figure 76. The static load also stiffens the panel and changes the mode shapes. As can be seen in the figure, the 600-Hz mode becomes more prominent. The preload effect is more pronounced in Figure 77, which shows the integral shear clip stress. From Figure 77, the linear model does not accurately predict either the magnitude or the spatial distribution of loads and stresses in the panel, so it is evident that a nonlinear simulation is required.

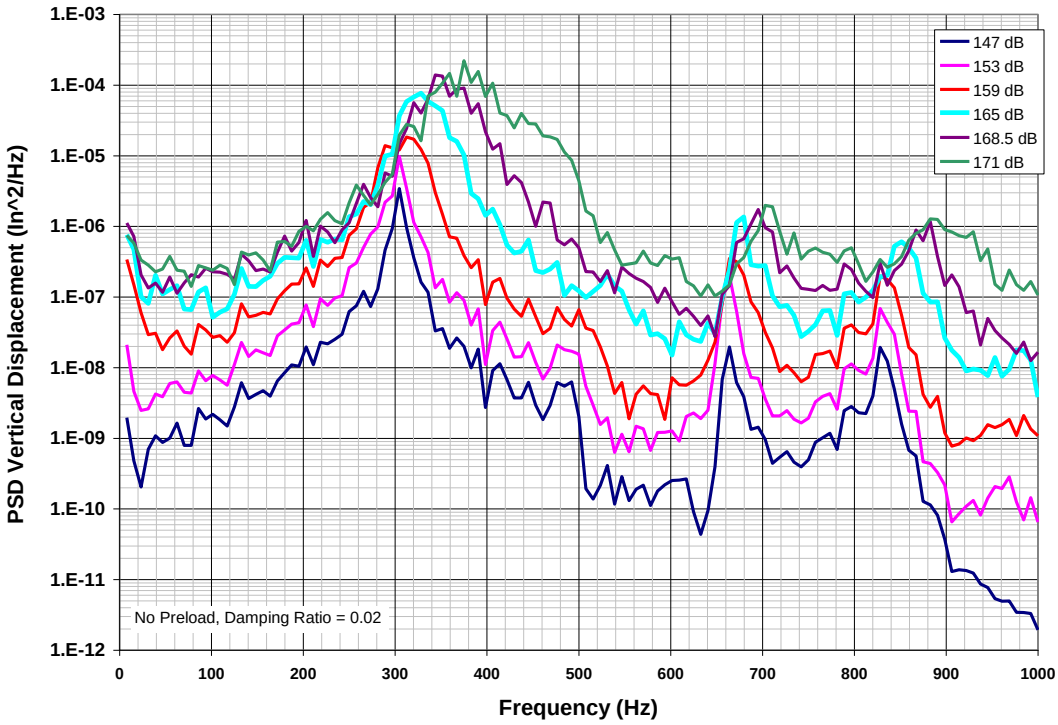

Figure 75 – NLROM Simulation at Different Load Levels and without Preload

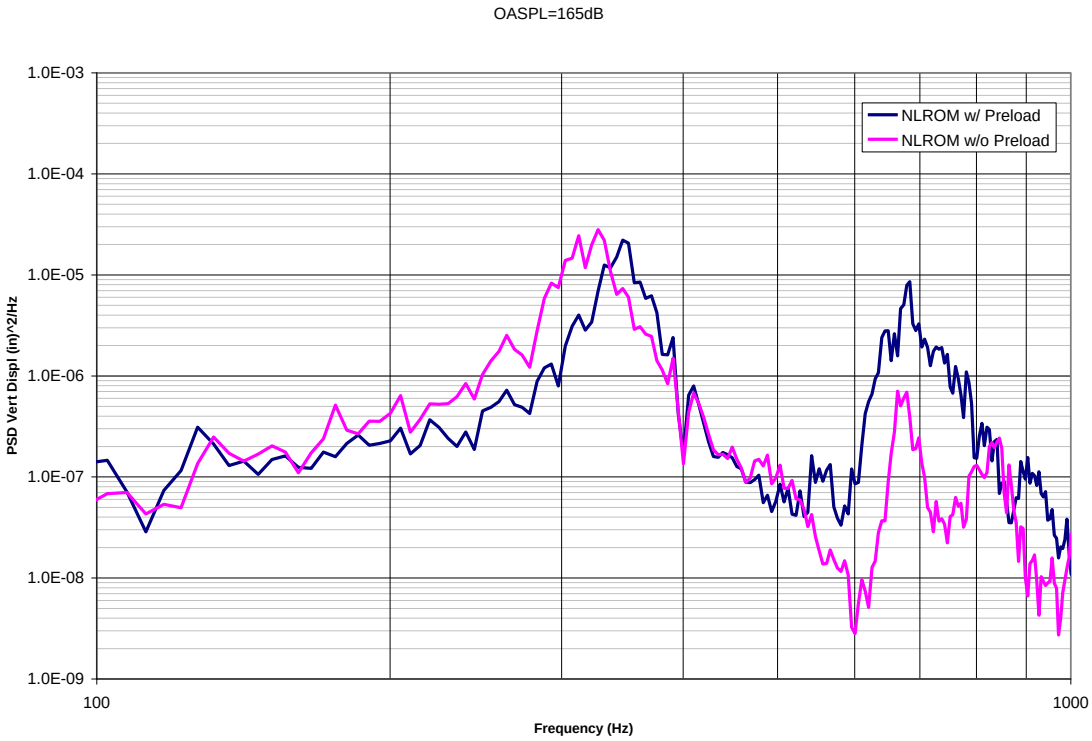

Figure 76 – Panel Displacement, NLROM simulation w/ and w/o 3-psi preload

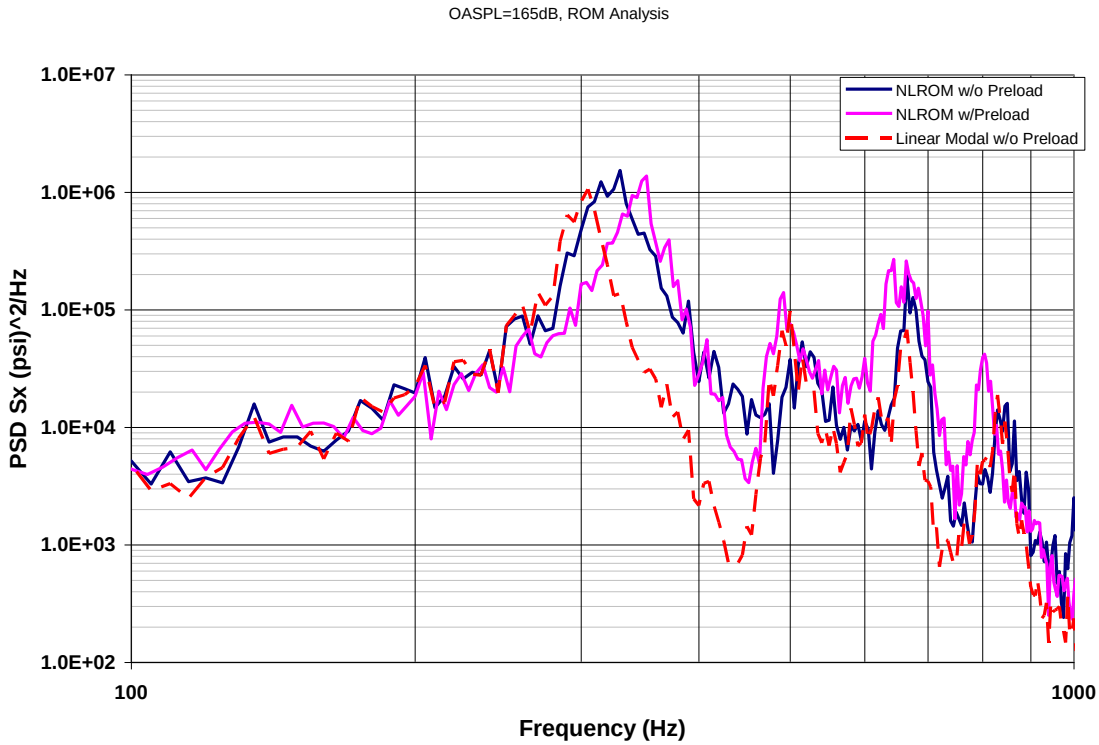

Figure 77 – Clip Stress, NLROM simulation w/ and w/o 3-psi preload

The ABAQUS/Explicit and NLROM solutions used the same mesh, boundary conditions, material properties, and damping. The NLROM solution compared well to the ABAQUS/Explicit solution, although there were some differences in the frequencies and mode shapes between the NASTRAN/NLROM model and the ABAQUS/Explicit full-order model. Because the comparison was not as close as it was in the curved panel test case, there were some differences in the response. However, overall the responses in the panel and at the critical stress location in the clip (Figure 78) match very well with the preload.

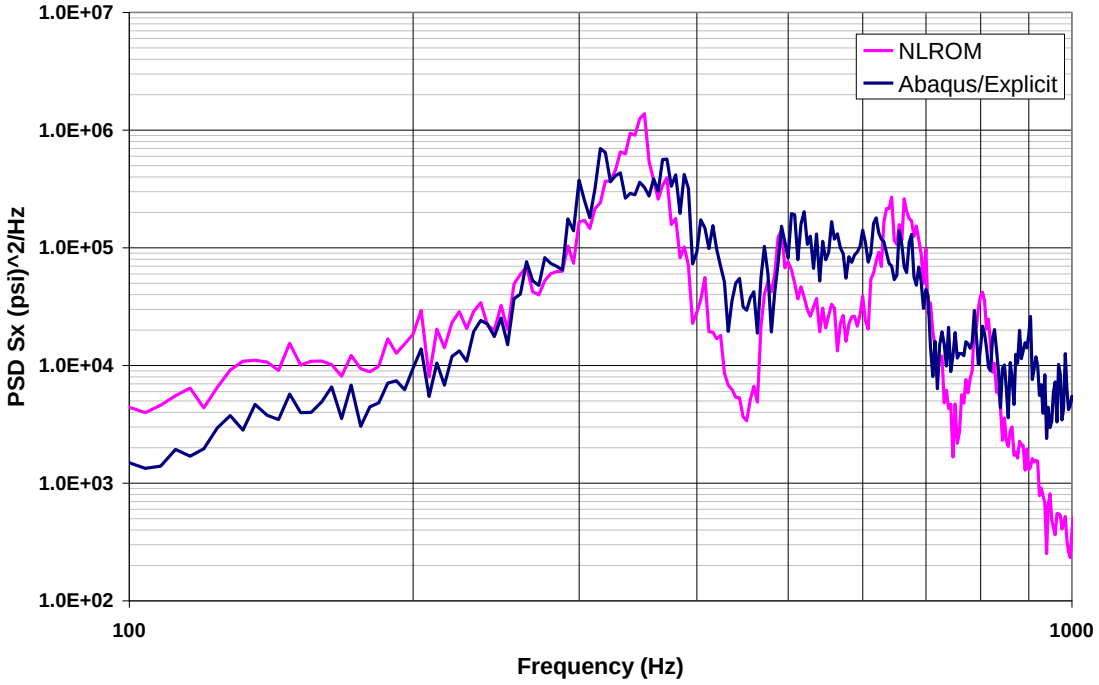

Figure 78 – Stress in the Clip at the Edge of Panel, OASPL = 165 dB, Ps=3psi

Fatigue-life prediction is carried out by counting the number of cycles to failure; results are shown in Table 3. The fatigue life as measured in the laboratory tests on several specimens ranged from 1800 to 3200 seconds.

Table 3 – Life Prediction Results

	OASPL =165dB Ps=3psi
	Life in Seconds to Failure
NLROM	4319
Full-Order	3705

No testing was performed as part of the Statement of Work of this program. However, lab test data was available for the stiffened curved test panel. The testing was performed in the Progressive Wave Acoustic Facility (Figure 79). An acoustic strain survey was performed on the panel at several combinations of static pressure and acoustic noise levels. Also, all testing was performed at ambient conditions. The panel was then tested to failure at OASPL=165dB and Ps=-3psi. The failure was a crack that initiated in the panel's stiffener integral shear clip, Figure

80. The panel was instrumented with 16 strain gages, three accelerometers, one static pressure transducer, 1 thermocouple, and two control microphones inside chamber, Figure 81. The NLROM analysis is compared to the laboratory test data.

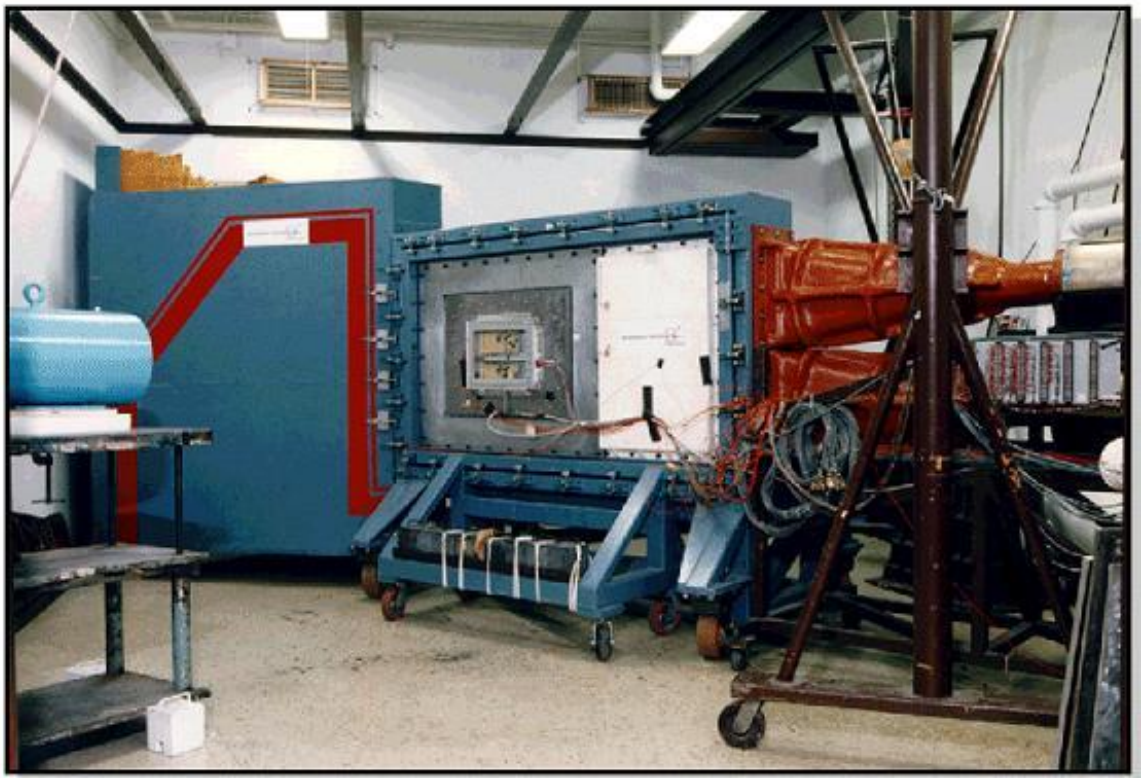

Figure 79 - Progressive Wave Chamber

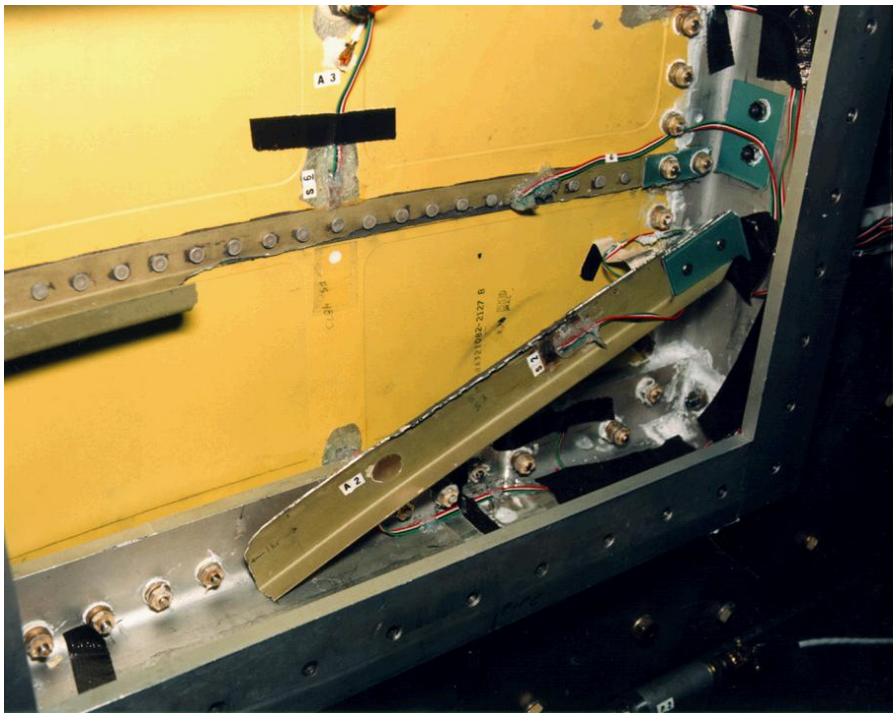

Figure 80 – Test Panel Failure Mode

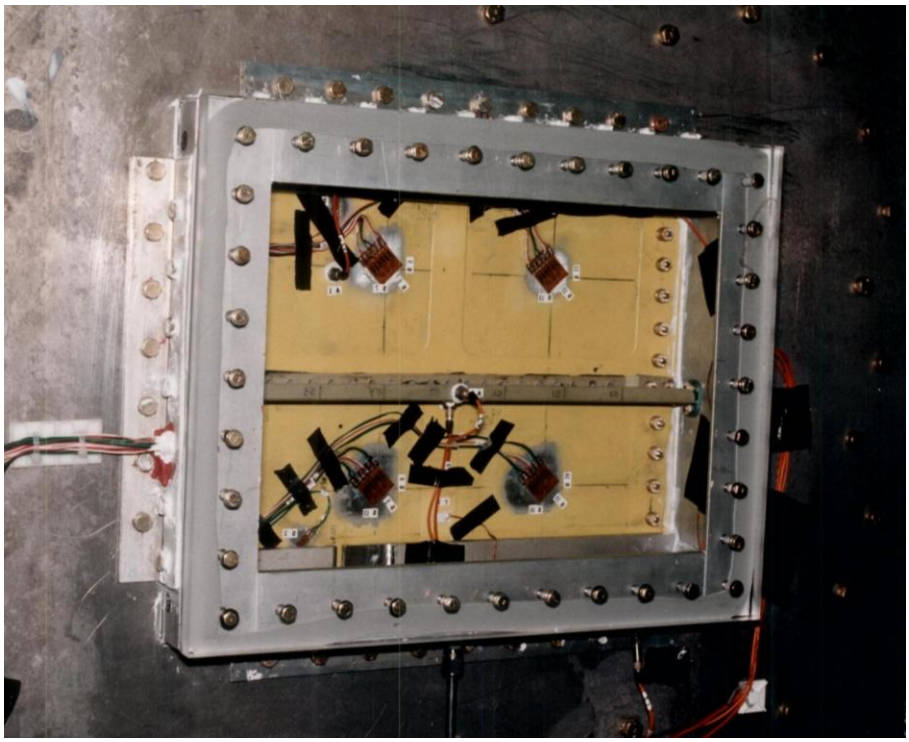

Figure 81 – Test Panel Mounted in Facility Side Wall in Pressure Plate Fixture

The panel frequencies are listed below in Table 4. These can be seen in the representative Frequency Response Functions (FRF) shown in Figure 82 and Figure 83.

Table 4 – Experimental Panel Frequencies

Mode Number	Frequency (Hz)
1	280.
2	309.
3	414.
4	433.
5	461.
6	515.
7	587.
8	635.
9	679.
10	698.
11	731.
12	792.

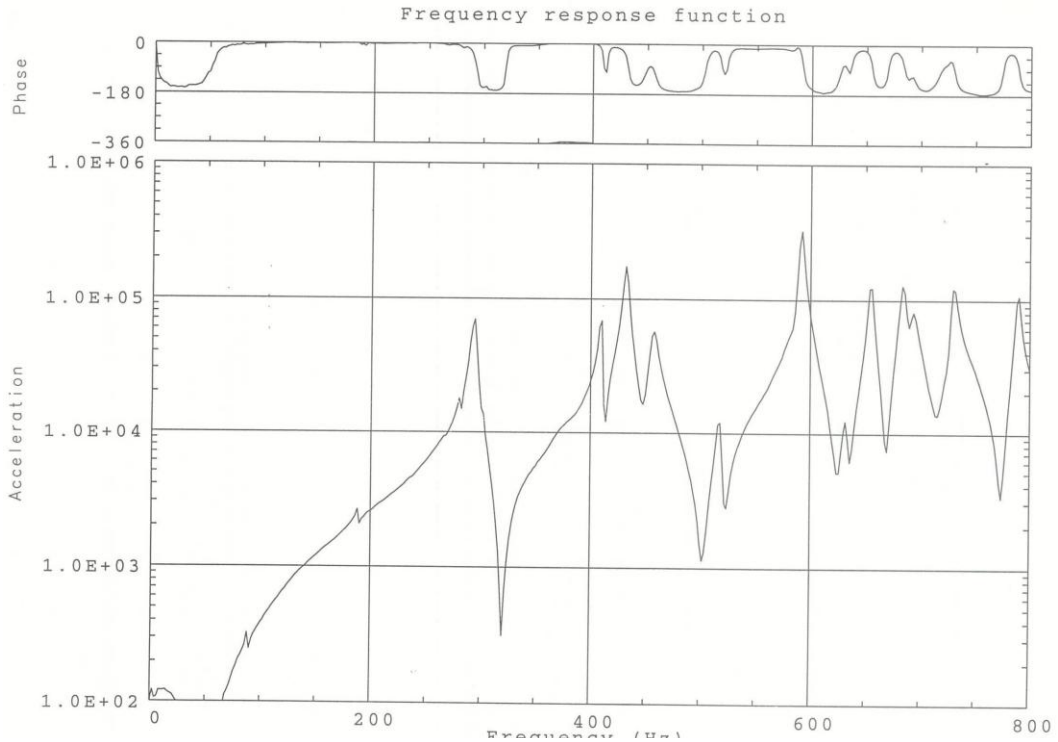

Figure 82 – Mid Panel Upper RHS Skin Pocket

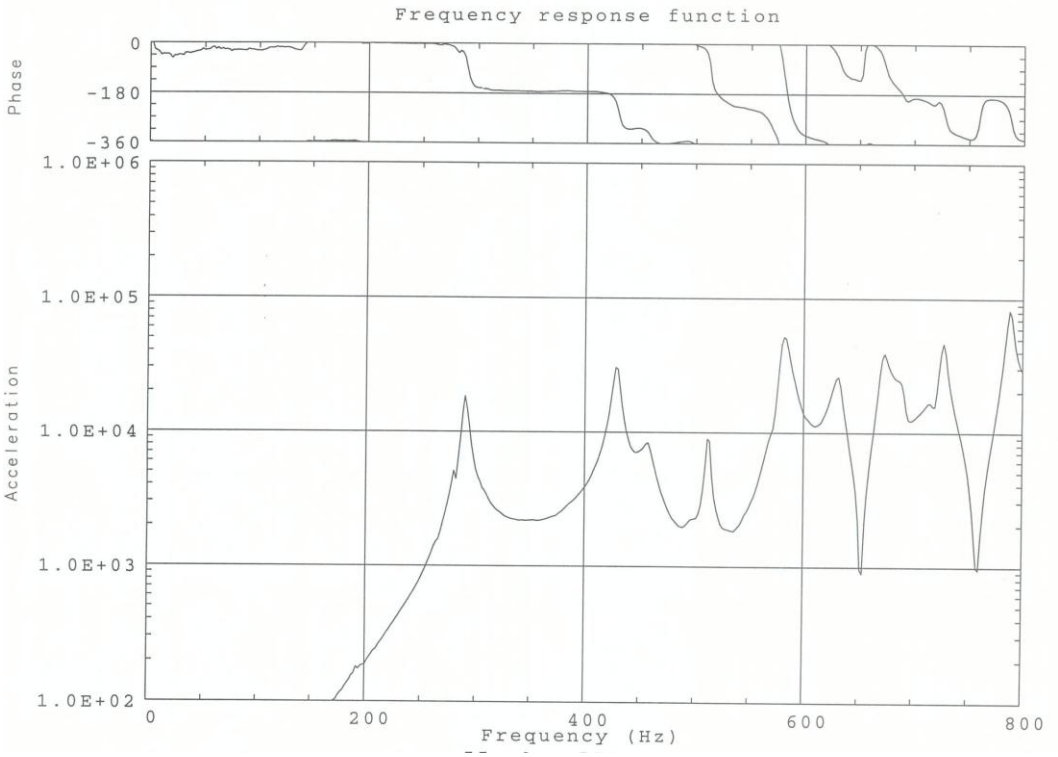

Figure 83 – Representative FRF Mid-Stiffener on the Web

The NLROM analysis is compared to the lab test data in Figure 84 and Figure 85. The NLROM analysis generally captures the same trend in the test data. In Figure 84, the RMS strain in the stiffener is shown compared to the test data. This was a gage approximately located at the end of the stiffener in the center of the web about 1 inch from the crack location in a lower strain

gradient location. The second plot, Figure 85, is from the reference accelerometer in the center of skin pocket. In general, the model does a good job of predicting the RMS trends in the test data.

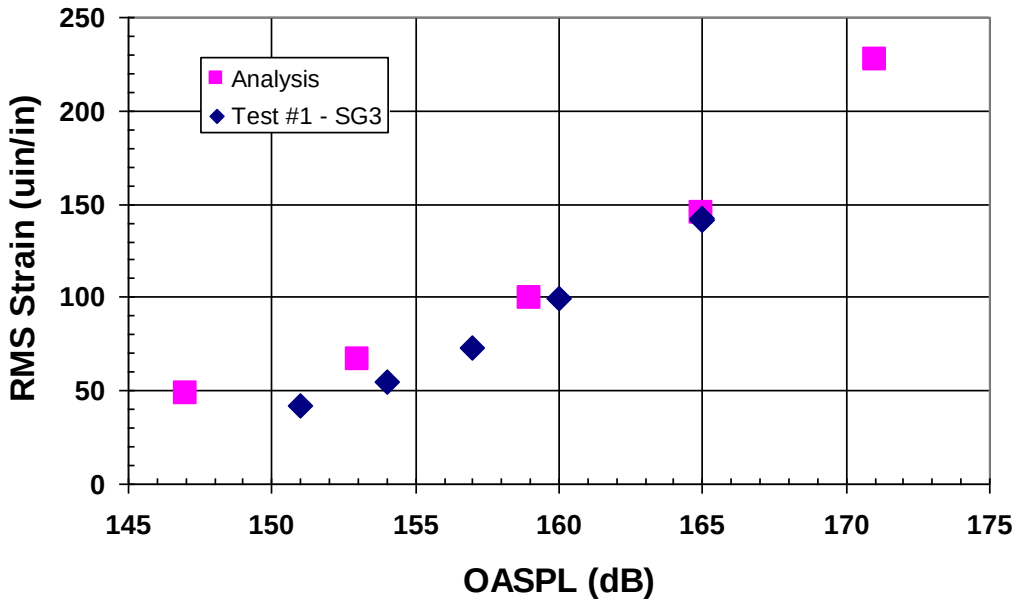

Figure 84 – Reference Strain (Sg3) on the Former.

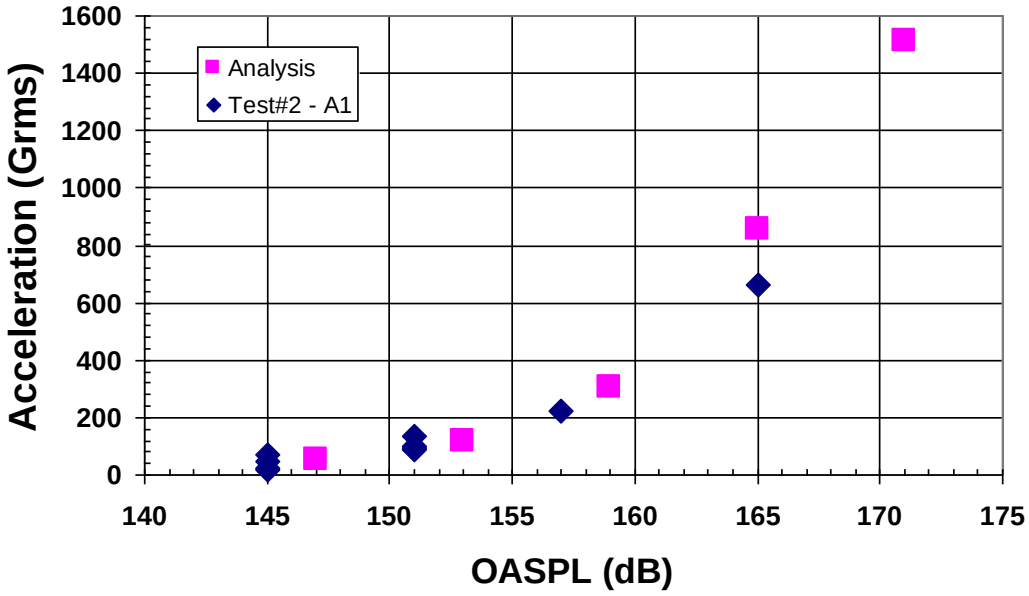

Figure 85 - Reference Acceleration (AC1) at the Center of the Panel Bay.

3.4 Acoustic Fatigue Design Study

3.4.1 Baseline Panel

The solution process for the baseline case began with a linear static and a modal analysis. In the linear static analysis, unit pressures were applied to the panel surface in two sets. The purpose of this was to attempt to excite anti-symmetric modes across the channel support structure. However, any number of pressure loading sets could be defined to excite desired modes. The pressure loading can be seen in Figure 86. The modal solution for the panel produced 32 modes between 1 and 1500 Hz.

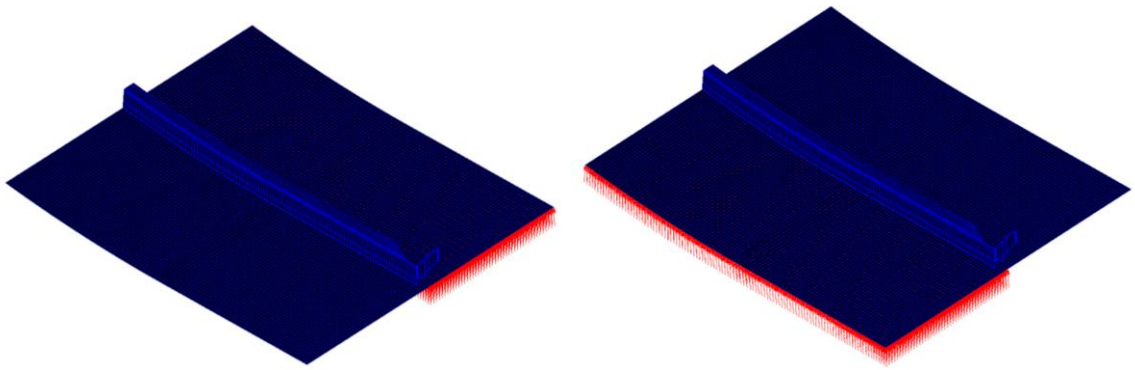

Figure 86 – Unit pressure loading in two separate sets to capture desired panel modes

Mode selection in the panel consisted of examining peaks in the PSD of a few representative nodes on the panel and channel. These nodes were selected arbitrarily to attempt to demonstrate that the process can be used for general structure, without the need to know the locations of critical fatigue locations. Three nodes were selected as shown in Figure 87.

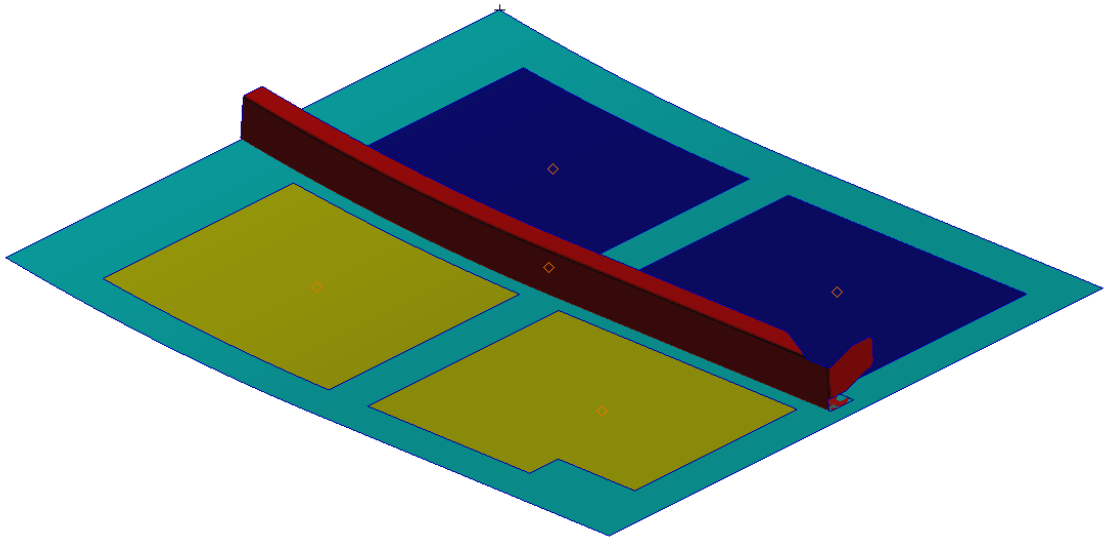

Figure 87 – Representative node locations for mode selection

A linear reduced order modal model solution was run with all modes up to 1500Hz, using a structural damping of 0.02 ($\zeta = 0.01$). This produced modal displacement data, which was then used to extract physical displacement information for the representative nodes. It is important to note that an inspection of the model was necessary for each node to determine the appropriate direction for which to examine nodal displacements. The physical time histories were transformed to the frequency domain to produce PSDs. These PSDs were the basis for the down-selection of modes for the nonlinear reduced order model (NLROM) solution. The PSDs for the representative nodes are shown in Figure 88, as well as the selected modes.

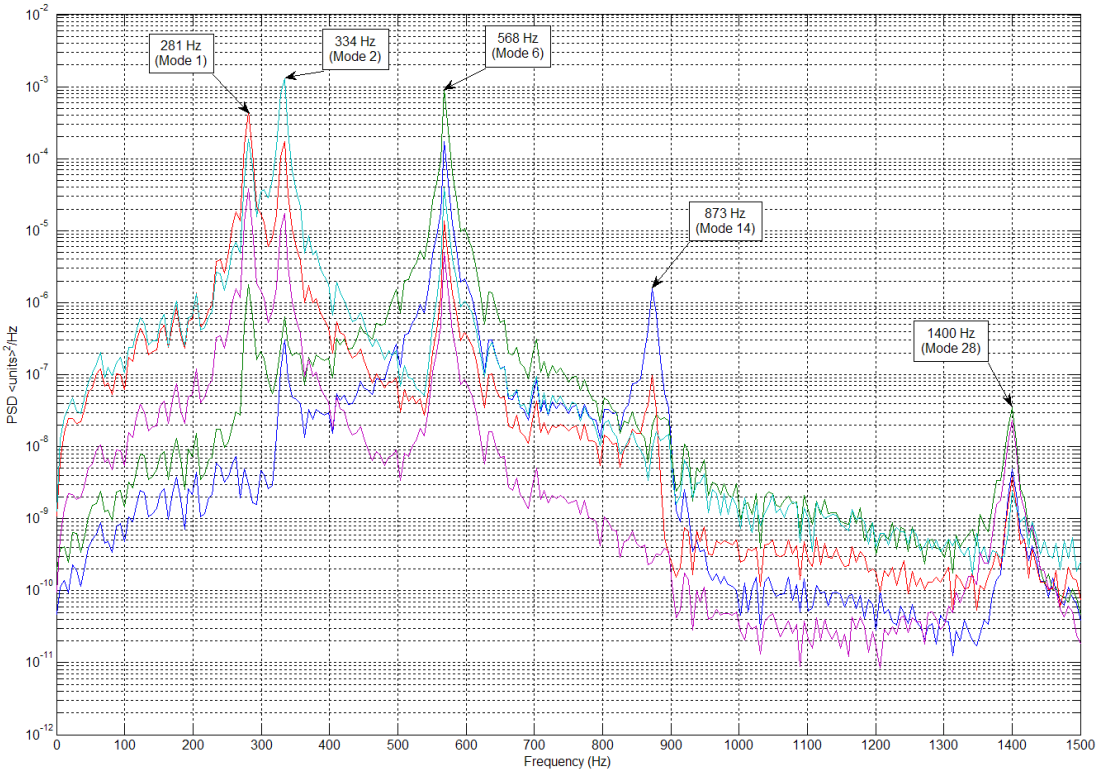

Figure 88 – Displacement PSDs for representative nodes and selected modes

As can be seen, each of the selected modes showed up as being dominant on multiple PSDs, and as such was deemed to be appropriate for the evaluation of the NLROM. The next step was to make an educated guess as to how to scale the loading for each of these modes in the NLROM solution. A general approach was used, choosing an initial scale factor for all modes using the equation:

$$s_f = \frac{2t}{|X|} \qquad \textbf{16}$$

where t is the thickness of the panel, and $|X|$ is the magnitude of the largest eigenvector value over all of the selected modes. In this case,, the panel consists of areas of different thicknesses. So a representative thickness of 0.05" was chosen. Using the maximum eigenvector value yielded an initial scale factor for all modes of 0.0004. This was used for the positive scaling, but due to the curvature of the panel, the negative scaling was set to 0.0002.

After setting the scale factors for the nonlinear loading, a nonlinear static solution was created, consisting of all one, two, and three mode combinations, including the positive and negative scale factors. The NLROM GUI was used to automatically generate the nonlinear static input file (NASTRAN SOL106) from the modes and scale factors selected by the user. Results from the solution 106 analysis were then read in to get displacement and applied load information.

The next step was to read in a physical load file. This file was created using the PSD_to_TH Matlab tool mentioned in a previous section. It contains a column for time, and then one column for each load set on the panel. For this panel there were two load sets, hence the file had three columns.

Once all of the above steps were taken successfully, the model was then ready to be converted to state-space format, and submitted to Matlab's ODE solver. Submittal options for the Matlab ODE solver include the solver type, dynamic scaling, static offset, solver evaluation time, and the number of data points to extract from the solution. The "Run Nonlinear" radio-button was selected, and the problem was submitted to the ode45 solver. Upon completion of the ODE solution, the computational routine automatically calculated a new set of nonlinear scale factors based on the RMS modal displacements.

Using these new calculated scale factors, the solution 106 process was then rerun up through the evaluation of the nonlinear ODE. Then the solution 106 result for the sub case with the maximum deflection was examined to locate the critical areas of the model. For the stiffened panel used in this study, an element in the radius of the clip was chosen for the explicit stress analysis. The Abaqus input file was automatically created for the selected element, including time versus displacement amplitude tables for each degree of freedom in the single element analysis. Running the explicit analysis then generated an output database, from which stresses were extracted for the final baseline fatigue analysis.

Using Lifeworks, Ref. (18), the stress spectrum was read in and used in a crack initiation analysis. Results were generated for Kt values from 0.5 to 2.0. The s-N plot is shown in Figure 89.

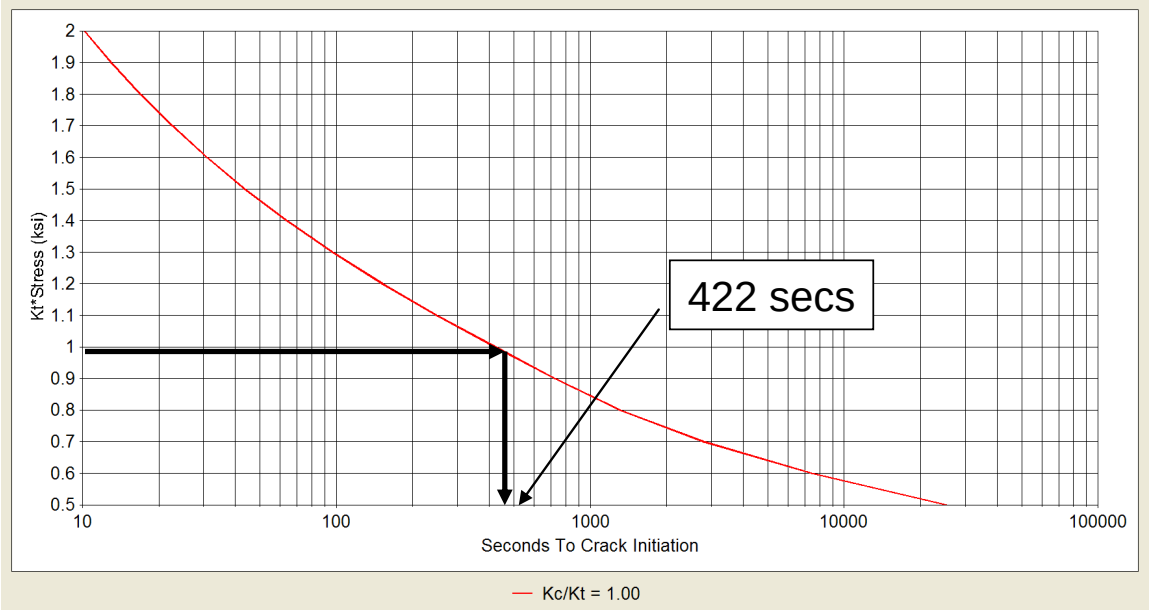

Figure 89 – Plot of fatigue prediction for critical element in baseline panel model

As can be seen in the figure, the fatigue prediction for this element is 422 seconds (7 minutes) to crack initiation. This is similar to what was seen in the testing performed on this panel design. Note: This fatigue life is much less than the fatigue life predicted in previous section. But, the design study does not include the static preload effect.

3.4.2 Improved Panel

An improved panel design was needed for better panel performance. For this new design, the entire channel thickness was doubled. A different, but also fairly general, mode selection process was used for the improved panel. The selection process consisted of choosing a mode that appeared essentially on one side of the channel, and also the corresponding mode that appeared on the other side. These "matched" pairs of modes, along with the correct set of scale factors, would allow for both symmetric and anti-symmetric modes to be excited. The selected modes are shown in Figure 90 through Figure 95.

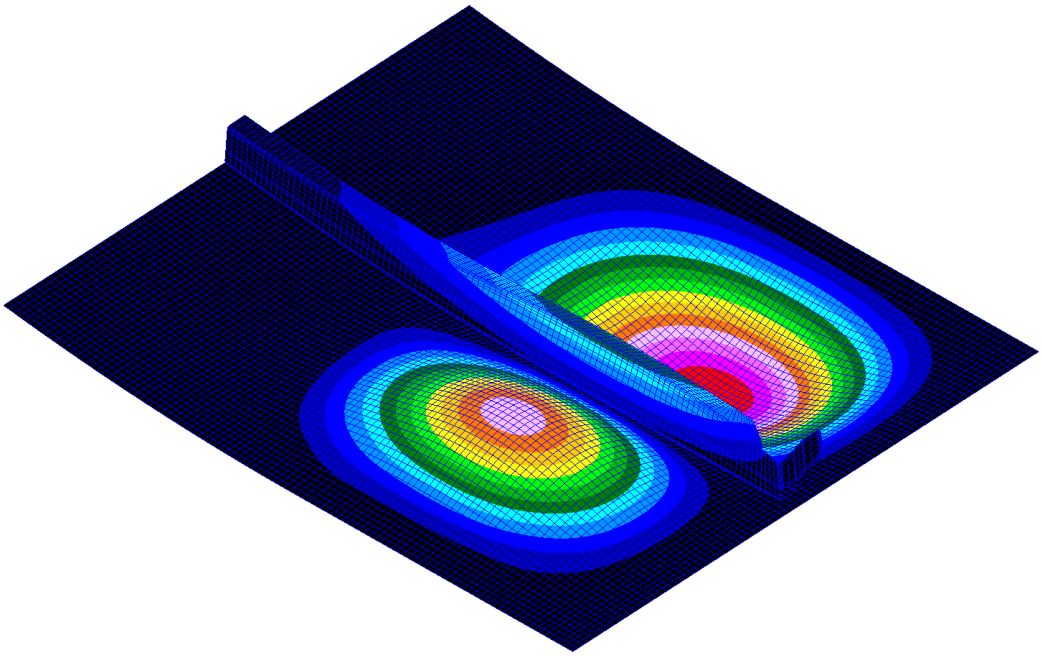

Figure 90 – Mode shape for improved model Mode 1, 293 Hz

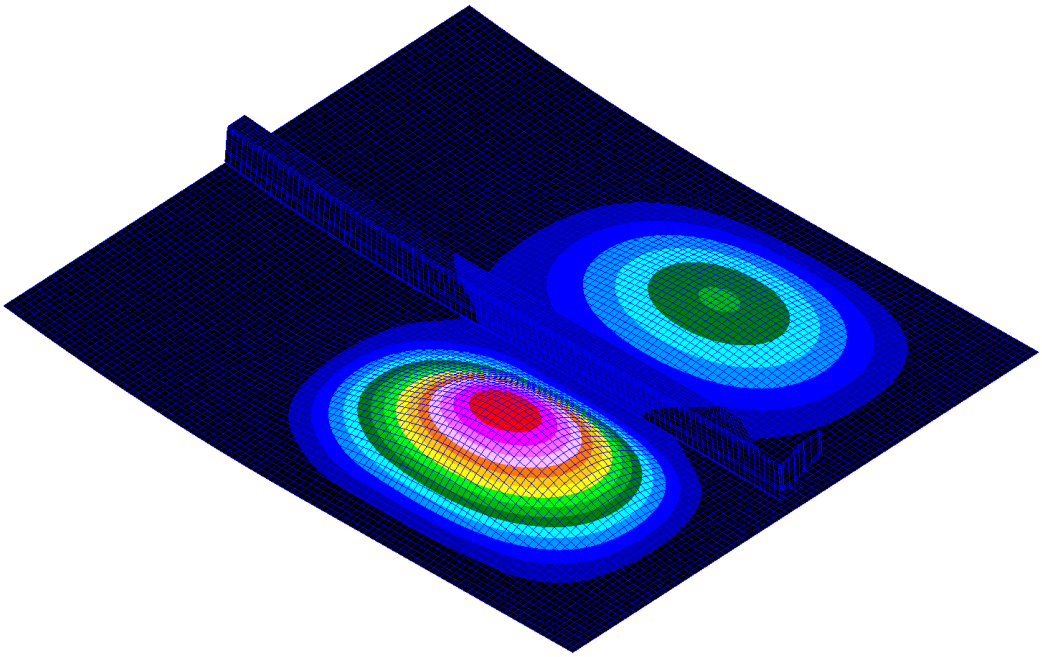

Figure 91 – Mode shape for improved model Mode 2, 350 Hz

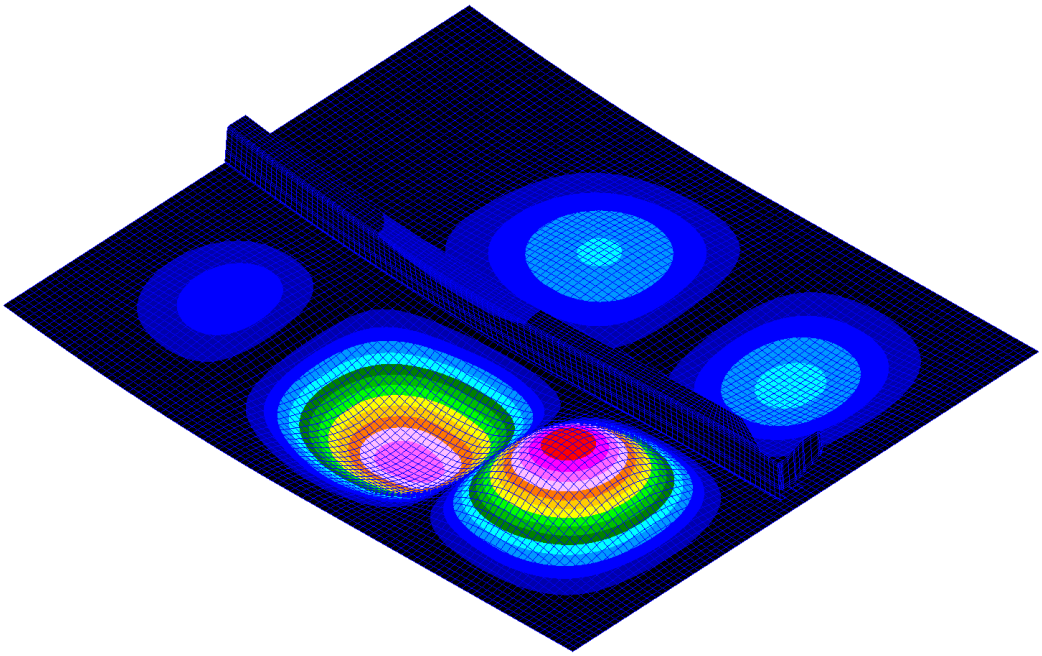

Figure 92 – Mode shape for improved model Mode 3, 454 Hz

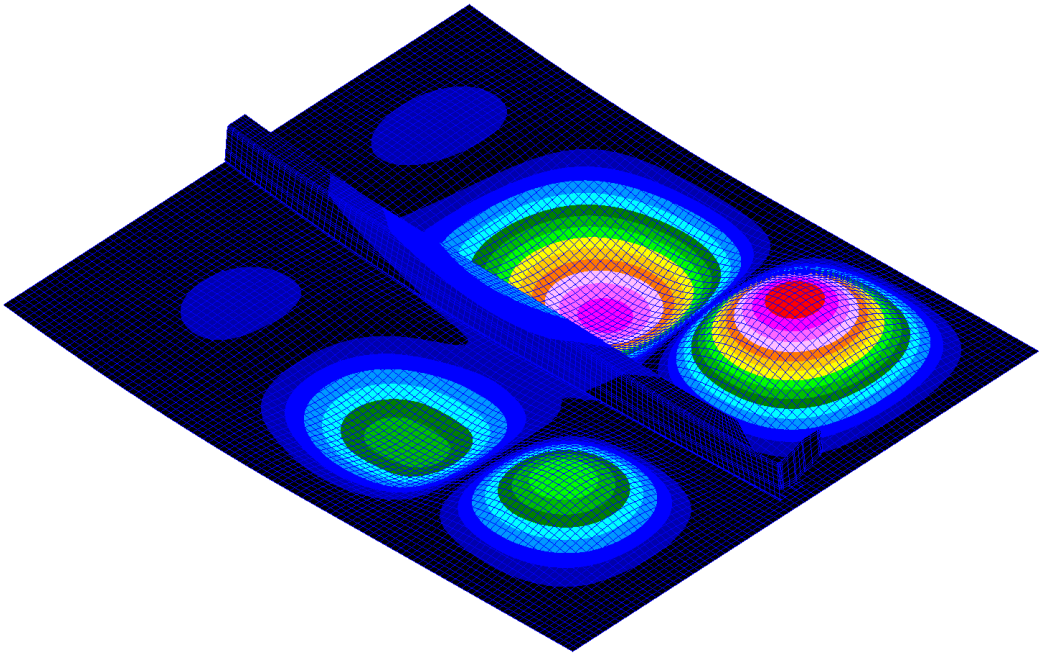

Figure 93 – Mode shape for improved model Mode 4, 491 Hz

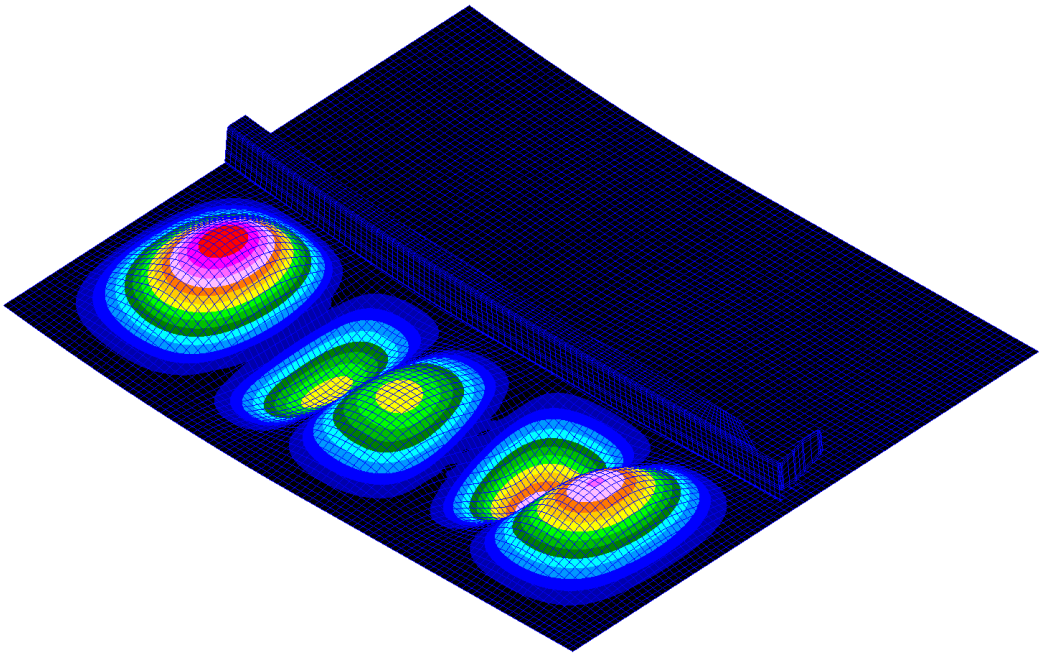

Figure 94 – Mode shape for improved model Mode 11, 776 Hz

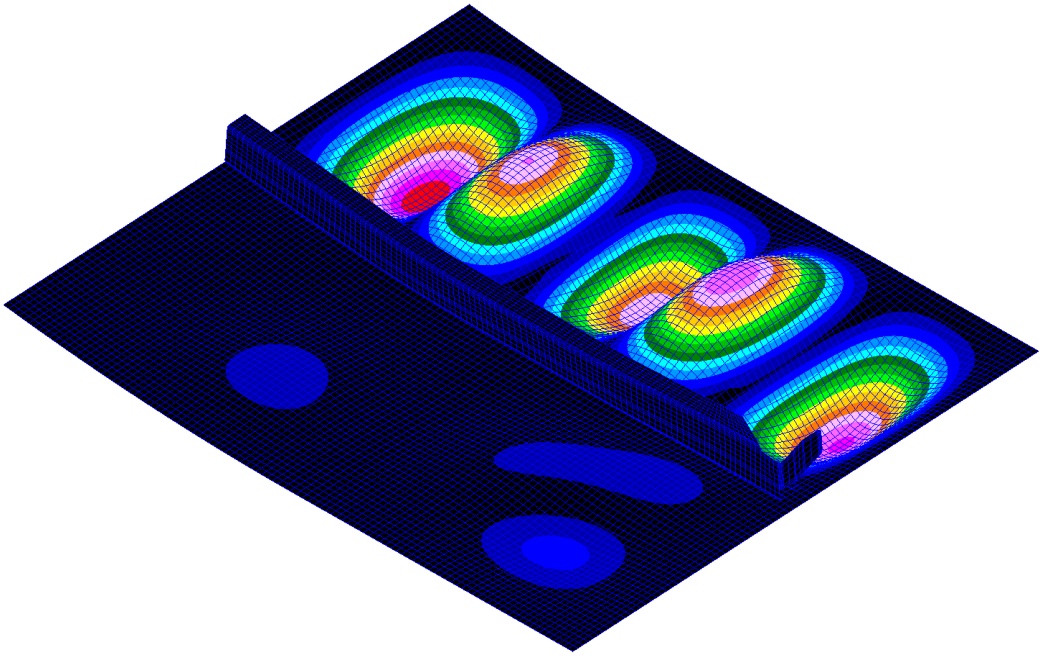

Figure 95 – Mode shape for improved model Mode 13, 888 Hz

The initial positive and negative scale factors were found to be 0.0004 and 0.0002, respectively, using Equation 1. Using the same process as for the baseline case, the solution 106 file was written using the GUI, and then the nonlinear ODE solution was solved. New scale factors were calculated automatically by the GUI and a newly scaled solution 106 file was created and run in NASTRAN. The nonlinear ODE solution was computed again.

For comparison purposes, the same element in the clip was chosen for closer examination. Using the GUI, an Abaqus explicit analysis input file was automatically generated. As in the baseline model, this explicit analysis file included time and displacement amplitude tables for all degrees of freedom in the single element analysis. Upon completion of the Abaqus analysis, the element stresses were used in a crack initiation analysis. As can be seen in Figure 96, the fatigue life of the improved panel is about eight times that of the baseline panel.

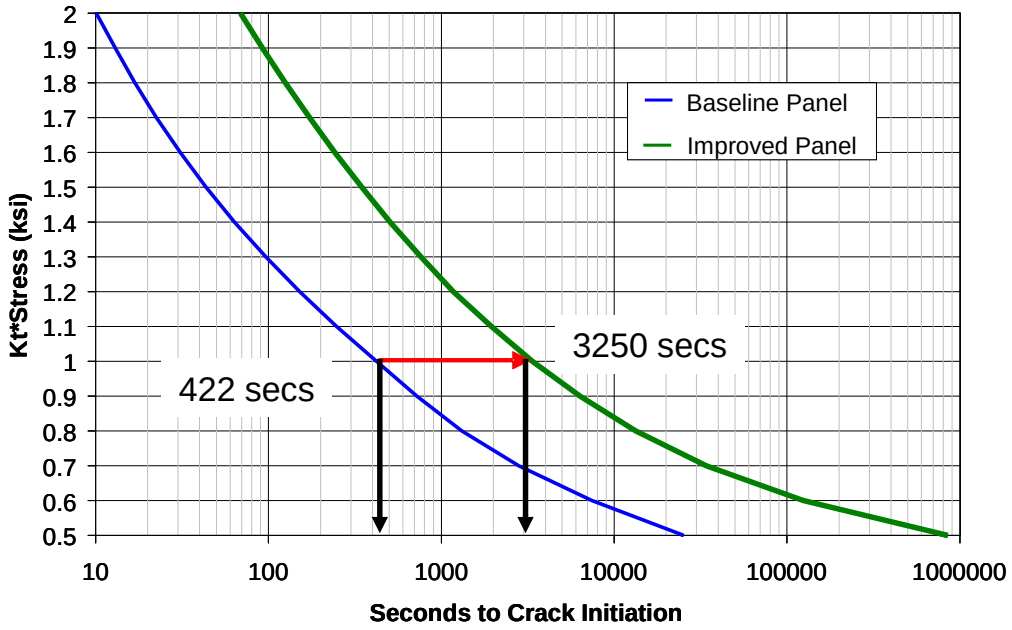

Figure 96 – Plot of fatigue prediction for critical element from baseline panel model

In this section, the NLROM was demonstrated to be very effective as a quick design tool. This study was run in 1/20th the time it would have taken to run the same analysis with a full-order method. The efficiency really improves with these bigger more detailed FEMs. Also, this was a 4 second simulation that used five modes. The full-order model would have taken four days to complete each simulation plus time to reduce the data, while the reduced order model too much less time approximately 4 hrs to complete the entire simulation.

4 CONCLUSIONS

The main objective of this project was to evaluate the NLROM method as applied to the acoustic fatigue analysis of representative fixed-wing aircraft structure and recommend technical improvements. This required that one of the NLROM methods be implemented into a standard commercial analysis tool. We chose to implement the applied force method using MSC/NASTRAN standard solution sequences and a Matlab program that calculated the nonlinear terms and evaluated the ODE. The method was verified to existing reduced order solutions available in the open literature. The method was then applied to two aircraft test cases: (1) a simple-supported curved fuselage panel, (2) a stiffened curved fuselage panel. Both of these test cases are actual aircraft applications, and used acoustic loads as measured in operation.

Based on a quantified evaluation, we found was that the NLROM method is a suitable and an efficient method for predicting acoustic fatigue of stiffened aircraft panels. What we know is that linear response methods tend to be conservative for these high intensity acoustic fatigue applications, but we don't know by how much. However, linear response methods generally do not predict the correct magnitude or spatial distribution of the critical stress response in a stiffened panel. Full-order nonlinear dynamic response methods are most accurate, but not very efficient when performing dynamic fatigue calculations. These methods are very computationally intensive for large detailed stress models. In general for fatigue calculations, models with accurate stress details are required. This significantly drives up the cost of performing the nonlinear full-order (explicit) analysis, because the stable time increment is dependent on the smallest element in the model. Hence, with a detailed stress model with a refined mesh in critical stress areas, the computational time can be significant. Also, for acoustic fatigue calculations long time simulations (>8 seconds) are required to get statistical convergence of the results. NLROM analysis is much more efficient as the models get larger (DOFs) and more detailed (smaller elements). The NLROM is not appreciably dependent on the solution time. Once the reduced order model has been developed, the time integration costs are low. Time simulations can be repeatedly performed at low cost. In fact, the NLROM method allows for more parametric solutions to be efficiently run on acoustic loading and damping level. The largest expense is the nonlinear static solutions. Full order explicit solutions are linearly dependent on the mesh size and simulation time. This was demonstrated in the Timing Study, section 3.1. Also, even though the method is a reduced order modeling approach, most acoustic fatigue damage is dominated by response of the lowest primary modes. This is ideal for the NLROM method since it doesn't require an extensive number of modes to capture the basic behavior. However, higher order modes bending modes and higher order (very high frequency) membrane modes do influence the lower order mode response. Higher order bending modes that contribute to the response or that are within the excitation forcing frequency range need to be included in the model. High order membrane modes need to be included based on the method being used. For the enforced displacement reduced order method, the membrane modes are essential to an accurate reduced order model. For the applied force method, the membrane modes are inherently statically condensed into the nonlinear stiffness terms.

This is a major advantage of the IMC method that no overt effort is necessary to model the membrane stretching. A membrane basis set is not required for the nonlinear model. When integrated, the model predicts modal bending amplitudes. Physical displacements that are spanned by the bending modes can be predicted accurately. However, the shortcoming of this method is that physical membrane displacements cannot be obtained. As a result, FEA based

stress/strain recovery is inaccurate. This shortcoming is overcome by estimating additional nonlinear functions to compute these quantities. This has been referred to as the ICE method. These functions are estimated from the nonlinear static solutions. The functions compute stress or strain, at a single location, directly from the modal bending amplitudes. Although, the stress/strain prediction can be accurate, the process is cumbersome.

For the stiffened panel test case, it was shown that response and fatigue life can be accurately predicted as compared to available test data. This was validated to both the full-order model and available test data. Also, the method was shown to be quite effective as a design tool as applied to the redesign study of the stiffened panel. Originally, this stiffened panel was redesigned using standard linear methods. The resulting redesign panel using the NLROM method resulted in a 3x weight savings over the redesign using linear methods. If these reduced methods are widely used throughout the airframe, then major weight savings can be realized.

In conclusion, the NLROM method is a suitable and efficient method for predicting sonic fatigue. Linear methods can not accurately predict the correct magnitude or spatial distribution of the critical stress response. Full-order nonlinear dynamic response methods are most accurate, but they are very computationally intensive when performing dynamic fatigue calculations. The NLROM method has equivalent accuracy to the full-order methods. Finally, the NLROM method allows the use of bigger (more refined) models in the analysis of acoustic fatigue; with bigger models better physics is captured. The NLROM method is an enabling technology that provides the means to generate a leap in performance and capability for the user.

5 RECOMMENDATIONS

This section lists the recommendations for technical improvements of the NLROM method. The recommendations will cover: Implementation of Method, Integration of the Method, Validation of the Method, Practicality of its Use, and Theoretical Extensions. Although, these recommendations are meant to be generally considered for all NLROM methods; it should be noted, that these recommendations are biased based on the NLROM method implemented and the nature of the test cases chosen for validation.

5.1 Implementation of Method

For this study, implementation refers to how the method is coded and with what tools. Acoustic fatigue of aircraft structure requires the use of complex built-up finite element models. These models can easily have upwards of hundreds of thousands of DOF. These models typically will mix element types: Solids, Shells, and Bars, Point (MASS, SPRING), Rigid Connectors, Fluid, etc… Also, the method requires the solution of linear static, normal mode, and nonlinear static solutions. Hence, the method needs to be implemented into a commercial finite element code that has all of these capabilities. For this program, we considered MSC/NASTRAN, ABAQUS, and ANSYS. The methodology could have been implemented with any of these codes. Other than the key features listed above, MSC/NASTRAN was chosen for this study based on our familiarity with using MSC/NASTRAN. But, also because of the ease of setting up (writing) models thru the Matlab interface, and ease of reading NASTRAN output files. NASTRAN also has the capability to retrieve, print, and manipulate internal matrices thru its Direct Matrix Abstraction Programming (DMAP) interface. The MSC/NASTRAN DMAP capability provides the ability to modify standard solution sequences or to write custom solution sequences to solve specialized problems. This capability can be used to either partially or fully implement the NLROM method. Another option for implementation of the NLROM method is the MSC/SimXpert. SimXpert is a fully integrated multidiscipline simulation environment with complete integrated solution (pre/post/solver) that speeds the process of simulation.

Simulia/ABAQUS and ANSYS also have programming interfaces and integrated simulation environments to allow a user to in write code or script to interact with the computer aided engineering environment. These scripts can manipulate objects to build models, setup and execute solutions, and access the solution databases. Likewise, this capability allows for partial to full implementation of the NLROM method. For this program, the NLROM method was essentially implemented as a stand-alone Matlab script, which used output results from MSC/NASTRAN standard solution sequences.

A similar integration approach is documented in Ref. (17), whereby the RANSTEP method was programmed in FORTRAN, and it interacts with either MSC/NASTRAN or ABAQUS thru standard input and output files. However, some DMAP is used for MSC/NASTRAN to output certain model and results data into INPUT4 format for manipulation by the RANSTEP executable. Also, the ABAQUS implementation uses Python script to do similar actions.

The recommendation on implementation is that these methods should be as an integrated solution sequence in a standard commercial finite element code. It's envisioned that the code would be an optional module for lease or purchase, but still be maintained by the supplier. This would be a preferred approach than as a special purpose script or program maintained by each

individual user. Consistent and standardized tools are a key requirement to designing quality products.

5.2 Integration of Method

The NLROM tool is only part of the total process by which an analyst designs structures to be acoustic fatigue resistant. First, a model needs to be developed in a Computer Aided Engineering (CAE) system, such as, MSC/PATRAN or ABAQUS/CAE. The geometry that the model will be developed from may be constructed in the CAE tool or imported from Computer Aided Design (CAD) tool; such as, CATIA. Most design applications will involve complex structural arrangements. The critical fatigue areas are usually in the structural details that need either fine meshing or breakout modeling. Therefore, the method needs to be implemented in a commercial finite element analysis tool that has a suitable CAD/CAE type interface. Second, the method needs to be integrated with tools that can perform fatigue analysis. The primary output from the NLROM method is a stress/strain time history. This time history needs to be in format that's easily manipulated by a fatigue life prediction tool. For this program, the NLROM time history output is read into LifeWorks, Ref. (18).

LifeWorks is the Boeing corporate standard software package for fatigue and fracture related analysis. The package contains modules for crack initiation, crack growth, spectrum processing, and stress analysis. It also contains an exhaustive database of material properties. The LifeWorks package is a comprehensive toolset that gives engineers the ability to perform advanced fatigue and fracture mechanics using a modern, robust, and easy to use graphical interface. The package can be used throughout the analysis process - from spectrum generation to final report documentation. A tool like LifeWorks is a critical for accurate prediction of fatigue and was essential to the evaluation process.

Acoustic fatigue analysis is part of the integrated design effort that occurs on any aircraft program. Early in a new development program, the acoustic fatigue margins are estimated using conservative linear methods. These linear methods might be handbook or spreadsheet based. If any structure is deemed acoustic fatigue critical, then the analysis will be proceeding to more detailed FEA based. The type of FEM used in the next step is dependent on the type of acoustic fatigue allowables available. A simplified FEM like the one used in Timing Study is common, Figure 97. This type of model is useful for either determining the max or RMS edge loads or for calculating the reference stress/strain response. The Max or RMS edge loads can then used in a detailed joint sizing tool; this might be a break out model or handbook equations. The reference stress/strain response is compared to an RMS strain allowable derived from coupon test data. In this case, the calculated RMS strain in the model is a reference that correlates directly to the RMS strain measured with the coupon. Several of these coupons are tested at different RMS strain levels to generate a fatigue curve. If no coupon or joint type data is available, then the analyst has to rely on basic material s-N data (preferably, R=-1, K_t=1.0). If only basic s-N data is available then, either the model needs to include the correct stress concentration factors; i.e., stress around hole, bolted joint, welded seam, bonded joint, chem-mill or machined step, or if the analyst knows the K_t, and applies it to the stress/strain time history during the fatigue analysis.

This is all applicable to this evaluation of the NLROM methods because the analyst needs to understand the process for developing the model, running the acoustic response solution, and

post-processing for fatigue. There shouldn't be any special restrictions on the type of models used or the type of results that come out of the nonlinear reduced order analysis. For instance, there shouldn't be any restriction on the choice or use of elements, the type of mesh (i.e. how it's numbered), geometry of the model (planar vs. 3-D, or coordinated systems), the boundary conditions (any linear classical constraints, spring elements, rigid connections, but not gaps or contact) , or structural loading (thermal, pressure, point load, acceleration, enforced motion.)

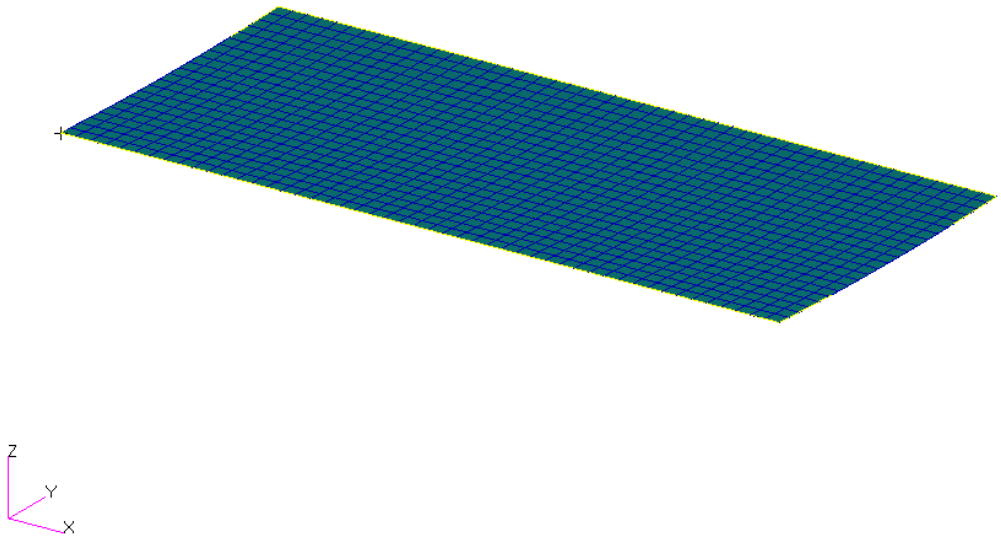

Figure 97 – FEM of Idealized Panel

The recommendations on integration are that the method needs to be implemented in a commercial finite element analysis tool that has a suitable CAD/CAE type interface. There can be no limits on the type of elements used with in the model. Second, the method needs to be integrated with tools that can perform time domain fatigue analysis.

5.3 Validation of Method

In this report, a test case was presented of a curved stiffened panel. This test case was deemed most appropriate as a first validation case, based on the Statement of Objectives for the program, which specified that these "new methods are applicable to the response of stiffened aircraft structural skins exposed to high-level aeroacoustic loading." The test case demonstrated that the reduced order model was orders of magnitude more efficient than the full-order model; that the methods are particularly well suited for acoustic response analysis of stiffened structure; that no special finite element modeling considerations are required; that the method can be used as a design tool or in a design environment; and that the predicted response is accurate enough to adequately predict fatigue life.

There are general guidelines for the validation and verification process (V&V), Ref. (19). Those developers of new software codes or methods have to be concerned about establishing credibility and confidence in the methods. This requires a rigorous V&V process, Ref. (20). With the implementation of any new method, the developer needs to first verify the accuracy of the simulation by comparison to another computational model. For this program, this was done by

comparing the full-order explicit finite element analysis. This establishes the credibility of mathematics, and verifies that the "equations were solved correctly." The validation is an assessment of the accuracy of the computational model with experimental data, and that the "right equations have been solved." The last step is quantifying the uncertainty in the simulation (e.g. fatigue life) and comparing this back to the reality.

In this report, a test case was presented that showed comparison to other validated computation models (verification) and to experimental data (validation). Simple beam and panel V&V test cases have been presented in the literature, and this is the first V&V test case to actual aircraft structure. In the next V&V steps, these NLROM method needs to be validated for other types acoustic and extreme environment loading; including, combined thermal and acoustic, and combined static and acoustic loading (note static loading can be in-plane loads or out-of-plane loads); pulse loading due to thermal shock, acceleration, or impact, blast; and base acceleration loading.

There are many types of nonlinear analysis: (1) boundary conditions (contact or gaps), (2) material, (3) geometric nonlinearity (large displacement), and (4) nonlinear loading (fluid-structure interaction). The NLROM method presented in the study was based on few linear assumptions: (1) constant non-changing boundary conditions, and (2) constant non-temperature or strain dependent material properties, (3) linear damping that is independent of the amplitude, and (4) deflection independent loads. The test case in this study only looked at geometric nonlinearity due to large displacements. In a geometric nonlinear solution, deflections of the structure are large (or at least on the same magnitude) with the dimensions of the original structure. When large displacements occur, there are changes in the stiffness and loads as the structure deforms. In a geometric nonlinear problem, there can be (1) large deflections, (2) deflection-dependent stiffness, (3) deflection-dependent loads, and (4) deflection-dependent damping. The first two situations were observed in the test case studied. But, deflection-dependent loading and damping were not considered. A common type of deflection-dependent loading would aerodynamic loading, which can lead to panel flutter. Nonlinear damping mechanisms commonly come from friction or from material nonlinearities, but damping is also dependent membrane loads, Ref. (21). When a steady-state tension membrane is present in a structure, the natural frequencies will increase, and the modal damping will decrease. Conversely, if steady-state compression load are present, then the natural frequencies decrease and the modal damping increases. This type of nonlinear effect is considered with the NLROM method, but the effect of alternating membrane loading brought on by large flexural dynamic deformations on the modal damping has not been verified in this model.

Another type of geometric nonlinear response would be snap-thru response caused by instability due to in-plane mechanical or thermal loads. This snap-thru response can be characterized by intermittent snap-thru when the structure is slightly below or at the buckling limit; persistent snap-thru when the structure at or slightly above the buckling limit; or post-buckled when the structure is responding to the acoustic loading in the statically post-buckled state. Any of these response types would be difficult to simulate with any confidence at this time. It should be noted that these are an important class of nonlinear problems for high temperature – high acoustic loading applications. This type of extreme loading is common in propulsion structures, engine exhaust structures, exhaust impinge structures, blow flaps, and thrust reverser structure, leading edge high acoustic/hypersonic structures, or environment control system (ECS) structures, which can exceed 350F normal, 580F discrete or 650F max operating. It's also possible that thin gage

aluminum fuselage structure exposed to normal operating conditions (-65F to 220F) can experience snap-thru buckling even though this isn't considered a "high temperature" application. Therefore, high temperature and high acoustic are relative to the application.

As new analytical methods (like NLROM) are introduced on a program, validation can be achieved through their application on a previous airplane and the subsequent correlation of results with those achieved earlier by using the original analysis method. Certification agencies, on the basis of FAR/JAR 25.307, 25.301, and 25.305, often require that new analytical predictions be corroborated by comparison with ground/lab test and/or flight test results, Ref. (22).

Therefore, the recommendation is that the NLROM method requires more validation uses test cases that demonstrate the most common and consequential types of geometric nonlinear problems; namely, extreme thermal/acoustic vibration applications. This will require a well-characterized thermal/acoustic laboratory test that verifies the degree of nonlinearity of the response. This test data would be used to validate the accuracy of the method.

5.4 Practicality of Use

In the development of new analysis methods, the general pursuit is faster and more accurate methods that lead to improved engineering quality and reduce design cycle time. For this program, we have established these practicality measures in the evaluation of the NLROM methods: CPU usage, model development requirements, user interaction, and user expertise level.

The NLROM method has been shown to reduce analysis time based on the test cases presented. The reduction in analysis can be significant. In fact, NLROM methods allow for a much more refined level of model detail, which is required for accurate fatigue life predictions, than conventional nonlinear explicit/implicit dynamic methods. Also, the accuracy was shown to be comparable to the full-order methods for the test cases presented. Finally, the reliability of the method or the ability for different users to duplicate results by others is reasonable or comparable to the full-order methods.

A method is practical if it can be used in a timely manner consistent with a program's schedule and man-power requirements. Generally, detailed acoustic response and fatigue analysis is performed by experienced structural dynamics engineers, who are familiar with the linear analysis methods. Nonlinear acoustic response analysis takes even more expertise. Full-order nonlinear analysis methods use conventional model development tools (e.g. MSC/PATRAN or Abaqus/CAE), but the setup, execution, and interpretation of results does require special skills. The NLROM uses conventional structural analysis methods (i.e., linear normal mode analysis, and nonlinear static analysis) to setup the nonlinear reduced order model.

The table below, Table 5, rates the NLROM method compared to the full-order method, and linear modal methods. In general, the CPU usage is much better than the full-order methods while establishing a suitable level of accuracy. The model development is high, mainly due to fact that the nonlinear stiffness terms need to be development using both linear modal and

nonlinear static analysis. The user interaction is also high, because the development of the NLROM does require the user to evaluate linear modal results to choose the proper modes, and the user needs to evaluate the nonlinear static solutions to ensure that the model has not buckled. The expertise level is high, mainly because this is a nonlinear transient solution. Any nonlinear and especially transient method requires a high level of expertise. Neither full-order or reduced order methods can be generally used by the average structures engineer.

Table 5 – NLROM Practicality Evaluation

Method	CPU Usage	Model Development	User Interaction	User Expertise Level
Linear Modal	Low	Low	Average	Average
Nonlinear Full-order	Very High	Average	High	High
NLROM	Average	High	Very High	High

The recommendation on practicality is that any new developments or implementations of the method should stress efficiency and ease of use. The most significant uncertainty in using the IMC method was the selection of the nonlinear scaling constants. There needs to be a practical and consistent method developed to appropriately select these constants. Also, the current state of the method is more practical for smaller (fewer) mode problems. But, for more complex built-up structures (with several panels), there will need to be many modes used in the solutions, which may make the development of a NLROM just as unyielding as trying to solve a full-order model. Hence, there needs to be a practical method for selecting modes most required for the NLROM.

5.5 Theoretical Extensions

The section describes potential extensions or developments of the method. The first recommendation would be to extend the method to the aeroelastic analysis of highly flexible structures. One particular application would be the nonlinear aeroelastic gust response of highly flexible wings of a High Altitude Long Endurance (HALE) vehicle. Other applications would be for the panel flutter response of highly flexible membrane structures being considered for morphing aircraft. The second recommendation would be to the nonlinear coupling of structural-acoustic systems. In a pressurized aircraft fuselage, the internal pressure adds stiffness to the structure; such that, structural waves become acoustically fast which can result in a decrease in Transmission Loss (TL). The higher frequency membrane modes couple to the lower frequency bending modes and there is a transfer of energy. All of these phenomena can not be analyzed using linear response methods and requires the use of nonlinear reduced order modal transient methods.

6 REFERENCES

(1) Rogers, L., et al., "Durability Patch: Repair and Life Extension of High Cycle Fatigue Damage on Secondary Structures of Aging Aircraft," proceedings of the 1st Joint DoD/FAA/NASA Conference on Aging Aircraft, July 1997.

(2) Beier, T.H., "AVTIP DO #27 Identification of Dynamic Loads Problems and Solutions," December 1, 2002.

(3) Locke, J. E., "A Finite Element Formulation for the Large Deflection Random Response of Thermally Buckled Structures," Ph.D. Dissertation, Old Dominion Univ., Norfolk, VA, 1988.

(4) Mei, C., "Large Deflection Multimode Response of Clamped Rectangular Panels to Acoustic Excitation," Wright-Patterson Air Force Base, Ohio, AFWAL-TR-83-3121, Vol. I, Dec. 1983.

(5) Rizzi, S.A. and Muravyov, A.A., "Improved equivalent linearization implementations using nonlinear stiffness evaluation," NASA TM-2001-210838, March 2001.

(6) McEwan, M.I., "A Combined Modal/Finite Element Technique for the Nonlinear Dynamic Simulation of Aerospace Structures," Ph.D. Dissertation, School of Engineering, University of Manchester, Manchester, UK, 2001.

(7) Liguore, S.L., "Identification of Uncertainties and Application of Probabilistic Analysis in Acoustic Fatigue Design, " Conference on Recent Advances in Structural Dynamics, Southampton England, UK July 2006

(8) Gordon, R.W., and Hollkamp, J.J., "Nonlinear Acoustic Response Prediction using Reduced-order Models," AFRL Workshop Notes, November 2007.

(9) Hollkamp, J.J., and Gordon, R.W., "Modeling Membrane Displacements in the Acoustic Fatigue Response Prediction Problem," AIAA-2005-2095, 2005.

(10) Gordon, R.W., and Hollkamp, J.J., "Reduced Order Modeling of the Random Response of Curved Beams Using Implicit Condensation," AIAA-2006-1926, 2006.

(11) Hollkamp, J.J., Gordon, R.W. and Spottswood, S.M., "Nonlinear Acoustic Fatigue Response Prediction from Finite Element Modal Models: A Comparison with Experiments," AIAA-2003-1709, 2003.

(12) Gordon, R.W., and Hollkamp, J.J., "Nonlinear Random Response of a Clamped Plate: A Well-Characterized Experiment," AIAA-2006-1924, 2006.

(13) Hollkamp J.J., Gordon R.W., and Spottswood S.M., "Nonlinear Modal Models for Acoustic Fatigue Response Prediction: A Comparison of Methods," *J. of Sound and Vibration*, Vol. 284 (3-5), 2005, pp. 1145-1163.

(14) Rizzi, S.A. and Przekop, A., "Estimation of Sonic Fatigue by Reduced-Order Finite Element Based Analyses," *Structural Dynamics: Recent Advances, Proceedings of the 9th International Conference*, Southampton, UK, 2006.

(15) Przekop, A., and Rizzi, S.A., "Nonlinear Reduced Order Random Response Analysis of Structures with Shallow Curvature,"AIAA-2005-2260, 2005.

(16) WAFO Tutorial – A Matlab Toolbox for Analysis of Random Waves and Loads, Lund Institute of technology, August 2000.

(17) Przekop A., Rizzi, S.A., "Reduced Order Analysis Using A Nonlinear Stiffness Evaluation Procedure (RANSTEP) User's Manual," NASA/TM-2007-XXXX.

(18) Sermersheim, J.S., "LifeWorks User's Manual," Dec 2007, The Boeing Company. Internal Report.

(19) Oberkampf, W.L., Trucano, T.G., and Hirsch, C., "Verification, Validation and Predictive Capability in Computational engineering and Physics," Foundations for V&V in the 21st Century Workshop, Oct 2022, John Hopkins University.

(20) Schlesinger, S. Terminology for Model Credibility, Simulation, Vol. 32, No.3, 1979.

(21) Lesieutre, G.A. "How Membrane Loads Influence the Modal Damping of Flexural Structures, " AIAA 2008-2188.

(22) Mohaghegh, M., "Validation and Certification of Aircraft Structures," Collected Papers in Structural Mechanics Honoring Dr. James H. Starnes, Jr.; February 2006, pp. 567-584

APPENDIX – LINEAR STATIC MODEL SETUP

```
$ NASTRAN input file created by the MSC MSC.Nastran
$ Linear Static Analysis, Database
SOL 101
CEND
SEALL = ALL
SUPER = ALL
TITLE = Curved Beam Test Case
ECHO = NONE
SUBCASE 1
$ Subcase name : LOAD_CASE.1.SC1
   SUBTITLE=LOAD_CASE.1.SC1
   SPC = 2
   LOAD = 3
   DISPLACEMENT(PLOT,SORT1,REAL)=ALL
   OLOAD(PUNCH,SORT1,REAL)=ALL
SUBCASE 2
$ Subcase name : LOAD_CASE.1.SC1
   SUBTITLE=LOAD_CASE.1.SC1
   SPC = 2
   LOAD = 4
   DISPLACEMENT(PLOT,SORT1,REAL)=ALL
   OLOAD(PUNCH,SORT1,REAL)=ALL
$ Direct Text Input for this Subcase
BEGIN BULK
PARAM    POST    0
PARAM    AUTOSPC NO
PARAM    WTMASS  .00259
PARAM    LGDISP  1
PARAM,NOCOMPS,-1
PARAM   PRTMAXIM YES
$ Direct Text Input for Bulk Data
$ Elements and Element Properties for region : beam
PSHELL   1       1       .09     1               1
$ Pset: "beam" will be imported as: "pshell.1"
CQUAD4   1       1       1       2       39      38
CQUAD4   2       1       2       3       40      39
CQUAD4   3       1       3       4       41      40
CQUAD4   4       1       4       5       42      41
CQUAD4   5       1       5       6       43      42
CQUAD4   6       1       6       7       44      43
CQUAD4   7       1       7       8       45      44
CQUAD4   8       1       8       9       46      45
CQUAD4   9       1       9       10      47      46
CQUAD4   10      1       10      11      48      47
```

```
CQUAD4   11      1       11      12      49      48
CQUAD4   12      1       12      13      50      49
CQUAD4   13      1       13      14      51      50
CQUAD4   14      1       14      15      52      51
CQUAD4   15      1       15      16      53      52
CQUAD4   16      1       16      17      54      53
CQUAD4   17      1       17      18      55      54
CQUAD4   18      1       18      19      56      55
CQUAD4   19      1       19      20      57      56
CQUAD4   20      1       20      21      58      57
CQUAD4   21      1       21      22      59      58
CQUAD4   22      1       22      23      60      59
CQUAD4   23      1       23      24      61      60
CQUAD4   24      1       24      25      62      61
CQUAD4   25      1       25      26      63      62
CQUAD4   26      1       26      27      64      63
CQUAD4   27      1       27      28      65      64
CQUAD4   28      1       28      29      66      65
CQUAD4   29      1       29      30      67      66
CQUAD4   30      1       30      31      68      67
CQUAD4   31      1       31      32      69      68
CQUAD4   32      1       32      33      70      69
CQUAD4   33      1       33      34      71      70
CQUAD4   34      1       34      35      72      71
CQUAD4   35      1       35      36      73      72
CQUAD4   36      1       36      37      74      73
$ Referenced Material Records
$ Material Record : aluminum
$ Description of Material
MAT1     1       1.06+7          .3      .1
$ Nodes of the Entire Model
GRID     1               18.     0.00000 0.
GRID     2               17.5019 .053965 0.
GRID     3               17.0035 .104855 0.
GRID     4               16.5047 .152671 0.
GRID     5               16.0057 .19741  0.
GRID     6               15.5064 .239072 0.
GRID     7               15.0069 .277653 0.
GRID     8               14.5071 .313154 0.
GRID     9               14.0071 .345572 0.
GRID     10              13.5069 .374906 0.
GRID     11              13.0066 .401155 0.
GRID     12              12.5061 .424319 0.
GRID     13              12.0055 .444396 0.
GRID     14              11.5047 .461385 0.
GRID     15              11.0039 .475287 0.
GRID     16              10.503  .486099 0.
```

```
GRID     17              10.002  .493823 0.
GRID     18              9.50101 .498457 0.
GRID     19              8.99999 .500002 0.
GRID     20              8.49896 .498457 0.
GRID     21              7.99796 .493823 0.
GRID     22              7.49699 .486099 0.
GRID     23              6.99608 .475286 0.
GRID     24              6.49524 .461385 0.
GRID     25              5.9945  .444395 0.
GRID     26              5.49388 .424318 0.
GRID     27              4.99339 .401154 0.
GRID     28              4.49305 .374905 0.
GRID     29              3.99288 .34557  0.
GRID     30              3.4929  .313152 0.
GRID     31              2.99313 .277652 0.
GRID     32              2.49359 .23907  0.
GRID     33              1.9943  .197408 0.
GRID     34              1.49527 .152669 0.
GRID     35              .996526 .104853 0.
GRID     36              .498102 .053964 0.
GRID     37              0.00000 0.00000 0.
GRID     38              18.     0.00000 1.
GRID     39              17.5019 .053965 1.
GRID     40              17.0035 .104855 1.
GRID     41              16.5047 .152671 1.
GRID     42              16.0057 .19741  1.
GRID     43              15.5064 .239072 1.
GRID     44              15.0069 .277653 1.
GRID     45              14.5071 .313154 1.
GRID     46              14.0071 .345572 1.
GRID     47              13.5069 .374906 1.
GRID     48              13.0066 .401155 1.
GRID     49              12.5061 .424319 1.
GRID     50              12.0055 .444396 1.
GRID     51              11.5047 .461385 1.
GRID     52              11.0039 .475287 1.
GRID     53              10.503  .486099 1.
GRID     54              10.002  .493823 1.
GRID     55              9.50101 .498457 1.
GRID     56              8.99999 .500002 1.
GRID     57              8.49896 .498457 1.
GRID     58              7.99796 .493823 1.
GRID     59              7.49699 .486099 1.
GRID     60              6.99608 .475286 1.
GRID     61              6.49524 .461385 1.
GRID     62              5.9945  .444395 1.
GRID     63              5.49388 .424318 1.
```

```
GRID     64              4.99339 .401154 1.
GRID     65              4.49305 .374905 1.
GRID     66              3.99288 .34557  1.
GRID     67              3.4929  .313152 1.
GRID     68              2.99313 .277652 1.
GRID     69              2.49359 .23907  1.
GRID     70              1.9943  .197408 1.
GRID     71              1.49527 .152669 1.
GRID     72              .996526 .104853 1.
GRID     73              .498102 .053964 1.
GRID     74              0.00000 0.00000 1.
$ Loads for Load Case : modal
SPCADD   2       1
LOAD     3       1.      1.      1
LOAD     4       1.      1.      5
$ Displacement Constraints of Load Set : fixed-edges
SPC1     1       123456  1       37      38      74
$ Pressure Loads of Load Set : Unit
PLOAD4   1       1       -1.                             THRU    18
PLOAD4   5       19      -1.                             THRU    36
$ Referenced Coordinate Frames
ENDDATA
```

APPENDIX – LINEAR MODAL SOLUTION SETUP

```
$ NASTRAN input file created by the MSC MSC.Nastran
$ Normal Modes Analysis
SOL 103
TIME 600
$
$ Direct Text Input for Executive Control
CEND
SEALL = ALL
SUPER = ALL
TITLE = Curved Beam Test Case
ECHO = NONE
$ Direct Text Input for Global Case Control Data
SUBCASE 1
$ Subcase name : modal
   SUBTITLE=modal
   METHOD = 1
   SPC = 2
   VECTOR(PUNCH,SORT1,REAL)=ALL
   GPFORCE(PUNCH)=ALL
$ Direct Text Input for this Subcase
BEGIN BULK
PARAM    POST    -1
PARAM    AUTOSPC YES
PARAM    WTMASS  .00259
PARAM    GRDPNT  1
PARAM,NOCOMPS,-1
PARAM   PRTMAXIM YES
EIGRL    1       0.      1500.           0                       MASS
$ Direct Text Input for Bulk Data

.
. see SOL 101 input file
.

$ Loads for Load Case : modal
SPCADD   2       1
$ Displacement Constraints of Load Set : fixed-edges
SPC1     1       123456  1       37      38      74
$ Referenced Coordinate Frames
ENDDATA
```

APPENDIX – NONLINEAR STATIC SOLUTION SETUP

```
$ NASTRAN input file created by MATLAB NLROM GUI
$ Nonlinear Static Analysis,Database
SOL 106
CEND
SEALL = ALL
SUPER = ALL
TITLE = Curved Beam Test Case
ECHO = NONE
SPC = 2
DISPLACEMENT(PUNCH,REAL) = ALL
OLOAD(PUNCH) = ALL
SUBCASE 1
$ Subcase name : lc0001
   SUBTITLE = lc0001
   NLPARAM = 101
   LOAD = 101
SUBCASE 2
$ Subcase name : lc0002
   SUBTITLE = lc0002
   NLPARAM = 102
   LOAD = 102
SUBCASE 3
$ Subcase name : lc0003
   SUBTITLE = lc0003
   NLPARAM = 103
   LOAD = 103
SUBCASE 4
$ Subcase name : lc0004
   SUBTITLE = lc0004
   NLPARAM = 104
   LOAD = 104
SUBCASE 5
$ Subcase name : lc0005
   SUBTITLE = lc0005
   NLPARAM = 105
   LOAD = 105
SUBCASE 6
$ Subcase name : lc0006
   SUBTITLE = lc0006
   NLPARAM = 106
   LOAD = 106
SUBCASE 7
$ Subcase name : lc0007
   SUBTITLE = lc0007
   NLPARAM = 107
```

```
   LOAD = 107
SUBCASE 8
$ Subcase name : lc0008
   SUBTITLE = lc0008
   NLPARAM = 108
   LOAD = 108
SUBCASE 9
$ Subcase name : lc0009
   SUBTITLE = lc0009
   NLPARAM = 109
   LOAD = 109
SUBCASE 10
$ Subcase name : lc0010
   SUBTITLE = lc0010
   NLPARAM = 110
   LOAD = 110
SUBCASE 11
$ Subcase name : lc0011
   SUBTITLE = lc0011
   NLPARAM = 111
   LOAD = 111
SUBCASE 12
$ Subcase name : lc0012
   SUBTITLE = lc0012
   NLPARAM = 112
   LOAD = 112
SUBCASE 13
$ Subcase name : lc0013
   SUBTITLE = lc0013
   NLPARAM = 113
   LOAD = 113
SUBCASE 14
$ Subcase name : lc0014
   SUBTITLE = lc0014
   NLPARAM = 114
   LOAD = 114
SUBCASE 15
$ Subcase name : lc0015
   SUBTITLE = lc0015
   NLPARAM = 115
   LOAD = 115
SUBCASE 16
$ Subcase name : lc0016
   SUBTITLE = lc0016
   NLPARAM = 116
   LOAD = 116
SUBCASE 17
```

```
$ Subcase name : lc0017
   SUBTITLE = lc0017
   NLPARAM = 117
   LOAD = 117
SUBCASE 18
$ Subcase name : lc0018
   SUBTITLE = lc0018
   NLPARAM = 118
   LOAD = 118
SUBCASE 19
$ Subcase name : lc0019
   SUBTITLE = lc0019
   NLPARAM = 119
   LOAD = 119
SUBCASE 20
$ Subcase name : lc0020
   SUBTITLE = lc0020
   NLPARAM = 120
   LOAD = 120
SUBCASE 21
$ Subcase name : lc0021
   SUBTITLE = lc0021
   NLPARAM = 121
   LOAD = 121
SUBCASE 22
$ Subcase name : lc0022
   SUBTITLE = lc0022
   NLPARAM = 122
   LOAD = 122
SUBCASE 23
$ Subcase name : lc0023
   SUBTITLE = lc0023
   NLPARAM = 123
   LOAD = 123
SUBCASE 24
$ Subcase name : lc0024
   SUBTITLE = lc0024
   NLPARAM = 124
   LOAD = 124
SUBCASE 25
$ Subcase name : lc0025
   SUBTITLE = lc0025
   NLPARAM = 125
   LOAD = 125
SUBCASE 26
$ Subcase name : lc0026
   SUBTITLE = lc0026
```

```
   NLPARAM = 126
   LOAD = 126
BEGIN BULK
PARAM    POST    0
PARAM    AUTOSPC NO
PARAM    WTMASS  .00259
PARAM    LGDISP  1
PARAM,NOCOMPS,-1
PARAM   PRTMAXIM YES
$ Direct Text Input for Bulk Data

.
. see SOL 101 input file
.

$ Loads for Load Case : modal
SPCADD   2       1
SPC1     1       123456  1       37      38      74
$ Referenced Coordinate Frames
$ Nonlinear Parameters for all Load Cases
NLPARM   101     10              AUTO    5       25              NO
NLPARM   102     10              AUTO    5       25              NO
NLPARM   103     10              AUTO    5       25              NO
NLPARM   104     10              AUTO    5       25              NO
NLPARM   105     10              AUTO    5       25              NO
NLPARM   106     10              AUTO    5       25              NO
NLPARM   107     10              AUTO    5       25              NO
NLPARM   108     10              AUTO    5       25              NO
NLPARM   109     10              AUTO    5       25              NO
NLPARM   110     10              AUTO    5       25              NO
NLPARM   111     10              AUTO    5       25              NO
NLPARM   112     10              AUTO    5       25              NO
NLPARM   113     10              AUTO    5       25              NO
NLPARM   114     10              AUTO    5       25              NO
NLPARM   115     10              AUTO    5       25              NO
NLPARM   116     10              AUTO    5       25              NO
NLPARM   117     10              AUTO    5       25              NO
NLPARM   118     10              AUTO    5       25              NO
NLPARM   119     10              AUTO    5       25              NO
NLPARM   120     10              AUTO    5       25              NO
NLPARM   121     10              AUTO    5       25              NO
NLPARM   122     10              AUTO    5       25              NO
NLPARM   123     10              AUTO    5       25              NO
NLPARM   124     10              AUTO    5       25              NO
NLPARM   125     10              AUTO    5       25              NO
NLPARM   126     10              AUTO    5       25              NO
$ Loads for all Load Cases
```

```
LOAD     101     1.      1.000-3 2
LOAD     102     1.     -4.000-4 2
LOAD     103     1.      1.000-4 3
LOAD     104     1.     -1.000-4 3
LOAD     105     1.      1.000-4 8
LOAD     106     1.     -1.000-4 8
LOAD     107     1.      1.000-3 2       1.000-4 3
LOAD     108     1.      1.000-3 2      -1.000-4 3
LOAD     109     1.     -4.000-4 2       1.000-4 3
LOAD     110     1.     -4.000-4 2      -1.000-4 3
LOAD     111     1.      1.000-3 2       1.000-4 8
LOAD     112     1.      1.000-3 2      -1.000-4 8
LOAD     113     1.     -4.000-4 2       1.000-4 8
LOAD     114     1.     -4.000-4 2      -1.000-4 8
LOAD     115     1.      1.000-4 3       1.000-4 8
LOAD     116     1.      1.000-4 3      -1.000-4 8
LOAD     117     1.     -1.000-4 3       1.000-4 8
LOAD     118     1.     -1.000-4 3      -1.000-4 8
LOAD     119     1.      1.000-3 2       1.000-4 3       1.000-4 8
LOAD     120     1.      1.000-3 2       1.000-4 3      -1.000-4 8
LOAD     121     1.      1.000-3 2      -1.000-4 3       1.000-4 8
LOAD     122     1.      1.000-3 2      -1.000-4 3      -1.000-4 8
LOAD     123     1.     -4.000-4 2       1.000-4 3       1.000-4 8
LOAD     124     1.     -4.000-4 2       1.000-4 3      -1.000-4 8
LOAD     125     1.     -4.000-4 2      -1.000-4 3       1.000-4 8
LOAD     126     1.     -4.000-4 2      -1.000-4 3      -1.000-4 8
.
.
.
ENDDATA
```